Roger Van Eperen

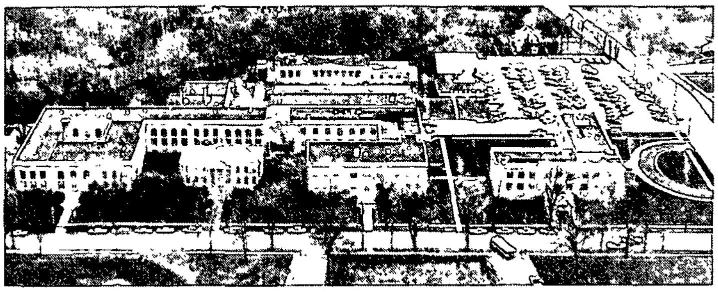

THE INSTITUTE OF PAPER CHEMISTRY, APPLETON, WISCONSIN

STATUS REPORTS

To The

PAPER PROPERTIES AND USES

PROJECT ADVISORY COMMITTEE

March 25-26, 1987
The Institute of Paper Chemistry
Continuing Education Center
Appleton, Wisconsin

NOTICE & DISCLAIMER

The Institute of Paper Chemistry (IPC) has provided a high standard of professional service and has exerted its best efforts within the time and funds available for this project. The information and conclusions are advisory and are intended only for the internal use by any company who may receive this report. Each company must decide for itself the best approach to solving any problems it may have and how, or whether, this reported information should be considered in its approach.

IPC does not recommend particular products, procedures, materials, or services. These are included only in the interest of completeness within a laboratory context and budgetary constraint. Actual products, procedures, materials, and services used may differ and are peculiar to the operations of each company.

In no event shall IPC or its employees and agents have any obligation or liability for damages, including, but not limited to, consequential damages, arising out of or in connection with any company's use of, or inability to use, the reported information. IPC provides no warranty or guaranty of results.

This information represents a review of on-going research for use by the Project Advisory Committees. The information is not intended to be a definitive progress report on any of the projects and should not be cited or referenced in any paper or correspondence external to your company.

Your advice and suggestions on any of the projects will be most welcome.

THE INSTITUTE OF PAPER CHEMISTRY
Post Office Box 1039
Appleton, Wisconsin 54912
Phone: 414/734-9251
Telex: 469289

February 27, 1987

TO: MEMBERS OF PAPER PROPERTIES AND USES PROJECT ADVISORY COMMITTEE

Attached for your review are the Status Reports for the Projects to be discussed at the Paper Properties and Uses PAC meeting scheduled for March 25-26, 1987, in Appleton. A meeting agenda can be found inside the booklet.

For those of you staying at the Continuing Education Center, the attached pink card gives the combination to the front door so that you may gain entrance if you arrive after the doors are locked. Room schedules are posted in the lobby. If you have not indicated whether you will be attending the meeting or have not yet reserved a room, please do so by notifying Sheila Burton at 414/738-3259.

We look forward to seeing you on March 25-26. Best regards.

Sincerely yours,

Gary

Gary A. Baum
Director
Paper Materials Division

GAB/sb
Enclosure

TABLE OF CONTENTS

MEETING AGENDA

PAPER PROPERTIES AND USES PROJECT ADVISORY COMMITTEE

March 25-26, 1987
The Institute of Paper Chemistry
Continuing Education Center
Appleton, WI

Wednesday -- March 25

8:30 a.m.	Welcome/Introductions	Van Liew/Baum
8:45	OVERVIEW OF PROJECTS	Baum
9:15	PROJECT REVIEWS	
	Process, Properties, Product Relationships	Baum/Habeger
	Student Presentation	Berger, B. J.
10:30	COFFEE BREAK	
10:45	PROJECT REVIEWS	
	Internal Strength Enhancement	Stratton
12:00 noon	LUNCH (CEC Dining Room)	
1:00	TOUR OF PAPER MATERIALS DIVISION LABORATORIES	
2:15	PROJECT REVIEWS	
	Board Properties and Performance	Whitsitt/Halcomb/ Dees
3:00	COFFEE BREAK	
3:15	PROJECT REVIEWS	
	Strength Improvement and Failure Mechanisms	Waterhouse
	On-Line Measurement of Paper Mechanical Properties	Habeger/Baum/Hall
5:15	SOCIAL TIME	
6:00	DINNER (CEC Dining Room)	

Thursday -- March 26

7:15 a.m.	BREAKFAST (CEC Dining Room)	
8:00	DISCUSSION OF PROJECTS (Krannert 108/109)	Committee
9:30	COFFEE BREAK	
10:00	DISCUSSION OF PROJECTS (continued)	
11:00	CLOSING COMMENTS	
	NEXT MEETING - October 21-22, 1987	
11:30	ADJOURNMENT/LUNCH (CEC Dining Room)	

PAPER PROPERTIES AND USES
PROJECT ADVISORY COMMITTEE

Dr. Gary Van Liew, Chairman -- 6/88*
Department Manager, Shipping
Container & Containerboard R&D
Weyerhaeuser Company
WTC 2h42
Tacoma, WA 98477
(206) 924-6464

Mr. James E. Beatty -- 6/89
Technical Director
Amricon Corporation
800 South Lawe
Appleton, WI 54915
(414) 733-3070

Dr. Robert L. Beran -- 6/89
Research Director
Westvaco Corporation
Covington Research Center
Covington, VA 24426
(703) 962-2111

Mr. Dennis Betz -- 6/89
Assistant Research Director
P. H. Glatfelter Co.
228 S. Main Street
Spring Grove, PA 17362
(717) 225-4711

Mr. Marvin D. Cooper -- 6/89
Resident Manager
Western Kraft Paper Group
Red River Mill
Willamette Industries, Inc.
P.O. Box 377
Campti, LA 71411
(318) 476-3392

Dr. John L. Firkins -- 6/88
Director of Product Development
Thilmany Pulp and Paper Company
P.O. Box 600
Kaukauna, WI 54130
(414) 766-4611

Mr. Richard P. Grant -- 6/89
Senior Engineer
Eastman Kodak Company
1669 Lake Avenue
Bldg. 36
Rochester, NY 14650
(716) 477-6537

Dr. Peter F. Lee -- 6/88
Director, Pulp and Paper Technology
Mead Corporation
Central Research
8th and Hickory St.
Chillicothe, OH 45601
(614) 772-3528

Dr. R. Heath Reeves -- 6/89
Sr. Research Associate
James River Corporation
Neenah Technical Center
1915 Marathon Avenue
Neenah, WI 54956
(414) 729-8148

Mr. Lowell Schleicher -- 6/89
Director of Basic Research
Appleton Papers Inc.
P.O. Box 359
Appleton, WI 54912
(414) 735-8857

Mr. Robert L. Smathers -- 6/89
Manager of Technical Services
MacMillan Bloedel Inc.
P.O. Box 336
Pine Hill, AL 36769
(205) 963-4391

Mr. David South -- 6/89
Technical Director
Chesapeake Corporation
P.O. Box 311
West Point, VA 23181
(804) 843-5252

Mr. Gary White -- 6/89
Supervisor, Materials Development
Owens-Illinois, Inc.
One Seagate
Toledo, OH 43666
(419) 247-5786

*Date of retirement from committee.

2/87

THE INSTITUTE OF PAPER CHEMISTRY

Appleton, Wisconsin

Status Report

to the

PAPER PROPERTIES AND USES

PROJECT ADVISORY COMMITTEE

Project 3467

PROCESS, PROPERTIES, PRODUCT RELATIONSHIPS

February 13, 1987

PROJECT SUMMARY

PROJECT NO. 3467: PROCESS, PROPERTIES, PRODUCT RELATIONSHIPS

PROJECT STAFF: G. A. Baum, C. C. Habeger February 13, 1987

PROGRAM GOAL:

Develop relationships between the critical paper and board property parameters and how they are achieved in terms of raw material selection, principles of sheet design, and processing conditions.

PROJECT OBJECTIVE:

(1) To improve our capability of characterizing paper and board materials,
(2) to relate measured parameters to end-use performance (especially in the case of Z-direction measurements), and
(3) to relate measured parameters to machine and process variables.

PROJECT RATIONALE, PREVIOUS ACTIVITY, AND PLANNED ACTIVITY FOR FISCAL 1987-88 are on the attached 1987-88 Project Form.

SUMMARY OF RESULTS LAST PERIOD: (April 1986 - September 1986)

(1) The automatic device for measuring the in-plane elastic stiffnesses of paper has been improved mechanically in several ways. Plans are underway for the third generation device which will use the latest technology and "off-the-shelf" components.

(2) The carriage translation on the in-plane robotic system is now driven by a magnetic linear motor resulting in a great reduction in maintenance.

(3) There also have been a number of software changes in the automatic device. These include specific software for testing handsheets and changes in the reporting format for the polar data results.

(4) The apparatus for measuring the out-of-plane specific stiffness has been automated, significantly reducing operator time. There have been other improvements in transducer design.

(5) A Fourier analysis capability was added to the automated ZD system.

(6) A study of rubber to sample coupling was undertaken. This could lead to loss tangent measurements on paper at high loading pressures.

(7) Work is underway to elucidate those papermaking variables that affect the shape and size of the polar graphs of specific stiffness <u>vs.</u> angle. During the past period we have been studying (1) CD profiles, (2) the effects of drying restraints, and (3) stress relaxation of the sheets by rewetting.

(8) Work on the impact of refining and yield on the ZD properties is continuing. Recent work has involved measurements of single fiber transverse modulus.

(9) A device which will be able to measure specific scattering coefficients in heavy board materials is being designed and constructed.

(10) A paper "Automatic Determination of Ultrasound Velocities in Planar Materials" (Technical Paper Series 181) was submitted to Ultrasonics for publication.

(11) A paper "Elastic Properties, Paper Quality, and Process Control" (Technical Paper Series 186) was written for publication in Tappi.

(12) A paper "Roughness Anisotropy in Paper" (IPC Technical Paper Series 190) has been submitted to J. Pulp and Paper Science.

SUMMARY OF RESULTS THIS PERIOD: (October 1986 - March 1987)

(1) Construction of the instrument for measuring scattering coefficients in heavy board materials is now underway.

(2) Work on the variables which affect polar diagrams is continuing with measurements on carton boards and a study of the z-direction distribution of properties.

(3) A new in-plane robotics system is under construction using commercially available robots and electronics. IPC will supply software to member companies upon request.

(4) Work to automate the out-of-plane shear measurements is nearly complete.

(5) Work with z-direction loss measurements suggests that they may be useful for establishing ply bond failures in multiply boards.

(6) A paper describing the effect of transverse slice flows on sheet properties was written for presentation at the TAPPI Process Control Conference in March, 1987. (Appendix 1).

(7) The paper concerning the use of microwave attenuation as a measure of fiber orientation anisotropy was published in TAPPI 70(2):109(1987). (Appendix 2.)

(8) In student work, Brian Berger is making good progress on his thesis concerning the relationships between transverse fiber properties and z-direction sheet properties.

PROJECT TITLE: Process, Properties, Product Relationships	Date: 1/14/87
PROJECT STAFF: G. Baum, C. Habeger	Budget: $200,000
PRIMARY AREA OF INDUSTRY NEED: Properties related to end uses	Period Ends: 6/30/88
	Project No: 3467

PROGRAM AREA: Performance and Properties of Paper and Board

PROGRAM GOAL:

Develop relationships between the critical paper and board property parameters and how they are achieved in terms of raw material selection, principles of sheet design, and processing conditions.

PROJECT OBJECTIVE/GOAL:

(1) To improve our ability to characterize paper and board materials,
(2) to relate measured parameters to end-use performance,
(3) to relate measured parameters to machine and process variables.

PROJECT RATIONALE:

It is important to understand the relationships between process variables, end-use performance, and paper and board properties in order to improve these products or maintain performance within close tolerances while effectively utilizing available raw materials, minimizing energy requirements, and minimizing environmental impacts.

RESULTS TO DATE:

The major areas of activity and results can be separated into three areas: development of instrumentation; the impact of process variables on elastic properties; and the relationships between elastic properties and the end-use performance of paper. Ultrasonic techniques and instruments have been developed which enable us to measure all four of the in-plane elastic stiffnesses of paper and three of the five out-of-plane elastic stiffnesses. These instruments also are suitable for measurements on other planar materials. Some of the equipment has been automated, so that the measurements are carried out under computer control, appropriate calculations made, and the results printed out in a report format. A soft rubber platen caliper system was developed under this project to provide accurate caliper and density measurements. The ability to measure the three dimensional elastic behavior of paper has led to an extensive study of how process variables affect the elastic response. To date, process variables examined include wood species, pulping method, yield, refining, jet-to-wire speed ratios, wet pressing, wet stretching, drying restraints, and calendering. The effects of coatings, fillers, sheet composition, sheet structure, and environmental factors (temperature and relative humidity) have also been investigated. Several useful relationships between the elastic stiffnesses have been discovered. Finally, the elastic stiffnesses have been shown to be related to a number of the parameters now used to predict end-use performance and/or convertability. The elastic stiffnesses are fundamental properties of a material, and are good indicators of operating conditions on the paper machine and of final product quality. A microwave technique for determining fiber orientation has also been developed.

PLANNED ACTIVITY FOR FY 1987-88:

In recent years this project has been concerned with measuring the elastic properties of paper, and relating these to process variables and end use performance, where possible. These activities will continue in FY 1987-88.

The in-plane and out-of-plane elastic constants will be measured on a representative group of samples made from fibers differing in composition and structure (yield and refining) at different ambient environments. The data will be compared to individual fiber measurements and to use-oriented test results.

A device currently under construction that can measure specific scattering coefficients in heavy board materials will be used to test boards differing in composition and structure.

The use of polar diagrams to evaluate machine operating characteristics will continue.

With respect to instrumentation development, we plan to automate the Z-direction shear measurement apparatus and construct a second generation in-plane automatic system.

We will be working to develop out-of-plane loss measurement techniques. These may lead to non-destructive tests for determining poor ply bonding. We will also study the in-plane loss process using the strip resonance and attenuation techniques.

We will continue the study of the linear transient effect.

A study of formation will be undertaken in Project 3469, which will be complementary to the work in this project.

STUDENT RELATED RESEARCH:

B. F. Berger, Ph.D.-1987, B. J. Berger, Ph.D.-1987, R. R. Willhelm, MS-1988.

Status Report

PROCESS, PROPERTIES, PRODUCT RELATIONSHIPS

Project 3467

INTRODUCTION

This project is moving forward on several fronts. Hence this report is separated into different sections. Section 1 is concerned with polar diagrams and how they are impacted by paper machine process variables. This topic was discussed at some depth in the last report. The current section reviews some of that work and outlines our plans for the near future. Section 2 describes the work planned to update the in-plane measurement system. In the last report we discussed the automation of the z-direction longitudinal measurements and indicated we planned to do the same with the shear measurements. This is near completion and is discussed in Section 3. Section 4 describes some new work concerned with z-direction loss measurements.

SECTION 1. - Polar Diagrams

In the last status report, dated October 21-22, 1986, we discussed how the polar diagrams were obtained and how their shape, size, and angle of inclination to the MD were dependent on paper machine variables such as jet-to-wire speed differentials, wet straining, and drying restraints. Rewetting experiments showed that the angle of inclination was not affected by reducing internal stresses (by wetting the sample) or drying conditions, implying that fiber orientation off the MD, due to transverse flows from the headbox, was solely responsible for the effect. Experiments with specially prepared laboratory sheets, showed that the area enclosed by the polar diagram was related to wet pressing and the general shape to fiber orientation, wet straining, and drying conditions. The "peanut" shape often observed was attributable to CD shrinkage effects. Both of the above experiments, together with data obtained on commercial papers, showed that the geometric mean stiffness, defined as $(E_{MD} \cdot E_{CD})^{0.5}$, was not always a good measure of product quality (or machine operating conditions). A better measure seemed to be the "effective" stiffness, defined as the radius of a circle having the same area as the polar diagram. Figure 1, taken from the last report, illustrates this by plotting effective stiffness vs. geometric stiffness. The latter is typically less than the former. The magnitude of the difference seems to be related to the MD/CD ratio, becoming larger as the ratio increases. For the samples studied, this appears to result from the increasing tendency toward the peanut shape, which leads to a higher anisotropy ratio and an underestimated geometric mean.

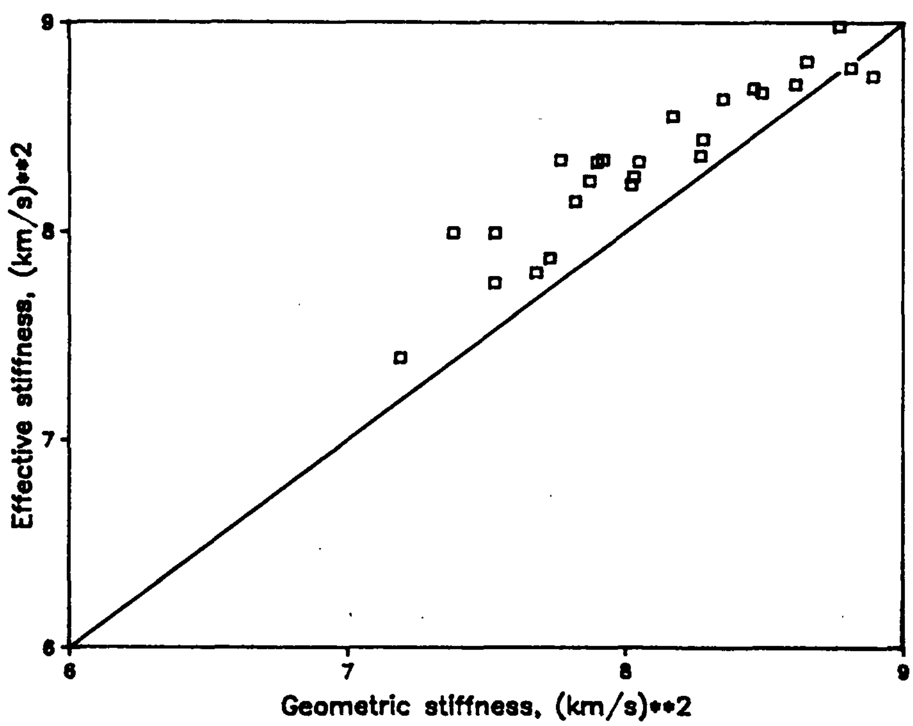

Figure 1. Effective stiffness vs. geometric stiffness.

The work presented in the last status report will be presented at two upcoming conferences. A discussion of how transverse jet flows affect paper properties will be given at the TAPPI Process Control meeting in March, 1987.

A copy of the paper prepared for that conference is attached as Appendix A. The work describing how the shape and size of the polar diagrams is affected by machine variables will be given at the 1987 International Paper Physics Conference in Mont Gabriel in September.

Current work in this area includes:

(1) Measurements on carton boards, to examine cylinder machine formers and to ascertain, if possible, the impact of multilayered structures on the polar diagrams. Figure 2 illustrates one such diagram. Note the high stiffness ratio and the necking down in the CD.

(2) Measuring polar diagrams as a function of z-direction on the special laboratory sheets described in the last report. This involves grinding away the surface(s) of the sheets in a controlled fashion.

(3) Measurements of z-direction properties as a function of CD direction to go along with the polar diagram information.

Future work planned in this area includes measurements of polar diagrams on CD strips of commercial samples. Letters have been written to companies producing fine papers or board, requesting such samples. This work would involve:

(1) Measurements on CD strips before and after the slice screws have been adjusted in known ways.

(2) Measurements on CD strips in which the machine speed has been changed in a series of steps.

In order to better understand the nature of machine operations or manufacturing conditions on the CD profiles of polar diagrams, we are interested

THE INSTITUTE OF PAPER CHEMISTRY
LONGITUDINAL SPECIFIC STIFFNESS (VEL SQR) VS ANGLE TO MD

OPERATOR: D BRENNAN
PROJECT : 3467

DATE :2 16 87
SAMPLE : CB 2

ANGLE DEGREES	VEL SQR KM2 / SEC2	STD DEV	ANGLE DEGREES	VEL SQR KM2 / SEC2	STD DEV
0	9.35	.33	90	2.87	.11
5	9.40	.28	95	2.82	.13
10	9.25	.25	100	2.79	.10
15	8.87	.29	105	2.78	.10
20	8.15	.28	110	2.85	.10
25	7.40	.26	115	2.98	.08
30	6.67	.19	120	3.16	.09
35	5.93	.19	125	3.39	.07
40	5.32	.15	130	3.64	.08
45	4.69	.13	135	3.93	.04
50	4.11	.15	140	4.45	.09
55	3.74	.09	145	5.04	.11
60	3.46	.07	150	5.64	.13
65	3.24	.07	155	6.31	.12
70	3.06	.09	160	7.08	.18
75	2.94	.10	165	7.87	.16
80	2.90	.07	170	8.61	.23
85	2.86	.10	175	9.09	.28

TEST PER 5 DEGREE INCREMENT = 8
SIGNALS AVERAGED = 6
THE ANGLE TO MAJOR PRINCIPAL AXIS = 3.6
STIFFNESS RATIO = 3.26
AREA (KM^4/SEC^4) = 101.1

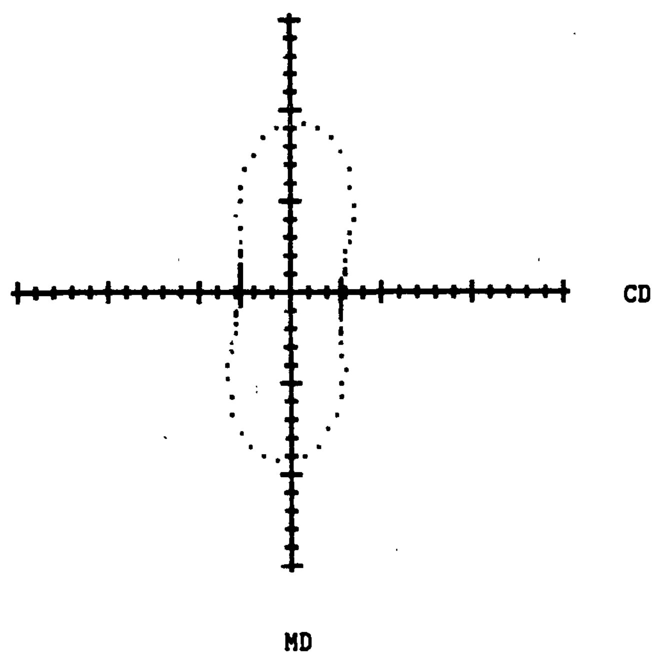

PLOT OF VEL SQR VS ANGLE AS SEEN FROM FELT SIDE

Figure 2. Ultrasonic polar diagram of multilayered board.

in any "before and after" CD strips that your company may have that may help us expand our knowledge. We would urge you to discuss these with us.

SECTION 2 - In-Plane Robotics System

The next version of the in-plane automatic system will be constructed around a Mitsubishi model RM-501 Move Master II. This is a small robot of appropriate size to transport the ultrasonic transducers over a sample. The transducers will be mounted in a custom built "end effector". Through pneumatic control, the end effector will (1) position the transducers at either of two separations, (2) rotate the transducers about their axes for shear and longitudinal mode generation, (3) provide individual ball bushing mounts for the transducers so that sheet loading is determined by dead weights regardless of caliper, and (4) provide positive feedback for transducer displacement and rotation. The end effector will bolt to the end of the robotic arm. The robot will translate the end effector in three dimensions, scanning the transducers over the sample and applying the probes to the sample. Through a "wrist rotation" the robot will also orient the end effector for measurement at arbitrary angle to the machine direction. A preliminary design of the end effector has been negotiated with Johnson Scale Co., who will provide the robot and build the first end effectors. Two systems are planned, one for the Institute and one for a member company which is collaborating closely on this effort. Delivery of robot and end effector is expected about the end of May, 1987. Some of the advantages of robotic design are: (1) standard mechanical construction which could be duplicated by member companies through a third party; (2) the versatility to test multiple sheets located around the periphery of the robot or to automatically test a roll of paper fed under the arm; and (3) dead weight loading of the transducers.

To further ease technology transfer to member companies, the electronics will be configured from off-the-shelf instruments. There will be some minor custom wiring, but duplicating a system should be very easy. Also, we are upgrading the computer from an Apple IIe to an IBM AT. This increases the speed of operation, eases programming and raises the complexity of possible operations. We are already developing software and expect to be well along when the robot and end effector are received. Once we are happy with our system, we plan to provide software and instructions for assembly to interested member companies. Total present cost of a system is about $30,000 (~$16,000 for robot, controller and end effector, ~$12,000 for electronics, and ~$2,000 for surprises).

SECTION 3. - Automation of Out-of-Plane Shear

Work is nearly complete for an automatic out-of-plane shear cross-correlation velocity and hard platen caliper gage. Special electronics for computer control of probe raising and lowering are in operation and special software has been written. After the technique has been checked out, we will be able to use the digital oscilloscope and IBM AT to make and print out hard caliper and shear velocities. This will improve the quality of the velocity determination, speed data taking, and automate reporting.

SECTION 4. - Out-of-Plane Ultrasonic Loss Measurements

The development of the broadband Kynar transducers (described in the last two PAC reports) gives us the opportunity to make out-of-plane loss measurements as well as the normal velocity measurements. A single, well-defined pulse can now be sent through a sample, and its amplitude can be related to loss processes in the sample. Knowing the velocity of sound propagation and density of the sample and the acoustic properties of the rubber which couples energy into and out of the sample, the energy reflected at the rubber-sample interfaces can be determined and the losses due to sound propagation can be calculated (see last PAC report). The fly in the ointment here is that the calculation of the reflected energy depends on the assumption of "perfect coupling" between the sample and the soft rubber. Less than perfect coupling leads to greater than calculated interface reflections and an over estimate of the loss through the sample. We have demonstrated in a number of ways that the interface between the sample and rubber affords less than perfect coupling at low loading pressure (~50 kPa), but improves rapidly as the mechanical load is increased. Figure 3 is one such demonstration. The time difference in the 0.98 MHz frequency component of the signal in going through a thick (42 μm) and a thin (8 μm) aluminum foil is plotted versus loading pressure and compared to the formula derived from the perfect coupling assumption. Notice that for these rigid, smooth samples surface cleanliness can also have dramatic effects. Usually poor coupling leads to large decreases in signal amplitude and very small changes in signal transit time. Very thin foil is a special case in which this situation is reversed.

Most of the effort over the last six months has been toward accounting for less than perfect coupling. However, as this is of a very specialized technical nature and as the results are inconclusive, this work is not presented at this time. Instead improvements in the technique and possible practical applications are discussed.

An important recent enhancement to the automated out-of-plane system is the addition of a fast fourier transform capability to the data analysis

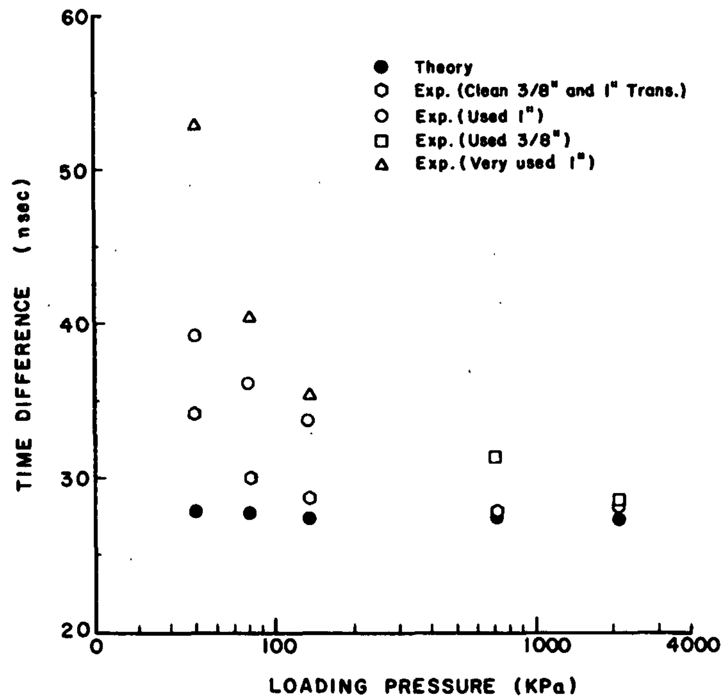

Figure 3. The effect of loading pressure on the time shifts through thin aluminum foils.

system. This allows the sample and reference signals to be broken into sinusoidal components and their relative amplitudes and phase shifts to be compared as a function of frequency. In addition to the cross correlation velocity determinations (discussed in previous PAC reports), meaningful amplitude ratio and phase velocities are routinely printed out for a discrete set of frequencies between 0.5 MHz and 2 MHz. The attenuation coefficients (α) and loss tangents ($\tan\delta$) are calculated at each frequency, assuming perfect coupling.

One way to assess the ability of this system to make accurate loss measurements is to test samples whose viscoelastic parameters can be determined independently. This was done for polystyrene, a brittle low-loss plastic, and Kynar, a very lossy plastic. Modulus and loss tangent were determined by comparing signals through samples of different thicknesses. This cancels out the effects of poor coupling. Figure 4 and 5 show the loss tangent results on single samples at 1.220 MHz, assuming perfect coupling. The loss tangent in polystyrene as determined by multiple samples is 0.0012, with a standard deviation of 0.0014, while tanδ for Kynar at 1.22 MHz is 0.076 ± 0.006. Notice that on these smooth samples the calculated loss tangents are within about 0.01 of these values at high loading pressures. The effect of surface roughness is also demonstrated on these plots. Grooves of approximately equal depth, width, and separation were cut into both sides of separate plastic discs. The results for 0.5 mil, 1.0 mil, and 2.0 mil deep grooves are presented. Surface roughness on these rigid samples obviously has a deleterious effect that abates at high loading pressure.

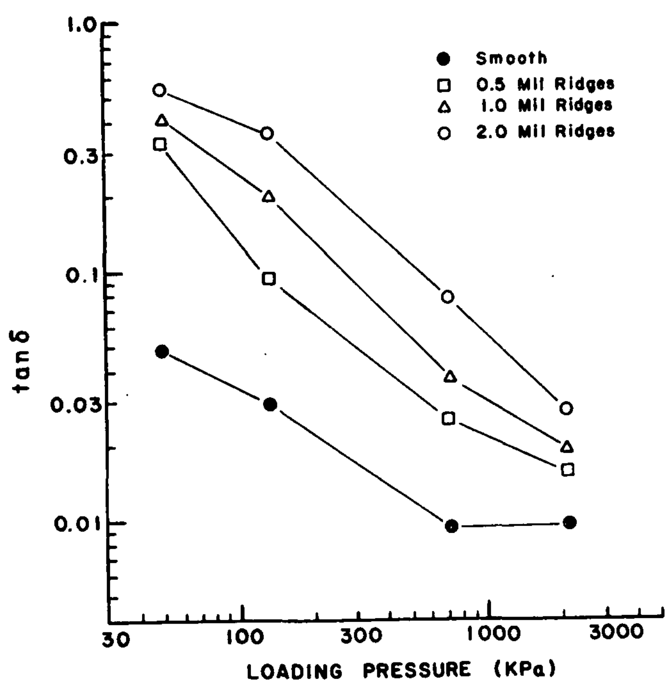

Figure 4. Loss tangent measurements in polystyrene.

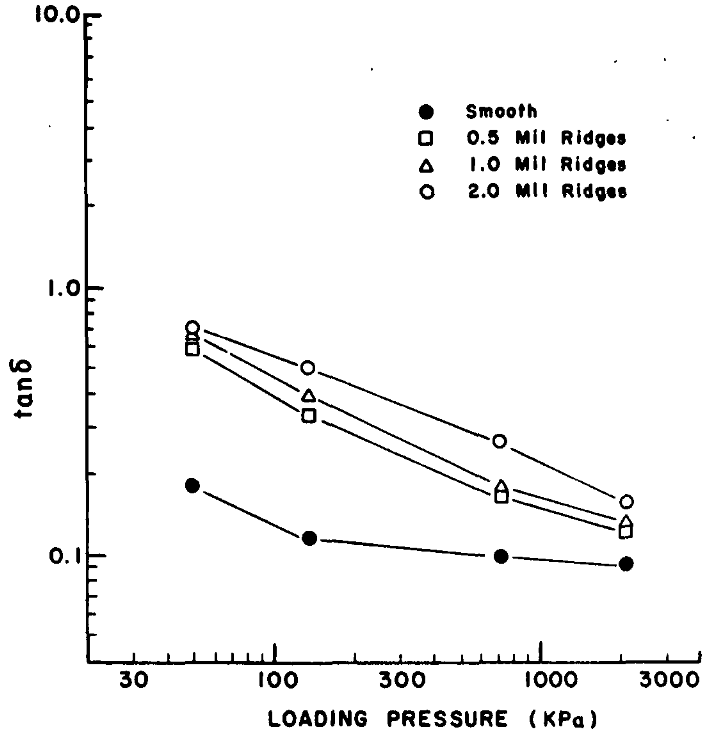

Figure 5. Loss tangent measurements in Kynar.

The effects of poor coupling and the meaning of loss measurements are tougher to assess on paper samples. It is difficult to obtain identical sheets of different thicknesses in order to cancel out coupling effects; loading pressure consolidates the structure thus increasing velocity and decreasing loss significantly; and surface roughness cannot be independently varied. Since the calculated loss coefficient increases rapidly with loading pressure, especially on rough surfaces, we expect the error from coupling to be significant at the 50 kPa standard pressure. Also the cellulose fibers are more conformable than the plastic and the deterioration from surface roughness should be less pronounced than with the plastic disks. Readings at the higher pressures probably measure loss processes in the sheet. One should keep in mind that at higher pressures, out-of-plane velocity and loss tangents values are more of a function of cell wall properties, less dependent on structure, and less affected by process variables.

There is more than one parameter that can be used to characterize loss in paper. The attenuation coefficient, α, is the natural log of the amplitude ratios at two locations along the wave divided by their separation. This is a measure of loss per unit distance of propagation. The loss tangent is $\alpha\lambda/\pi$, where λ is the wavelength and is a measure of the loss per wavelength. As velocity increases or frequency decreases, $\tan\delta$ increases at constant α. For out-of-plane properties of paper, it is often wise to define parameters in terms or basis weight rather than of caliper. In this case, the logical choice is the natural log of the amplitude ratio divided by the basis weight traversed. This is α/ρ, the natural log of amplitude ratios of signals separated by unit basis weight. Since α/ρ is a pure attenuation and is mass specific, we think in most cases it is the best indicator of loss in paper in the ZD.

The influence of process variables on our ZD loss measurements was investigated by testing samples (made by Brian Berger for his thesis research) having a common furnish but variable wet pressing, refining, and yield. The effect of refining at 1.22 MHz and at four loading pressures is presented in Fig. 6. Here α/ρ is plotted versus density measured at the loading pressure of the test. In analyzing these results keep in mind the following points: (1) low loading pressure results are inflated by poor rubber to sample coupling; (2) high pressure results probably are good indicators of losses in the sample; and (3) out-of-plane mechanical properties are generally dependent on loading pressure.

The high loading pressure decrease in α/ρ with refining is partially due to the reduction in scattering sites with densification. Since scattering increases rapidly with frequency, this conclusion is supported by results (not shown) at lower frequencies where the effect is much smaller. The α/ρ decrease with refining at low pressure is less frequency dependent and is more a result of changing surface conditions. Another interesting point brought out by Fig. 6 is that changing density with loading pressure decreases α/ρ much faster than changing density by refining. The effects of wet pressing and yield on α/ρ were very similar to those of refining. In fact when compared at common density α/ρ seems independent of process. Figure 7 is a plot of all the data. Notice that there is roughly a single curve for each loading pressure.

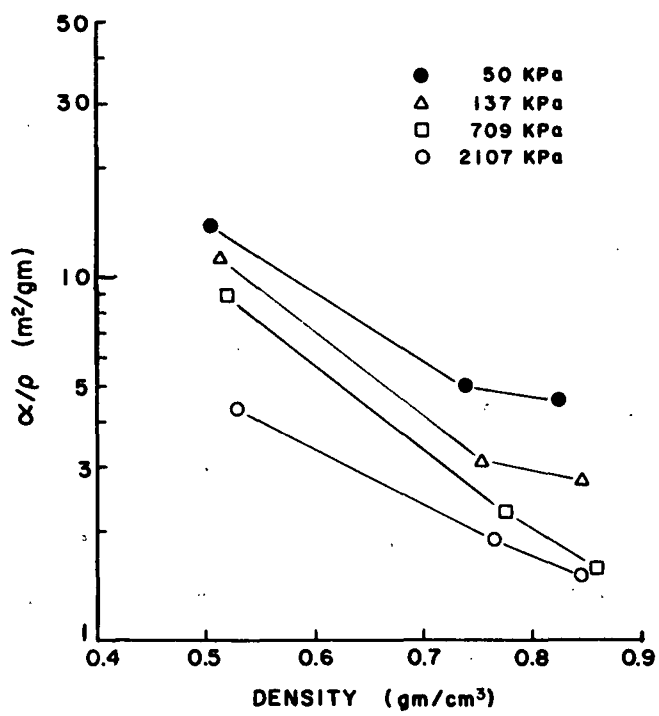

Figure 6. The effect of refining on α/ρ.

The sensitivity of the loss determinations to poor interface coupling at low loading pressure is a feature that might be used to advantage. In the past, we have found that out-of-plane longitudinal velocity correlated well with ZD tensile in homogeneous sheets. However, in multiply sheets, the velocity is relatively insensitive to properties in the thin interface regions where failure

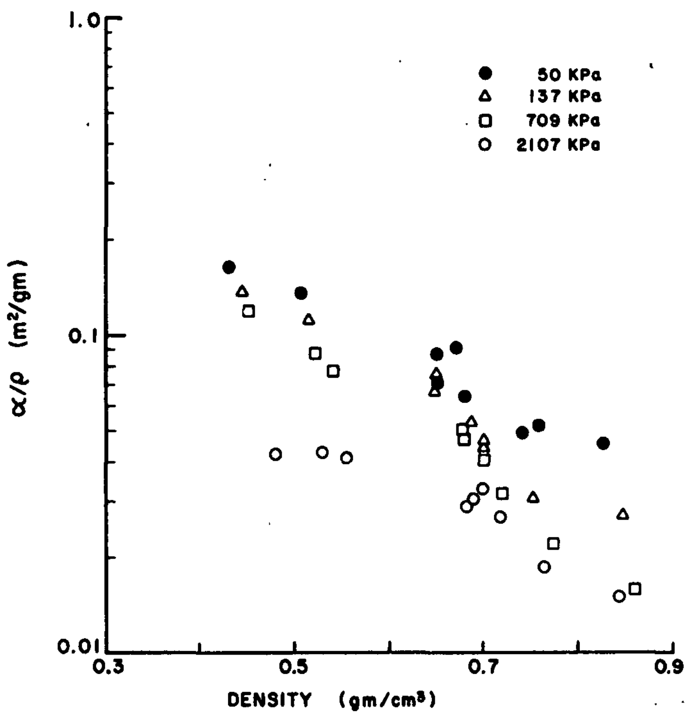

Figure 7. The effect of refining, wet pressing, and yield on α/ρ.

occurs. These interfaces could result in acoustic losses by the same mechanisms as at the boundaries and α/ρ might be a non-destructive predictor of ZD tensile strength in multiply sheets. To test this we damaged multiply sheets and looked at the effect on velocity and loss. Figure 8 and 9 show the results of bending a chipboard sample and a multilayer Fourdrinier sample around a 3-inch diameter and over a sharp edge. The results are plotted as α vs. loading pressure*. The out-of-plane longitudinal velocities are also given. Notice that damaging the sheet both lowers the velocities and raises the loss by an amount that decreases with loading pressure. This is consistent with the earlier conjecture that loss measurements are less influenced by interface conditions at high loading pressure. For small loads, loss and velocity both

*We could have used α/ρ here and, as ρ decreases a bit with bending, the conclusion would have been stronger.

reflect the damage done to the sheet; however, the relative effect is significantly greater in loss, especially for the milder treatment. The ZD tensile values for these sheets in kPa are chipboard (375, 303, and 279) and Fourdrinier board (304, 303, and 217).

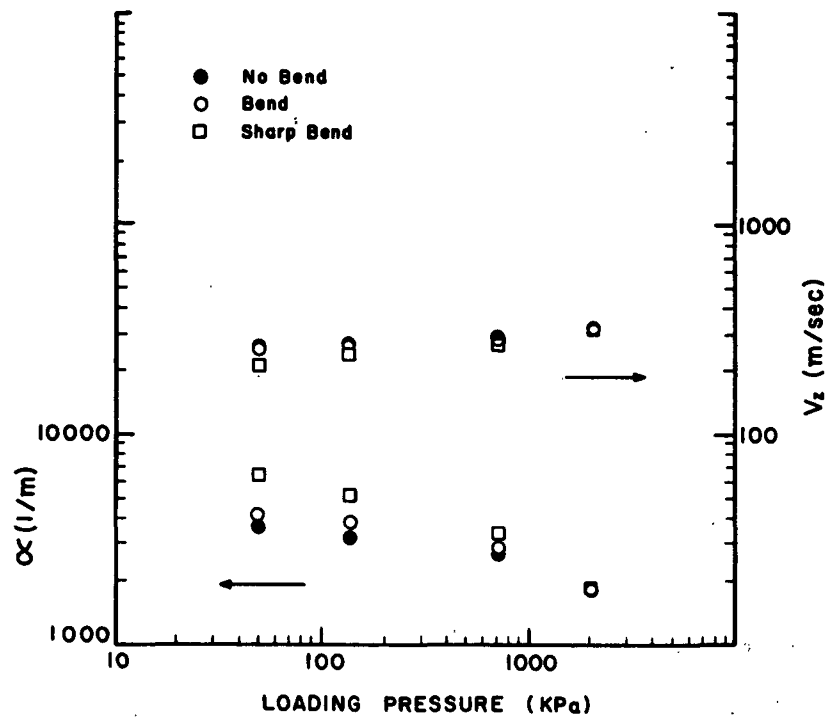

Figure 8. Acoustic measurements on damaged chipboard.

As another check of the possibility of relating loss to ZD tensile in multiply sheets, we made measurements on some multiply sheets that Roger Van Eperen had collected from different manufacturers. Tests were run on three samples of an eight layer clay coated newsprint, three samples of an eight layer clay coated kraft, and three samples of seven layer chipboard. Remember these are all from different companies and this is a rather severe test. The results obtained at 50 kPa loading pressure are in Table I. The correlation coefficient, R, between each parameter and ZDT is in the fourth row of each group.

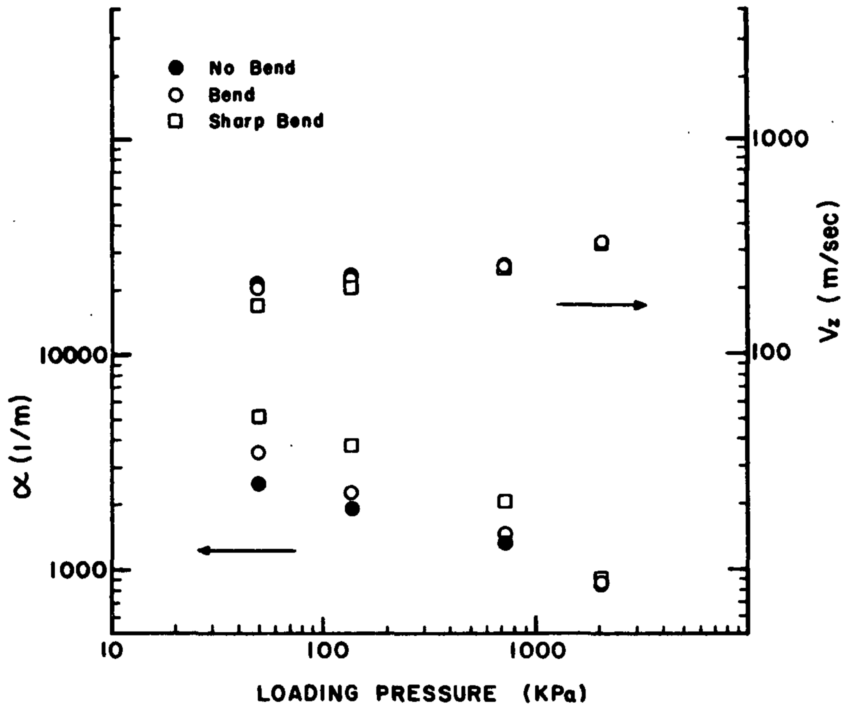

Figure 9. Acoustic measurements on damaged multilayer board.

The first group, clay coated kraft, is very well behaved: ZDT correlates well with density, ρ, out-of-plane velocity, V^2, and the α/ρ correlation coefficient is out-of-sight. The clay coated news correlates negatively with ρ and not at all with V^2, but the α and α/ρ results are not bad. In the chipboard series, the last sheet is a real maverick and messes up everything. It is of relatively high density, high velocity, and low loss; however, it's ZDT is low. The correlations between ZDT and the acoustic parameters were checked at the higher loading, and, as expected, the correlations were not as good.

Admittedly the results showing that acoustic loss is a practical indicator of ZDT in multiply sheets are very preliminary. However, we think it deserves further study and we would appreciate some real life problems to try our hand at.

Table 1. Acoustic parameters and ZD tensile.

Sample	ρ gm/cm^3	V^2 m/sec	α 1/m	α/ρ m^2/gm	ZDT kPa
Clay Coated Kraft					
1	0.788	250	42.3	5370	483
2a	0.684	212	42.4	6200	348
2b	0.765	192	46.6	6090	355
R to ZDT	(0.704)	(0.924)	(-0.478)	(-0.997)	
Clay Coated New					
1	0.722	266	38.7	5360	424
2a	0.756	245	31.3	4140	429
3b	0.714	255	25.3	3540	495
R to ZDT	(-0.598)	(-0.090)	(-0.867)	(-0.793)	
Chipboard					
6a	0.762	240	44.8	6180	417
6b	0.690	234	44.1	6390	384
7a	0.705	265	36.7	5210	341
R to ZDT	(0.506)	(-0.807)	(0.932)	(0.817)	

APPENDIX 1

TRANSVERSE JET FLOWS AFFECT PAPER PROPERTIES

G. A. Baum
Director
Paper Materials Div.
The Institute of
Paper Chemistry
P.O. Box 1039
Appleton, WI 54912

D. G. Brennan
Research Fellow
The Institute of
Paper Chemistry
P.O. Box 1039
Appleton, WI 54912

ABSTRACT

Measurements of specific elastic stiffness as a function of angle from the machine direction (MD) provide information about operating conditions on the paper machine. The shape and size of the resultant polar diagrams are related to headbox operation, jet-to-wire speed ratios, stretching of the web in open draws, and MD and CD drying restraints. This paper discusses how conditions at the slice, viz. jet-to-wire speed ratios and transverse slice flows from the headbox, affect the measurements. It appears that such information will be instrumental in improving headbox design and minimizing CD variations in paper mechanical properties.

INTRODUCTION

A considerable amount of work has been done at the Institute of Paper Chemistry in the last seven years to measure the orthotropic elastic stiffnesses of paper both in the laboratory and on the paper machine[1-4]. The elastic stiffnesses are sensitive indicators of paper machine operating conditions, and, in many cases, can be directly related to end use tests now used to characterize the paper[5]. A recent development is the ability to easily measure specific elastic stiffnesses as a function of angle from the machine direction. The instrument, described in detail elsewhere[6], is capable of measuring the longitudinal specific stiffness (related to C_{11} and C_{22} or the Young's moduli E_{MD} and E_{CD}) or the shear specific stiffness (related to C_{66} or G_{MD-CD}). Figure 1 shows a typical output from the instrument. The table at the top of the figure gives the angle from the machine direction and the corresponding value for the specific elastic stiffness (stiffness divided by density) and the standard deviation of the measurements (16 in this example) at each angle. The lower part of the figure plots the results as a polar graph, showing how the values change as a function of angle. The major axis of the generally elliptical shape is computed and the angle it makes from the MD is determined. The area of the ellipse is also calculated.

The shape and area of the polar diagrams typically vary across the width of the paper machine. These variations have been shown to be related to changes in the level of fiber orientation, of the wet paper web in open draws, and non-uniform drying conditions in the web[7]. In this paper we are primarily concerned with variations in the inclination of the major axis of the ellipse with the machine direction (MD) of the paper.

RESULTS

Figure 2 shows two laboratory sheets made from the same furnish and having the same nominal basis weights. The circular shape is the result obtained for a handsheet made on a Noble and Woods machine, for which the fiber orientation would be expected to be random (no preferred fiber orientation). The elliptical shape was obtained for a sheet made in a Formette Dynamique anisotropic sheet former, in which there is some fiber orientation along the machine direction. The ratio of the stiffnesses along the MD compared to the CD for this latter case is about 1.4. Clearly the elliptical shape is related to the extent of fiber orientation in the paper. It is also related to the extent of wet straining[7].

In Figure 2 the major axis of the ellipse for the Formette sheet is exactly along the MD. Figure 3 is a similar polar diagram for a commercial sheet in which the major axis is about 12 degrees clockwise from the MD. This angle of inclination is believed to be caused by jet flows from the headbox which have a transverse component, that is, a component of flow that is at right angles to the MD. Such transverse flows apparently deposit fibers onto the paper machine wire that have a preferred orientation at some angle to the MD.

In our experience such behavior is quite common. To date we have made measurements on numerous CD strips from many paper machines manufacturing a variety of grades. In most cases there is some angular offset of a few degrees, which typically varies from point to point across the paper machine. In severe cases, the angular displacement may be as large as plus or minus 15 degrees. In such cases, it is not unusual to experience some difficulty during a subsequent converting operation or end-use application. Figure 4 shows angle from the MD versus position for four CD strips taken from the same machine. In our experience the profile or pattern for a given machine seems to make a fairly reliable "fingerprint" of that machine. We plan to study, however, several factors which we believe should change the observed profile. There does not seem to be any common pattern in the measured CD profiles of angular displacement from machine to machine.

Experiments were conducted to determine if the observed angular displacement was a result of a maximum in the fiber orientation distribution not along the MD, or if drying conditions were also important. Commercial sheets of linerboard and fine paper having polar diagrams in which the major axes were noticeably off the MD were soaked in water for 24 hours, dried with no restraint, and remeasured. Figure 5 shows the initial and final polar diagrams for two of these sheets. In the top of the figure, A and B are the linerboard results before and after rewetting, respectively. There is very little change in the angle of inclination but a large change in the enclosed area. The linerboard sample had an initial clockwise displacement from the MD of 3.8 degrees with an enclosed area of 315 $(km/s)^4$. After rewetting and drying the angular displacement was about 4.4 degrees with an area of only 210 $(km/s)^4$. In the lower part of Fig. 5, before and after rewetting results are shown for the fine paper. In C, the original diagram shows a counterclockwise angular displacement of 8.4 degrees with an area of 214 $(km/s)^4$. In D, after rewetting, these two values are 8.2 degrees and 181 $(km/s)^4$, respectively. The rewetting and drying seems to have little effect on the angular displacement of the polar diagram, but a substantial effect on the area. These results are consistent with the notion that the angle of displacement from the MD is a result of fiber orientation effects, while the area of the diagram is affected by the fiber orientation, wet pressing, and drying conditions. Any stresses dried into the paper would be expected to be relieved by the rewetting so that the area should decrease, as observed. The release of such stresses, however, would not be expected to affect the distribution of the fibers.

Similar experiments were carried out on other specimens. Figure 6 shows the angle of the major axis of the elliptical diagram before and after rewetting for four specimens taken from a single CD strip of fine paper. The results fall along the one-to-one correspondence line, again indicating no change in the angular displacement of the polar diagram. For each of the specimens, however, the areas of the diagrams after rewetting are substantially less than the original areas.

Figure 7 shows the anisotropy ratio (MD/CD ratio) of the measured elastic stiffnesses, for the same four specimens, before and after rewetting. The ratio after wetting is slightly larger than before wetting, but the values are close to the one-to-one correspondence line. Even though both the MD and CD stiffnesses have decreased substantially with the rewetting, these results suggest that the changes in the two directions are about the same on a percentage basis. An increasing anisotropy ratio with rewetting would imply that the decrease in the CD was larger than in the MD, a reasonable situation.

CONCLUSIONS

The angle of inclination of a polar diagram of specific elastic stiffness seems to be due to a fiber orientation in which the maximum of the distribution is not along the MD. This behavior can most easily be explained as a consequence of jet flows coming from the headbox which have a velocity component in the cross machine direction. That is, at some CD positions, the velocity vector of the jet is not parallel to that of the wire. This understanding, and the ability to measure the polar diagrams across the width of the paper machine easily and quickly (in the laboratory), should lead to improved headbox designs that will eliminate or minimize such transverse flows, resulting in improved product uniformity (or quality) across the machine.

LITERATURE CITED

1. Mann, R. W., G. A. Baum, and C. C. Habeger, Tappi, 63(2):163(1980).

2. Baum, G. A., D. G. Brennan, and C. C. Habeger, Tappi, 64(8):97(1981).

3. Baum, G. A., C. C. Habeger, and E. H. Fleishman, "Measurement of the orthotropic elastic constants of paper", In The Role of Fundamental Research in Papermaking, Transactions of the Cambridge Symposium: September 1981. Mechanical Engineering Publications Ltd., London, 1983.

4. Habeger, C. C., and G. A. Baum, Tappi, 69(6):106(1986).

5. Baum, G. A., "Elastic properties, paper quality, and process control", presented at 1986 Tappi International Process & Materials Quality Evaluation Conference, Atlanta, GA, September 21-24, 1986.

6. Van Zummeren, M. L., D. J. Young, C. C. Habeger, G. A. Baum, and R. Treleven, "Automatic determination of ultrasound velocities in planar materials", submitted to Ultrasonics, 1986.

7. Baum, G. A., "The effect of paper machine variables on polar diagrams of specific elastic stiffness", to be presented at the 1987 International Paper Physics Conference, Mont Gabriel, Quebec, September 15-18, 1987.

THE INSTITUTE OF PAPER CHEMISTRY
LONGITUDINAL SPECIFIC STIFFNESS (VEL SQR) VS ANGLE TO MD

OPERATOR: D BRENNAN
PROJECT : FREE DRYING TEST

DATE 19 17 86
SAMPLE : LB1 (11)

ANGLE DEGREES	VEL SQR KM2 / SEC2	STD DEV	ANGLE DEGREES	VEL SQR KM2 / SEC2	STD DEV
0	11.84	.67	90	4.04	.35
5	11.70	.53	95	4.03	.46
10	11.59	.56	100	4.06	.45
15	11.35	.70	105	4.02	.43
20	10.88	.76	110	4.08	.40
25	9.82	.53	115	4.21	.33
30	9.10	.60	120	4.41	.36
35	8.19	.49	125	4.66	.37
40	7.33	.39	130	5.03	.39
45	6.59	.39	135	5.49	.39
50	5.97	.48	140	5.99	.43
55	5.45	.46	145	6.66	.43
60	5.03	.44	150	7.36	.51
65	4.66	.37	155	8.14	.61
70	4.34	.31	160	9.04	.69
75	4.25	.31	165	9.96	.43
80	4.14	.31	170	10.71	.51
85	4.01	.30	175	11.38	.48

TEST PER 5 DEGREE INCREMENT = 16
SIGNALS AVERAGED = 6
THE ANGLE TO MAJOR PRINCIPAL AXIS = 5.0
STIFFNESS RATIO = 2.93
AREA (KM^4/SEC^4) = 174.4

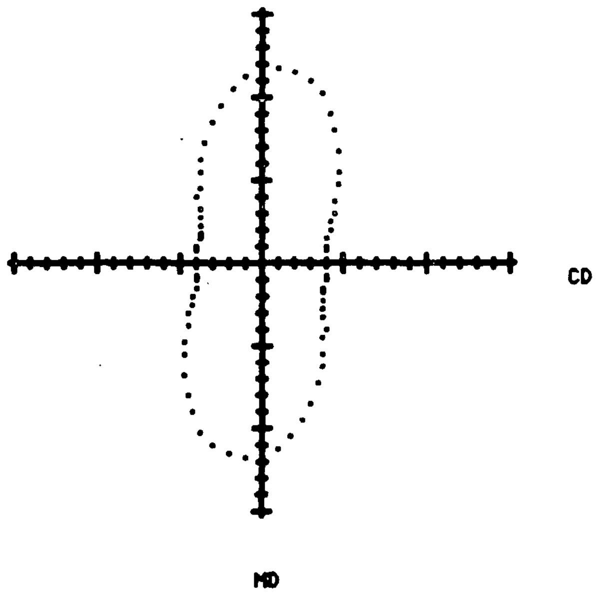

PLOT OF VEL SQR VS ANGLE AS SEEN FROM FELT SIDE

Figure 1. Typical in-plane polar plot.

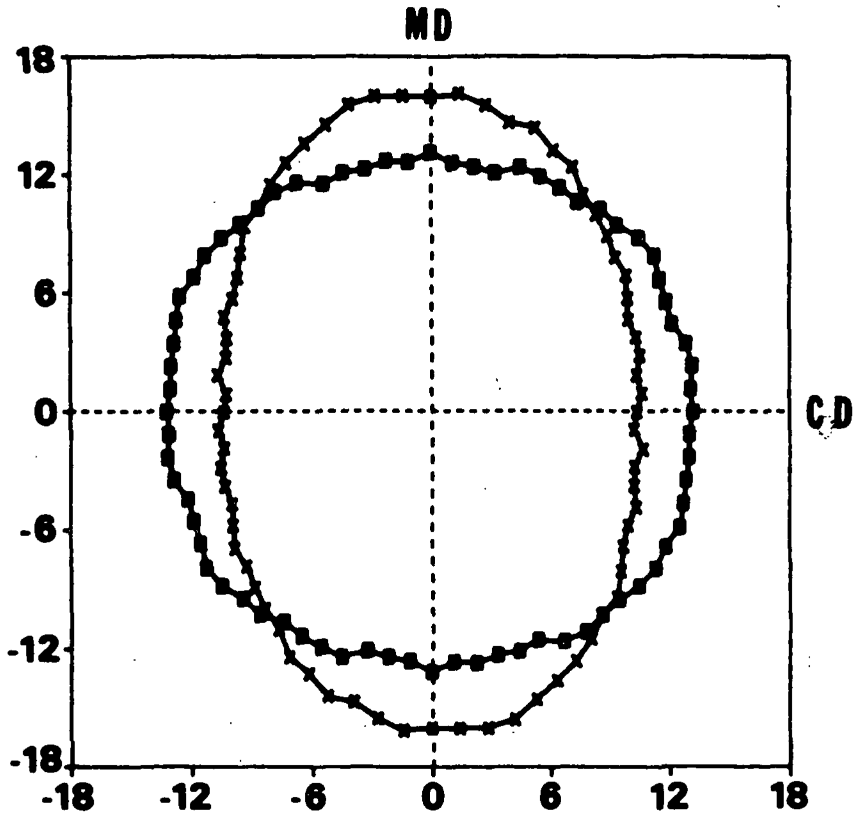

Figure 2. C_{11} measured at various angles to the MD for a handsheet and oriented paper.

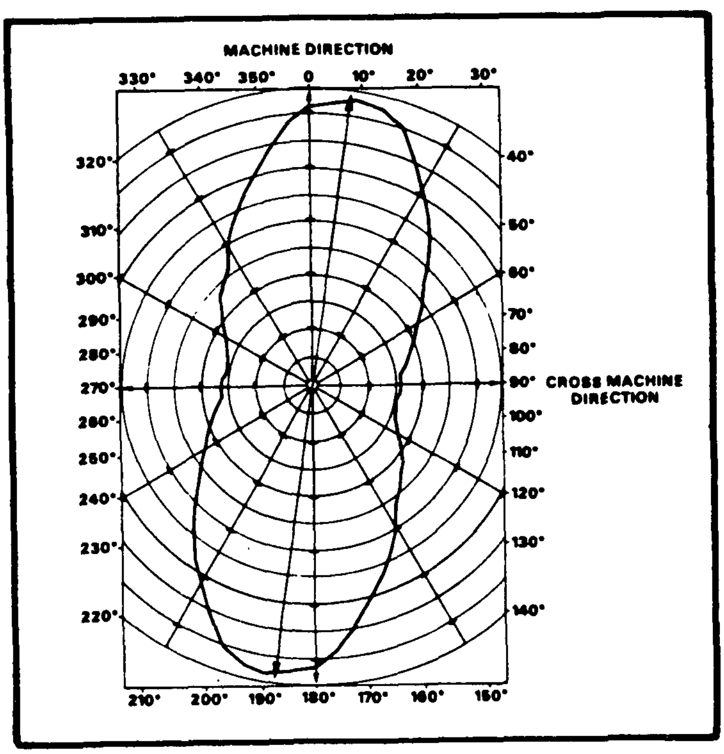

Figure 3. Polar graph of specific stiffness vs. angle.

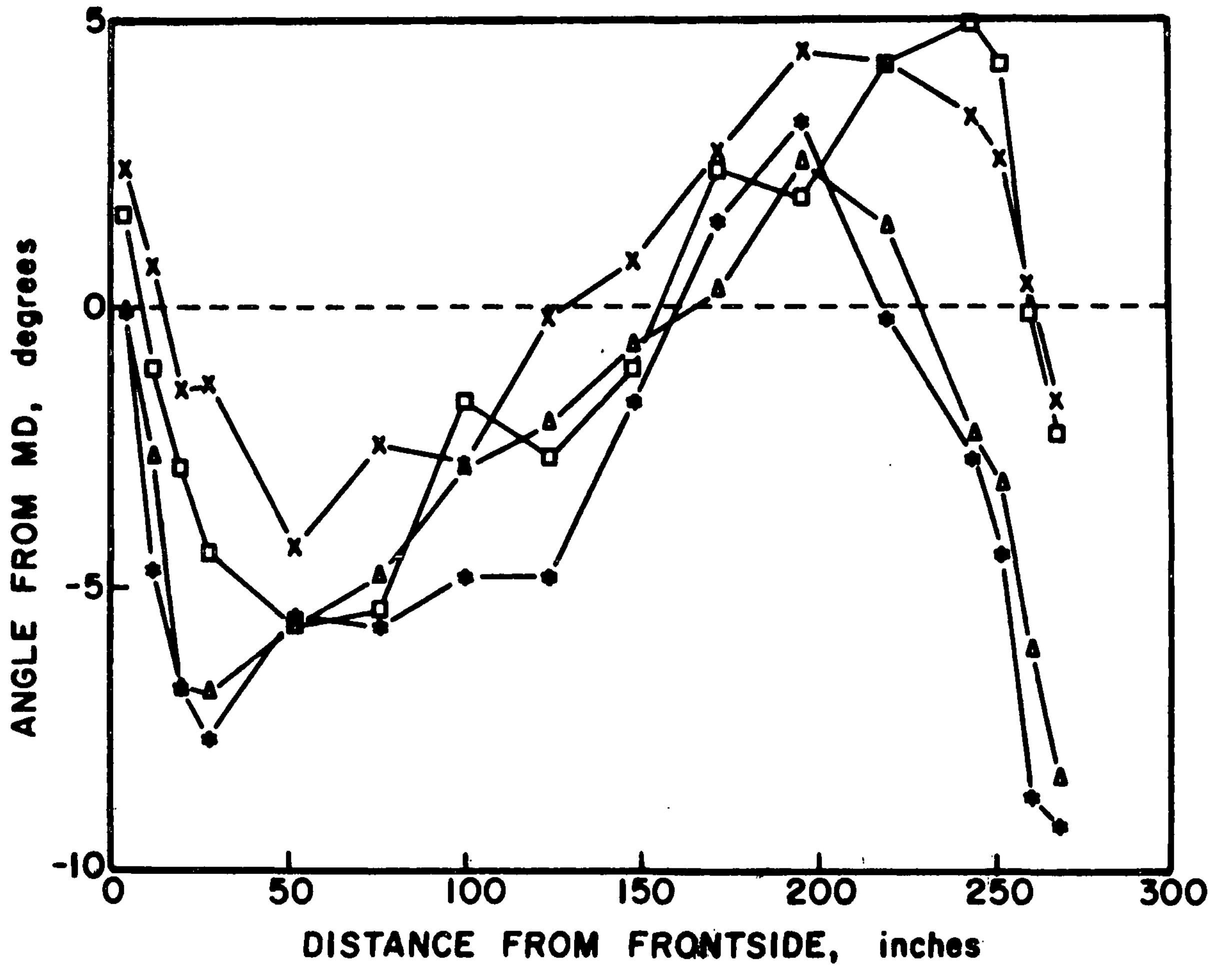

Figure 4. Angular displacement across the paper machine for four scans.

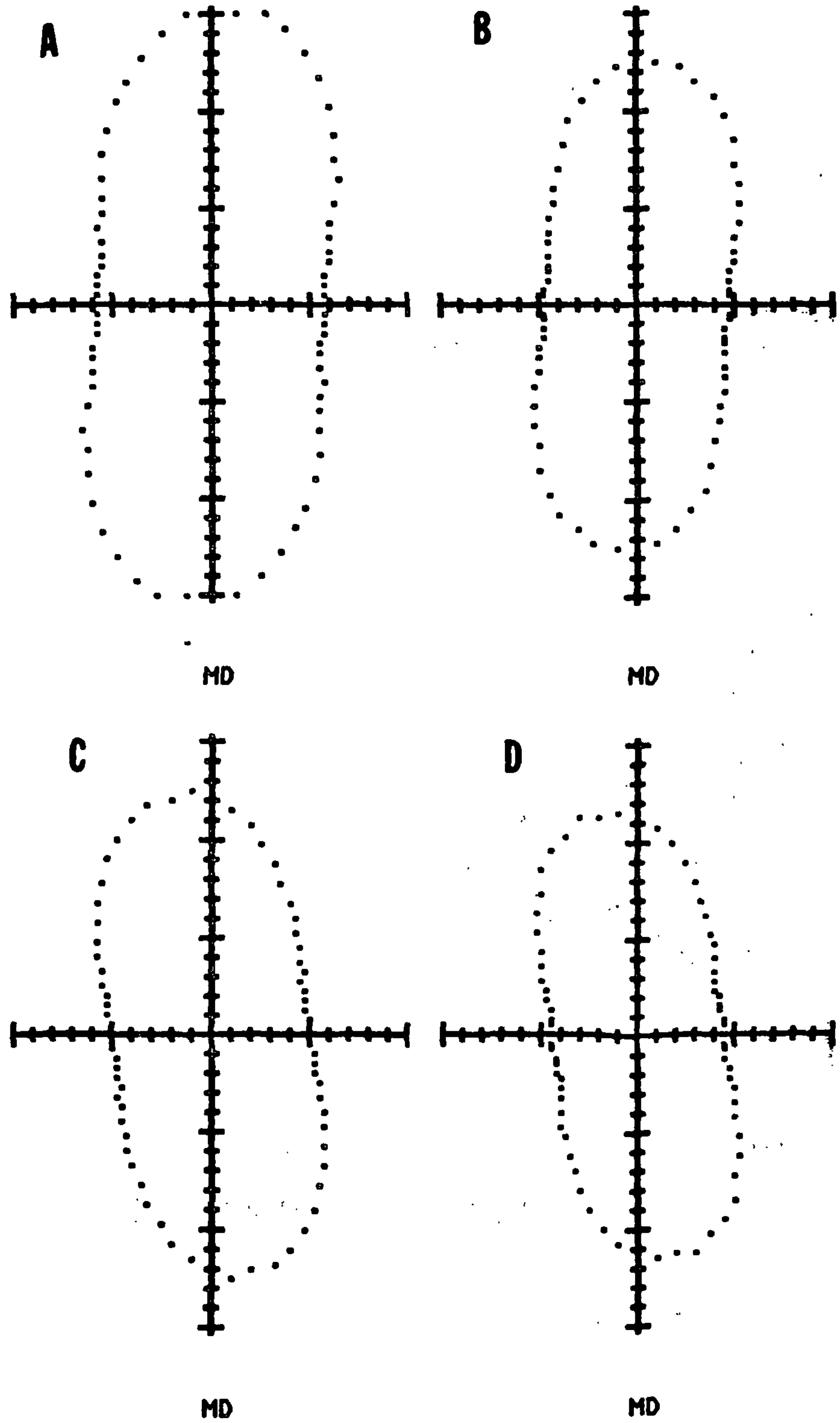

Figure 5. Top: Linerboard before (A) and after (B) rewetting.
Bottom: Fine paper before (C) and after (D) rewetting.

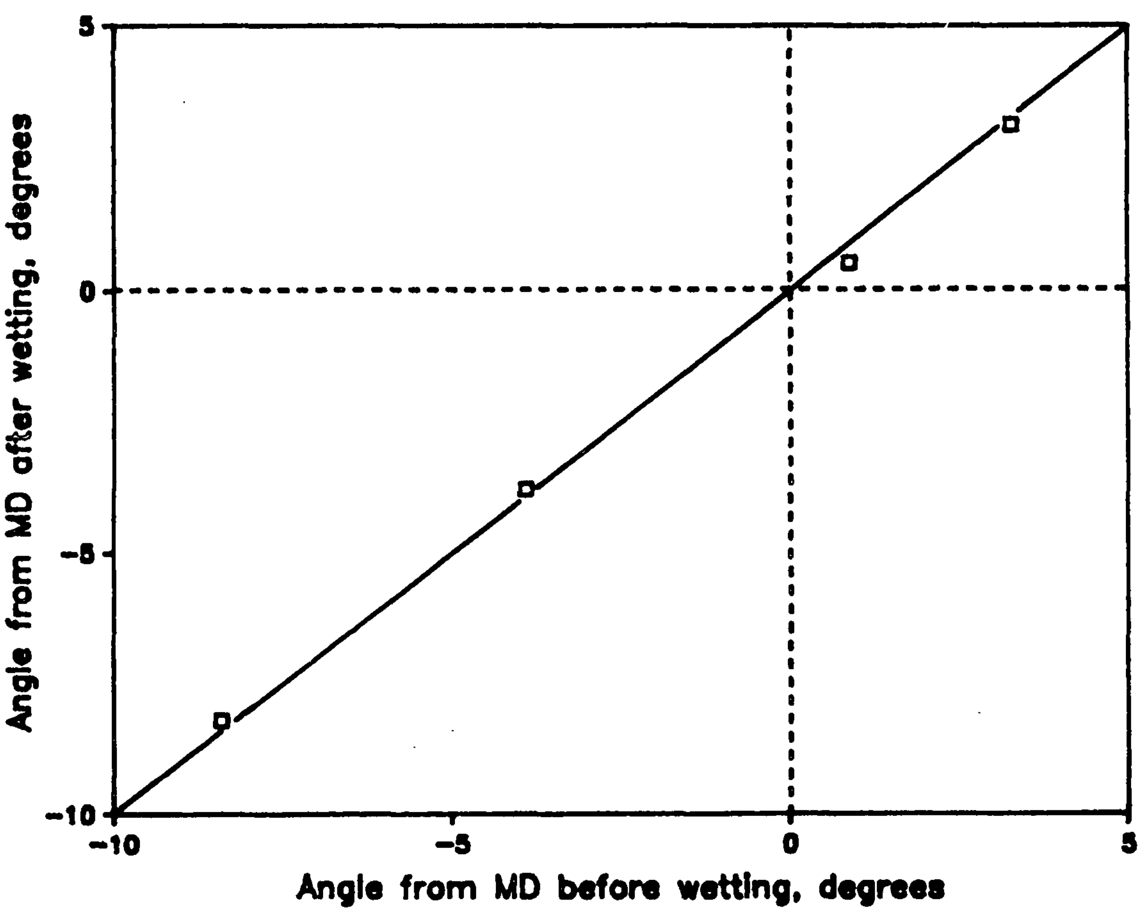

Figure 6. Angle from MD after wetting vs. angle from MD before wetting.

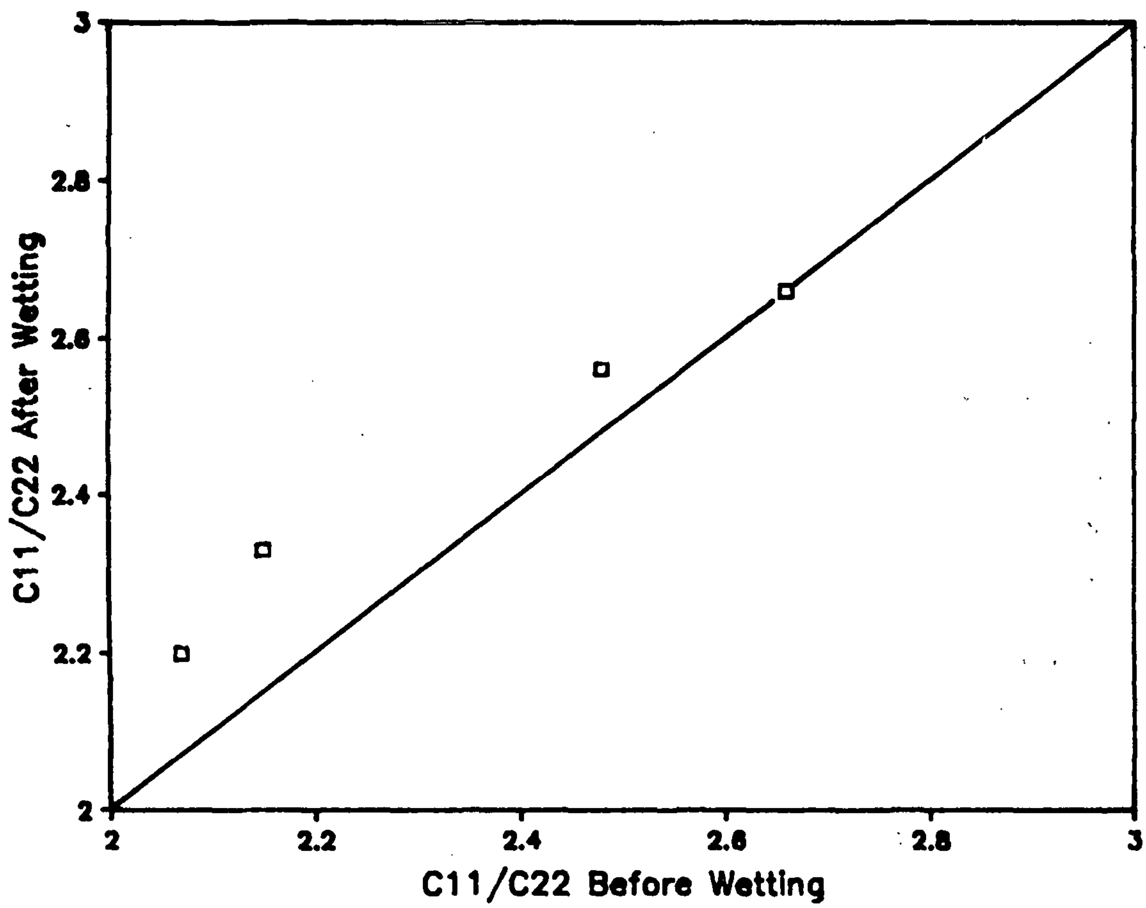

Figure 7. C_{11}/C_{22} after wetting vs. C_{11}/C_{22} before wetting.

APPENDIX 2

The use of microwave attenuation as a measure of fiber orientation anisotropy

C. C. Habeger and G. A. Baum

Associate Professor of Physics and Professor of Physics, respectively, The Institute of Paper Chemistry, P.O. Box 1039, Appleton, Wis. 54912

ABSTRACT *A laboratory instrument uses microwave attenuation to indicate fiber orientation anisotropy. The sensitivity of the instrument to fiber orientation, basis weight, furnish, moisture content, and density is discussed. The technique is recommended for on-line application if the results are corrected for varying moisture content.*

KEYWORDS
Analysis
Anisotropy
Attenuation
Instrumentation
Microwaves
Orientation
Testing

The distribution of fiber orientations in paper is primarily a function of conditions at the juncture of the pulp jet and the forming wire. The orientation distribution, which is skewed to the machine direction (MD), causes the physical properties of the paper to vary with the angle to the MD. Fiber orientation anisotropy is not the only source of sheet anisotropy. Wet straining in the open draws and MD tension during drying also produce MD to CD (cross-machine direction) differences in some properties. An online measurement of the anisotropy in a property sensitive to fiber orientation (but not to drying conditions) could be a monitor of pulp flow at the jet. A device that scanned the web in the CD would be particularly useful, because it would detect sheet variability resulting from the inhomogeneous application of pulp to the wire.

The distribution of fiber orientations was first determined on sheets formed from a pulp containing a small portion of darkly colored fibers, by manually measuring the angles of orientation of thousands of dyed fiber segments (*1*). Later, the angle tabulations were automated with a digitizer interfaced with a computer (*2*). This most direct fiber orientation determination has two limitations: (a) the sheet must contain dyed fabrics, and (b) if the sheet is not impregnated with a fluid whose index of refraction nearly equals that of the fibers, only dyed fibers near the surface are analyzed. Surface fiber orientation is often not representative of the entire sheet.

X-ray diffraction has also been used to find the fiber orientation distribution (*3-5*). The intensity of a Bragg diffraction peak is taken as a function of the angle from the line of intersection of the plane of radiation with the sheet to the machine direction. The axes of the cellulose crystals have preferential alignment to the fiber axis. Therefore, the diffraction pattern of a fiber depends on the angle of the radiation to the fiber axis, and in turn the pattern of the sheet depends on the fiber alignment to the MD. This is a relatively rapid off-line measurement that can be applied to a wide range of basis weights. However, the distribution of fibril angle alignments to the fiber axis must be known to relate X-ray anisotropy to fiber orientation anisotropy.

The ratio of MD to CD zero span tensile strength is another laboratory measure of fiber orientation anisotropy (*6, 7*). The zero span tensile strength is the breaking load per unit width when paper is clamped between closely spaced jaws (*8*). When properly performed (*9, 10*), it is a measure of fiber strength, which is insensitive to interfiber bonding. Since the fibers have greater tensile strengths along their axes, the ratio of MD to CD zero span tensile strength can be an indication of fiber orientation anisotropy. Fiber strength increases with drying stress, which is greatest in the MD. Thus, for this ratio to only reflect fiber orientation anisotropy, sheets are first soaked in water for 24 h to relieve drying stresses. The test for zero span tensile strength is an adequate test of fiber strength only for samples with a basis weight of 30–80 g/m^2 (*9*).

Information about the fiber orientation is also inferred from the pattern of visible light transmitted through a sheet. When an expanded beam of laser light passes through a thin sheet ($< 50\ \mu$m) and is focused on the plane of a detector, light diffraction by single fibers creates an elliptical pattern. The principal axis of the ellipse is aligned in the CD. The ratio of signal when the detector is rotated along the CD to that along the MD is an indication of fiber orientation anisotropy (*11, 12*). When laser light is focused on a sheet, preferred scattering along the fiber axes produces an anisotropy transmittance pattern. The major axis of the ellipse is now in the MD. (Lippke manufactures both laboratory and on-line instruments (*13*) that use the scattering principle to predict fiber orientation anisotropy.) Adequate light transmittance is achieved on sheets up to 250 g/m².

Microwaves and paper

The interaction of microwave radiation with paper is sensitive to moisture content. Water molecules have permanent dipole moments, which at low frequencies align with the electric field. The time required for dipole orientation is of the order of one cycle of the electric field at microwave frequencies. Therefore, the dielectric constant of water is larger below microwave frequencies (approx. 80) than at higher frequencies (approx. 5). In the microwave regime, water dipole moments trail the electric field in time, and the imaginary part of the dielectric constant is large. Substantial microwave energy is dissipated as heat. For sheets of moderate moisture content, water is the main source of labile dipoles, and the dielectric constant of paper (especially the imaginary part) depends on the amount of water, its molecular environment, and the geometry of its distribution. Other sheet variables have only small influences on microwave dielectric properties (*14*). Microwave techniques for measuring moisture content rely on this strong interaction between water and microwave radiation.

The effective dielectric constant of paper, ϵ_p, depends on the orientation of the electric field with respect to the principal axes of the paper. The absolute value of ϵ_p is greater for an in-plane than for an out-of-plane electric field (*15–18*). Also, ϵ_p is larger for an electric field parallel to the MD than for one parallel to the CD (*14, 19*). There are two explanations for this dielectric anisotropy (*14*). Paper is composed of fibers that lie in the plane of the paper and that are preferentially aligned in the MD. This fiber-induced anisotropy in the geometry leads to dielectric anisotropy. The fiber fraction, which has a higher dielectric constant, is more connected along the MD, and ϵ_p is thereby larger in the MD. Roughly speaking, the mixture is closer to a parallel alignment of capacitors in the MD.

While the dielectric anisotropy can be explained in terms of fiber geometry, a secondary mechanism may also contribute. The bond between the absorbed water and the fiber restricts the lability of the water dipoles. On the average, the water lability could be different along the fiber axis than it is transverse to the axis. This variation, along with the dielectric anisotropy of the dry fiber, could result in a fiber matrix that is not dielectrically isotropic. The anisotropy in the fiber would be reflected in the effective sheet properties. Regardless of the relative importance of the two mechanisms, sheet dielectric anisotropy will be sensitive to the fiber orientation distribution.

The change in in-plane dielectric constant with the angle of the electric field to MD is small; however, ϵ_p can be determined with sufficient repeatability to distinguish MD from CD and to detect changes in fiber orientation (*14*). Unlike mechanical anisotropy measurements, the ratio of MD to CD ϵ_D is insensitive to drying conditions (*19*). Therefore, microwave dielectric anisotropy could be a nondestructive indicator of in-plane fiber orientation anisotropy.

There is much experience with on-line microwave moisture gauges, and development of an on-line fiber orientation indicator should be straightforward. However, before on-line work is justified, a viable laboratory instrument must be developed and tested as a measure of fiber orientation and for sensitivity to sheet variables other than fiber orientation. The effective dielectric constant of paper is a well defined physical quantity whose direct measurement is tedious. A practical instrument for fiber orientation could determine an easily measured property related to ϵ_p. It is our purpose here to describe such a device and to discuss its benefits and limitations.

Experimental techniques

Instrumentation

This laboratory instrument provides a simple, rapid test of in-plane fiber orientation anisotropy based on a microwave dielectric anisotropy. It measures the attenuation of a microwave signal passing through a sample. The attenuation depends on the amount of energy reflected at the sample–air boundaries and the amount of energy dissipated in the sample. These quantities, in turn, depend on the real and imaginary parts of the dielectric constant and the sample thickness. The effective dielectric constant is greater when the electric field is aligned in the MD; therefore, the ratio of attenuation with the electric field in the MD to that in the CD (R_M) is a measure of fiber orientation anisotropy. Briefly, the technique is to measure attenuations for a sample placed in a microwave waveguide at different orientations to the electric field. This is a simpler approach than finding the complex dielectric constant.

Figure 1 is a schematic diagram of the gauge. The microwave signal is produced by a Polarad model 1108A-C X-band microwave signal generator having a frequency range of 8.2 GHz to 12.4 GHz. All results reported were taken at 9.25 GHz. The microwave signal is pulsed on and off with a 50% duty cycle at a 1-kHz rate. This amplitude-modulated microwave signal goes through a Hewlett Packard 11686A filter to eliminate spurious low frequency signals. The signal is next carried through a rigid coaxial cable to a rectangular X-band waveguide. The waveguide is 2.286 cm wide and 1.016 cm high, and the electric field is oriented vertically (along the smaller dimension).

The end of the waveguide is attached to a variable microwave attenuator (Systron Donner DBG 430) with spring-loaded bolts. The attenuator connects to a Systron Donner DBG 310 detector mount, which contains an Alpha Industries DDC4511D low-barrier Schottky diode. The attenuator and detector mount are attached to a custom-made carrier which can be manually translated to open a gap between the waveguide and the attenuator. A switch shuts off the signal generator when the gap is open. Samples can be inserted in the gap with the MD vertical or horizontal. The signal, after passing through the sample and the attenuator, is rectified by the diode. The resulting 1-kHz square wave is applied to a Hewlett Packard 415E standing-wave-ratio meter. This is a narrow-band amplifier centered at 1 kHz. It registers in decibels the incoming signal on a needle dial. Figure 2 is a photograph of the instrument.

The need for the attenuator

One of our early difficulties was the lack of repeatability in the standing-wave-ratio meter readings. These were sensitive to small movements of the signal generator and waveguides, to small movements of the then-flexible coaxial cable into the waveguide, and to variability of the seating of the sample between the attenuator and the waveguide. This problem was remedied by bolting the signal generator, waveguide, attenuator, and detector mount to a common rigid base, by replacing the flexible coaxial cable with a rigid one, and by carefully aligning the translating carriage to avoid seating variabilities.

The first tests were conducted without the attenuator between the sample and the detector. This led to unsatisfactory results because of the large standing wave ratio in the microwave cavity. The loss was not linear with the number of samples inserted, and sometimes there were unreasonably high or low readings. The attenuator removed this problem by preferentially reducing multiple reflected components in the signal. A setting of 10 dB was sufficient to avoid difficulties.

Procedure

The sample is cut into strips 2.78 cm wide and about 15 cm long. This width is selected so that the sample will fit snugly between the bolts when placed in the waveguide. Strips cut along both the MD and CD are used. The strips are stacked to a thickness of about 0.15 cm and stapled at the ends. Four small edge marks, about 2.5 cm apart, are made toward the middle of the stack.

The data gathering procedure is to (a) pull open the gap, (b) insert a stack with the waveguide edge flush to an edge mark, (c) close the gap, (d) wait 30 s for the meter reading to stabilize, and (e) record the meter reading less the "no-sample" value. This is done for each edge of the four marks with MD and CD stacks and with horizontal and vertical insertion. A total of 16 readings are taken.

The first reading from the MD vertical test is added to the first reading from the CD horizontal test. This quantity is divided by the sum of the other two first readings (CD vertical plus MD horizontal) to give a value of R_M. These calculations are carried out for each of the four edge marks and are averaged to get the R_M for the sample. The reason for using a relatively thick stack is to quickly average out sheet variability and to increase the signal-to-noise ratio in the attenuation reading. It is necessary to do both vertical and horizontal insertions of MD and CD stacks, since the boundary conditions at the waveguide–detector mount interface are different for horizontal and vertical insertion.

Results and discussion

The first experiments determined the sensitivity of R_M to fiber orientation changes. Sheets with four different fiber orientations were made in the laboratory using a Formette Dynamique (*20*). The common furnish was a predominantly Douglas-fir, bleached kraft, never-dried pulp. Since the samples were fully constrained in the MD and CD while drying, the differences in anisotropy of the physical properties could be attributed to fiber orientation anisotropy only.

Figure 3 is a plot of R_M vs. R_E, the ratio of the elastic stiffness (measured ultrasonically) in the MD to that in the CD. The error bars, which are typical for results reported later, are two standard deviations wide. Notice that although elastic anisotropy values are larger, the ratio of uncertainty in a reading to variability between the samples is nearly identical in the mechanical and microwave tests. This indicates that the uncertainty in both cases is largely caused by variability in the sample. Wet zero span anisotropy was also measured, and for this set of

1. Schematic diagram of the microwave fiber orientation gauge.

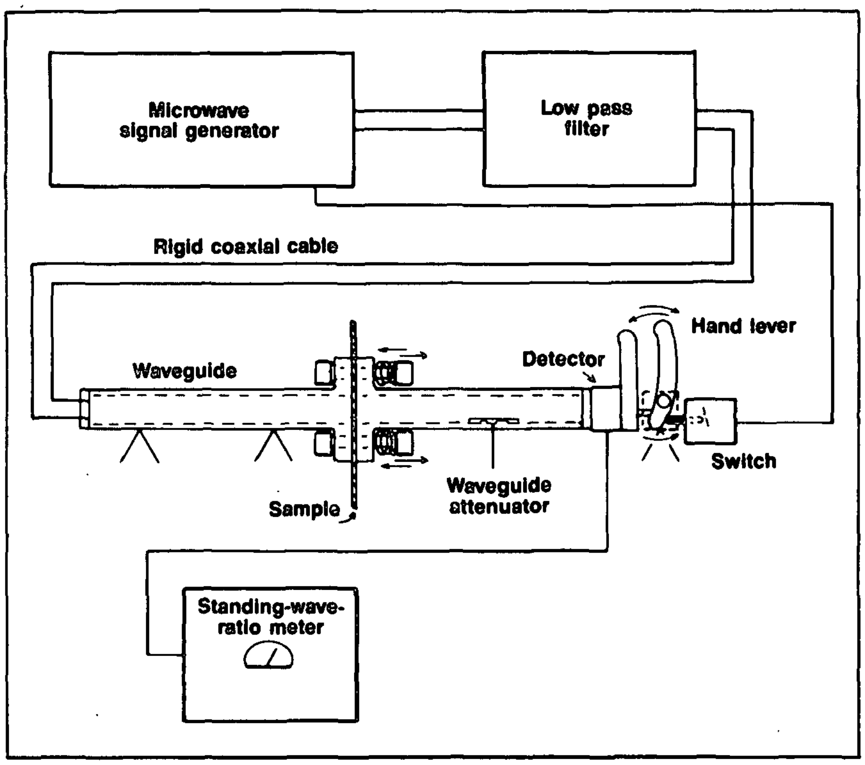

2. Photograph of the experimental apparatus.

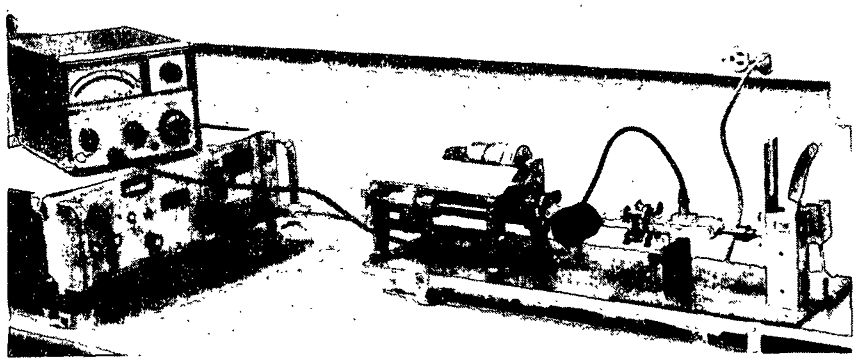

samples these values are close to the elastic anisotropy values.

These results demonstrate that, on fully restrained sheets, R_M is an indicator of orientation anisotropy of a quality equal to that of mechanical determinations. Further evidence of the utility of R_M comes from two measurements on commercial linerboard made at different rush-drag ratios and constant draw tension. The normal rush-drag setting produced an R_M of 1.056 ± 0.006 and an R_E of 2.27 ± 0.27, whereas a low rush-drag setting gave an R_M of 1.014 ± 0.005 and an R_E of 1.77 ± 0.21.

With the variable attenuator set at 10 dB, R_M is not sensitive to basis weight. This assertion is supported by the results in Table I. Here, R_M was determined on the same set of eight MD and eight CD linerboard strips in three different ways. The sheets were inserted into the waveguide in stacks of two, four, or eight strips. These results also justify the choice of about 0.15 cm for a standard stack height, which is near the thickness of the four-deep stack in Table I. This stack height provides enough sample to minimize reading variability without losing basis weight variability at high gap spacings.

One advantage of this technique is that the microwave attenuation is insensitive to thickness direction dependence in fiber orientation. To demonstrate this, an extremely two-sided stack was tested. The stack was made from MD and CD strips of the most oriented sample shown in Fig. 3. Eight MD strips were placed on the "top" side and eight CD on the "bottom." The stack was placed vertically into the waveguide, and average attenuation was recorded with the top side toward the detector (2.443 dB) and with the top side toward the generator (2.431 dB). The standard deviations in the readings were 0.021 dB and 0.023 dB, respectively.

The effect of furnish on the relationship between microwave anisotropy and elastic anisotropy was studied by plotting R_M vs. R_E for Formette sheets of three different bleached kraft furnishes, all dried under full restraint (Fig. 4). The results indicate that, except at high anisotropy, furnish has a similar effect on R_M and R_E.

The sensitivity of R_M to moisture content is shown in Fig. 5. Measurements of R_M were taken at 50% RH and 23°C and then in a variable-humidity room maintained at 15% RH or

3. Microwave anisotropy ratio vs. elastic anistropy ratio for sheets of bleached kraft and Douglas-fir, made to different distributions of fiber orientation.

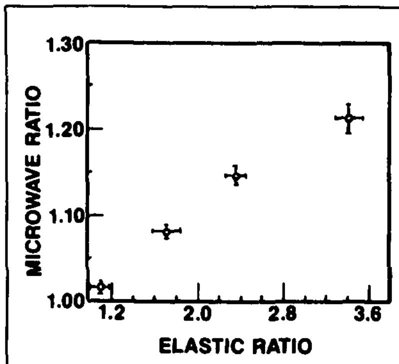

I. Basis weight sensitivity

Sample	Microwave anisotropy
4 each, 2 stack	1.070 ± 0.032
2 each, 4 stack	1.071 ± 0.007
1 each, 8 stack	1.063 ± 0.007

4. The effect of varying furnish on the relationship between microwave anisotropy ratio and elastic anisotropy ratio.

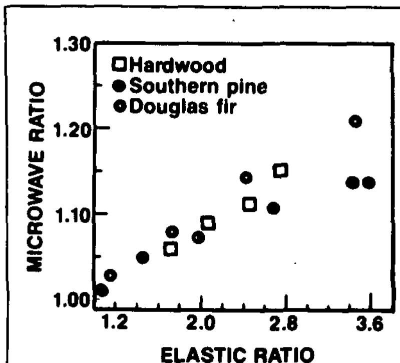

5. The effect of moisture on the microwave anisotropy ratio.

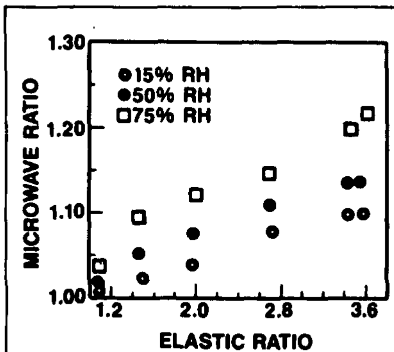

II. Wet pressing effects

Orientation	Wet pressing	Density, g/cm³	Microwave anisotropy	Elastic anisotropy
Medium	high	0.827	1.093	2.28
Medium	medium	0.656	1.127	2.55
Medium	low	0.418	1.138	2.73
High	medium	0.654	1.154	3.08
Low	medium	0.621	1.008	1.17

III. Equations

Ratio of the effective dielectric constant in the x-direction to that in the y-direction:

$$^{R}I = \{[^{\rho\epsilon}F + (1-\rho)\,^{\epsilon}A][^{\rho\epsilon}A + (1-\rho)\,^{\epsilon}F]\}/\,^{\epsilon}A\,^{\epsilon}F \qquad (1)$$

Derivative of Eq. 1 with respect to the dielectric constant of the F component

$$\frac{^{\epsilon}F\,\partial\,^{R}I}{^{R}I\,\partial\,^{\epsilon}F} = \frac{(1-\rho)[^{\rho\epsilon}F^2 + 2(1-\rho)\,^{\epsilon}F\,^{\epsilon}A - {}^{\rho\epsilon}A^2]}{[^{\rho\epsilon}F + (1-\rho)\,^{\epsilon}A][^{\rho\epsilon} + (1-\rho)\,^{\epsilon}F]} \qquad (2)$$

75% RH. The calculated values of R_M are plotted vs. R_E measured at 50% RH. Notice that R_M increases with moisture content.

Sheet density can change R_M at constant fiber orientation. Table II demonstrates the relative effects of fiber orientation and wet pressing on R_M. Although R_M is much more sensitive to fiber orientation, there is a decrease in R_M (also in R_E) with density.

A possible explanation for the increase in R_M with moisture content is attained by considering an extreme case. Imagine a two-phase mixture with dielectric constants ϵ_F and ϵ_A, and let ρ represent the volume fraction of the F component. The geometry of the moisture is such that all interfaces are perpendicular to the y-axis. Therefore, the phases are aligned in series in the y-direction and in parallel in the x-direction. The ratio of the effective dielectric constant in the x-direction to that in the y-direction is given in Table III as Eq. 1.

The major dielectric effect of adding moisture to a sheet is to increase the dielectric constant of the fiber fraction. This is analogous to increasing ϵ_F in Eq. 1. Taking the derivative of Eq. 1 with respect to ϵ_F gives Eq. 2 in Table III. This quantity lies between 0 (when ρ approaches 1) and 2 (when ρ approaches 0). Thus, R_I rises with moisture content, especially at low ρ. Increasing ϵ_F has a larger percentage effect on the dielectric constant in the parallel direction than in the series direction.

The effect of density could be studied similarly by taking the derivative of Eq. 1 with respect to ρ. However, the result is that $\partial R_I / \partial \rho$ equals a positive number times $(1 - 2\rho)$. This conflicts with our experimental results, which showed R_I decreasing as density increased even when the volume fraction was less than ½. The volume fraction was estimated by assuming that the fiber density was 1.5 g/cm^3. The parallel-series model is probably inappropriate in this case, since it does not allow for increasing y-direction connectedness with increasing density. That is, as ρ increases, the CD geometry becomes less series-like, and this oversimplified model does not account for that.

Conclusions

The measurement of microwave attenuation anisotropy ratio is a simple laboratory indicator of fiber orientation. Testing should be done in a humidity-controlled room to avoid the effects of changing moisture content. Also, caution should be taken when comparing results on sheets of greatly different densities.

The technique could be applied online to sheets over a wide range of basis weights, provided the results are corrected for moisture. To our knowledge, the Lippke fiber scattering device is the only existing on-line fiber orientation indicator. A microwave meter could operate above the 250 g/m^2 basis weight limit of the Lippke device. Below this limit, it is hard to compare the two techniques, since no study of the sensitivity of the Lippke device to sheet variables other than fiber orientation has been published.

Literature cited

1. Danielsen, R. and Steinberg, B., Svensk Papperstid. 50: 301(1947).
2. Crosby, C.M., Eusufzai, A.R., Mark, R.E., Perkins, R.W., Chang, J.S., and Uplekar, N.V., Tappi 64(3): 103(1981).
3. Prud'homme, R.W., Hein, N.W., Noach, J., and Marchessault, R.H., J. Appl. Polymer Sci. 19(9): 2609(1975).
4. Koran, Z., Bussiers, D., and Prud'homme, R.E., Tappi 65(8): 88(1982).
5. Paakkari, T., Serimaa, R., Hattula, T., and Ahtee, M., Paperi Puu 10: 569(1984).
6. Kallmes, O.J., Tappi 52(3): 482(1969).
7. Votava, R.J., Tappi 65(4): 67(1982).
8. Van den Akker, J.A., Lathrop, A.L., Voelker, M.H., and Dearth, L.R., Tappi 45(8): 416(1958).
9. Wink, W.A. and Van Eperen, R.H., Tappi 45(1): 10(1962).
10. Cowan, W.F. and Cowdrey, J.K., Tappi 57(2): 90(1974).
11. Rudstrom, L., and Sjolin, U., Svensk Papperstid. 73(5): 117(1970).
12. Sadowski, J.W., Paperi Puu 9: 588(1979).
13. Kohl, A. and Hartig, W., Zellcheming general meeting (Baden-Baden), 80th, June 24-28, 1985, p. 22.
14. Habeger, C.C. and Baum, G.A., J. Appl. Polymer Sci. 28: 969 (1983). Tappi 65(1): 115(1982).
15. Servant, R. and Gougeon, C. R., Acad. Sci. Paris 242:2318(1956).
16. Chene, M., Coumes, A., and Lafaye, C.R., Acad. Sci. Paris 260(13): 3632(1965).
17. M'Baye, K. and Pellisier, J.P., Rev. ATIP 29(2): 51(1975).
18. Dusiou, N., Balaneschu, G., and Liuiu, T., Celul. Hirtie 25(1): 34(1976).
19. Fleischman, E.H., Baum, G.A., and Habeger, C.C., Tappi 65(10): 115(1982).
20. Sauret, G., Bull. ATIP 1616: 446(1962).

Received for review Jan. 22, 1986.
Accepted April 16, 1986.

THE INSTITUTE OF PAPER CHEMISTRY

Appleton, Wisconsin

Status Report

to the

PAPER PROPERTIES AND USES

PROJECT ADVISORY COMMITTEE

Project 3526

INTERNAL STRENGTH ENHANCEMENT

February 13, 1987

PROJECT SUMMARY

PROJECT NO. 3526: INTERNAL STRENGTH ENHANCEMENT

PROJECT STAFF: R. Stratton, K. Hardacker February 13, 1987

PROGRAM GOAL: Bring new attributes to fiber based products

PROJECT OBJECTIVE:

To improve internal strength and moisture tolerance in paper and paperboard. The short term goals are to establish those parameters fundamental to inter-fiber and intra-fiber bonding in conventional and ultra high yield pulps and to control these parameters, if possible, by chemical or mechanical treatments.

PROJECT RATIONALE, PREVIOUS ACTIVITY, AND PLANNED ACTIVITY FOR FISCAL 1987-88 are on the attached 1987-88 Project Form.

SUMMARY OF RESULTS LAST PERIOD: (April 1986 - September 1986)

(1) The effectiveness of the CMC/PAE and PAA/PAE bonding systems was expanded to include a wide range of pulps in whole and classified conditions including a softwood bleached kraft. The results show that these agents, particularly CMC/PAE, were effective in all pulps with some variations in the degree of success. Of the whole pulps, the bleached kraft and once-dried, average-yield southern pine unbleached kraft tended to be the most responsive. Of the classified pulps, the TMP was the most responsive and a softwood CMP, the least responsive. Generally speaking, higher strength levels were attained with the whole pulps in the presence of the bonding agents but the greatest increases in strength due to the additives generally occurred in the classified pulps.

(2) The study of bonding agents was expanded to include carboxymethylated starch as an anionic polymer in combination with PAE. While anionic starch/PAE combinations did not quite match the overall performance of CMC/PAE, anionic potato starch/PAE approached or equalled CMC/PAE in some strength properties including moist Et and compressive strength.

(3) The incorporation of carboxymethylated fiber and PAE into a classified bleached kraft pulp failed to provide equivalent strength to that achieved by the addition of an equal amount of water-soluble CMC in the presence of PAE. In fact, the addition of up to 10% of carboxymethylated fiber failed to attain the same level of strength afforded by the external addition of 0.4/1.0 CMC/PAE. This is assumed to be due to lower accessibility of the reactive groups in the fibrous form of CMC.

(4) Diffuse reflectance/FTIR analysis indicated that covalent bonding (ester formation) occurred in the bleached kraft pulp whether the carboxymethyl group was included in the fibrous component or in an external treatment. FTIR analysis of papers treated with anionic potato starch/PAE also indicated the presence of covalent bonding. On the other hand, no evidence of

covalent bonding was found in papers containing PEI or polydiallyl dimethyl ammonium chloride (a cationic polymer) alone or in combination with PAA in spite of the fact that several of these papers possessed strength properties approaching or equalling those containing PAE or PAE/PAA.

(5) A brief examination of the external treatment of unbleached kraft handsheets with polystyrene in solvent solution indicated that high levels of moist Et and compressive strength can be achieved while maintaining high tensile properties. It would appear, however, that high add-on levels would be required to achieve these desired effects.

(6) Work is continuing in the development of techniques for measuring the axial and transverse mechanical properties of single fibers and of Z-direction deformation of single fiber/fiber bonds using the FLER II.

(7) Measurements of bond strength, bond area, and locus of failure for a well-refined, classified southern pine provide a contrast to the unrefined sample reported previously. Frequent tearing of the fiber wall was now found for both untreated and chemically-treated fibers. However, extensive external fibrillation of the fibers make an unambiguous assessment of the damage due to bond failure difficult. Both breaking load and bond strength are considerably higher for the refined compared with the unrefined fibers.

SUMMARY OF RESULTS THIS PERIOD: (September 1986 - March 1987)

(1) Strength aids added to the pulp prior to refining influence the rate of beating. The strength properties of handsheets made from such a pulp are inferior to those of handsheets for which the bonding agents are added after refining.

(2) Addition of a polymeric retention aid to a whole pulp to attach the fines to the long fibers prior to introducing the strength aids gave less strength enhancement than if the retention aid was not present.

(3) Comparison of sheets made with bonding agents at pH 7 and pH 4.5 shows that greater strength is produced at the higher pH.

(4) Further evidence was adduced that tensile strength and STFI compression strength are each affected to different extents by the various bonding agent combinations.

(5) A suitable hot melt adhesive has been found for cementing single fiber to the mounting fixtures of the FLER II.

(6) Latewood fiber/fiber bonds produce both higher average breaking load and specific bond strength than earlywood from the same unbleached loblolly pine kraft pulps.

(7) For fibers both untreated and treated with PAE/CMC refining did not change the bond breaking load, decreased the bond area, and increased the specific bond strength.

(8) Untreated TMP fibers produced rather weak bonds from the viewpoint of breaking load. The specific bond strength, however, was very high.

(9) Treatment of the several pulp fibers with the strength additive PAE/CMC enhanced breaking load, bonded area, and specific bond strength.

PROJECT TITLE: Fundamentals of Internal Strength Enhancement	Date: 1/28/86
	Budget: $230,000
PROJECT STAFF: R. Stratton/K. Hardacker	Period Ends: 6/30/87
PRIMARY AREA OF INDUSTRY NEED: Properties related to end use	Project No.: 3526

PROGRAM AREA: Moisture tolerant, superior strength paper and board

PROGRAM GOAL: Bring new attributes to fiber based products

PROJECT OBJECTIVE:

To improve internal strength and moisture tolerance in paper and paperboard. The short term goals are to establish those parameters fundamental to inter-fiber and intra-fiber bonding in conventional and ultra high yield pulps and to control these parameters, if possible, by chemical or mechanical treatments.

PROJECT RATIONALE:

Major limitations of paper and board for many uses are low internal bond strength and poor moisture tolerance. Improved internal strength and enhanced moisture resistance would allow a number of present grades to be produced using less fiber and would also allow new end uses to be developed.

At present, commercial papers do not attain strength levels that realize the full potential of the wood fibers. Most paper mechanical properties are markedly degraded with increasing moisture content. We need to better understand the nature of the changes in fiber properties and fiber-to-fiber bonding with increasing moisture content if we are eventually to improve the moisture tolerance of paper.

RESULTS TO DATE:

PART ONE: Improved bonding via chemical additives.

Results presented in previous reports indicated that cationic/anionic duopolymer additives (primarily CMC/PAE and CMC/PAA) were very effective in improving the strength properties of several softwood unbleached kraft pulps as well as a softwood TMP. In addition to high levels of dry, moist, and wet tensile properties, these combinations significantly improved tensile energy absorption (TEA), extensional stiffness (Et), and stretch. The addition of these bonding agents to the softwood TMP revealed that superior results were generally obtained when added to the long (classified fiber) fraction. A subsequent study of fines and bonding agents in an average yield softwood unbleached kraft pulp showed that readdition of fines to the classified pulp failed to match the original whole pulp in any of the measured dry or moist tensile properties. This differs somewhat from the TMP where readditions of fines produced dry tensile and Et values roughly comparable to the whole pulp. As was found in the case of the TMP, maximum strength in the kraft pulp was generally achieved when CMC/PAE was added to the long fiber fraction.

CMC/PAE and PAA/PAE also proved to be effective bonding agents for a spruce chemimechanical pulp. One or both of these combinations has proved effective in all pulps tested thus far. This favorable result is somewhat tempered by the fact that their efficiency is generally lower in whole pulps than in classified pulps.

Diffuse reflectance FTIR analysis has indicated that covalent bonding occurs when the duopolymer systems are applied to cellulose, but it has not been established if the bonding occurs between the added polymers or between the polymers and cellulose. This work is being extended to include polymer systems where covalent bonding is not possible but where other forms of bonding may occur.

PART TWO: Fundamentals of bonding.

A literature search has been conducted. An instrument to measure axial or transverse fiber mechanical properties and fiber-fiber bond strength has been designed and constructed and is currently being readied for data gathering.

Techniques were developed to study the details of the fracture of the bond between two single fibers. They consisted of:

a) forming the fiber/fiber bond,
b) measuring the bond area using vertical polarized illumination,
c) determining the bond strength, and
d) determining the locus of failure of the bond using the scanning electron microscope.

Results on loblolly pine earlywood fibers revealed a normal distribution of bond areas and a bimodal distribution of bond breaking loads. Examination of the formerly bonded areas with the SEM showed permanent deformation where the fibers had been pressed together but little rupture (tearing) of the external fiber surfaces.

A vibrating reed instrument has been developed to measure the bending modulus of paper and board samples. A range of temperature from ambient to 200°C and a range of relative humidities from 0 to 95% at room temperature can be covered.

PLANNED ACTIVITY FOR THE PERIOD:

PART ONE:

(1) The study of bonding agents will continue. While several anionic/cationic polymers combinations have been found to be quite effective, other materials will be given consideration based on chemical structure and known properties.

(2) The utilization of duopolymer bonding agents will be expanded to include one or more bleached pulps.

(3) Means will be sought to improve the efficiency of polymer bonding agents in whole (fines-containing) pulps.

(4) The study of bonding mechanisms through chemical analysis will be continued in an effort to differentiate between polymer-to-polymer bonds and polymer-to-fiber bonds.

PART TWO:

(1) We plan to measure single fiber properties as functions of moisture content, refining, yield, and pulping method. The measurements will include both axial and transverse properties. The initial work will be with softwoods.

(2) Failure of single fiber/fiber bonds will be continued, with correlations expected among bonded area, bond strength, and locus of failure.

(3) Effective chemical additives identified in Part One will be used in forming single fiber/fiber bonds, whose failure will then be examined as above.

(4) Studies on the effects of pulp yield and refining on mode of bond failure will begin.

Status Report

INTERNAL STRENGTH ENHANCEMENT

Project 3526

INTRODUCTION

The objective of this project, to improve the internal strength and moisture tolerance of paper and board, is being pursued along several fronts. In Part One we review the results of handsheet studies with a variety of polymeric additives. These were carried out under the direction of Joseph J. Becher. In Part Two the continuing development of the FLER II instrument and the results of single fiber/fiber bond testing are discussed.

PART ONE: Improved Bonding via Chemical Additives

Previously[1], we have contrasted the behavior of classified pulps with that of whole pulps with regard to their response to chemical additives. Although the strength additives enhance the mechanical properties of both kinds of pulps, the relative improvement is much greater in the case of the classified pulps. In the mill one is confronted with a headbox stock typically containing a large proportion of fines. It is important, therefore, to maximize the effect of the expensive additives.

In related studies[1] we also showed that, in a whole pulp, polymer additive adsorbed on the long fiber fraction was much more effective in improving strength than was a similar amount of polymer adsorbed on the fines fraction. Adsorption on the long fiber fraction was also more effective than simultaneous adsorption on both fines and fiber - the usual method in the mill. Separation of the fibers and fines in the mill situation followed by treatment of the fibers only and then reblending the two components before sheetmaking is not likely to be economically viable. We thus sought alternative approaches.

One potential method would be to treat the pulp before it was refined so that mainly long fibers were present. During refining, fines are produced by removal of portions of the outer layers of the cell wall of the individual fibers. For this method to be successful, the fraction of initial fiber surface area lost during refining should be somewhat less than one-half. Observation of individual refined fibers in the optical microscope supports this. Although considerable fiber wall disruption is evident, the majority of the fiber surface appears undamaged. (Whether what one is seeing is the original - i.e. before refining - fiber wall is, of course, open to debate.)

Assuming that most of the initial wall remained intact during refining, we studied the effect of adding the strength aids to the pulp prior to refining. Handsheets made from the refined pulp were then compared with sheets made from pulp similarly refined but in the absence of the strength aids. In the latter case comparable dosages of the strength aids were added to the refined pulp just prior to sheet formation. The pulp used was a laboratory - produced conventional southern pine unbleached kraft pulp. The yield was 47.5% and the kappa number was 34.2. The pulp was refined for 10, 25, or 50 minutes in a laboratory Valley beater. When polymer was used, it was added to the beater while the pulp was being circulated with no load on the bedplate. A variety of strength additives previously found effective were applied. A pH of 4.5 - 5.0 was maintained. The results are presented in Tables 1 (polymer added before refining) and 2 (polymer added after refining).

As might be expected, addition of the various polymer strength aids increases the freeness of the unbeaten pulp by 5 to 30 mls CSF (Table 1). The additives also influence the subsequent rate of beating. Up to 25 minutes

Table 1. The effect of refining on polymer effectiveness - polymers added to pulp before refining, softwood unbleached kraft - whole pulp.

Set No.	Additives % Based on Fiber	Basis Weight, g/m^2	Apparent Density, g/cc	Dry Strength Properties: Breaking Length, km Av.	SD	TEA, kgm/m^2 Av.	SD	Et, kg/cm Av.	SD	Stretch, % Av.	SD	Moisture Content, % at 91-93% RH	Moist Strength Properties: Breaking Length, km Av.	SD	TEA, kgm/m^2 Av.	SD	Et, kg/cm Av.	SD	Stretch, % Av.	SD	Moist Tensile Factor
	Pulp slushed 5 min, no beating																				
1	Blank Control	63.9	0.349	2.79	0.133	3.11	0.421	229	10.7	2.49	0.215	15.4	1.29	0.092	1.87	0.193	103	9.5	3.15	0.158	1.00
2	PAE, 1.5	64.0	0.376	4.88	0.170	7.9	0.975	293	5.0	3.73	0.322	14.8	2.95	0.164	6.66	0.586	109	6.2	5.46	0.314	2.29
3	PAE, 1.0; CMC, 0.4	63.1	0.375	5.64	0.142	9.83	0.671	309	20.7	4.11	0.200	15.3	3.44	0.186	7.96	0.940	119	5.7	5.87	0.307	2.67
4	PAE, 1.0; PAA, 0.2	62.3	0.374	4.67	0.448	7.49	1.091	273	21.8	3.73	0.207	15.9	2.63	0.191	6.53	0.974	93.9	8.52	5.68	0.362	2.04
5	PAE, 1.0; CMPS, 1.0	63.6	0.383	5.03	0.355	7.63	1.071	295	16.0	3.48	0.313	16.3	3.00	0.167	6.65	0.780	108	8.5	5.51	0.303	2.33
6	PEI, 1.0; PAA, 0.2	62.4	0.372	4.39	0.176	6.19	0.560	292	11.6	3.25	0.245	15.9	2.13	0.120	4.64	0.625	102	7.8	4.98	0.339	1.65
	Pulp slushed, then beaten 10 min																				
7	Blank Control	62.6	0.407	4.62	0.241	5.30	0.831	339	26.5	2.73	0.368	15.1	2.51	0.051	3.75	0.240	1.59	9.3	3.45	0.215	1.00
8	PAE, 1.5	63.4	0.426	7.22	0.270	11.0	0.65	374	17.4	3.77	0.173	16.0	4.48	0.277	9.21	1.261	134	4.7	5.34	0.280	1.78
9	PAE, 1.0; CMC, 0.4	61.0	0.421	7.20	0.296	10.1	0.925	374	9.1	3.59	0.230	15.6	4.62	0.232	8.47	0.918	131	12.5	5.21	0.323	1.84
10	PAE, 1.0; PAA, 0.2	62.8	0.423	6.43	0.305	10.2	0.84	346	11.3	3.87	0.171	16.1	3.83	0.158	8.13	0.361	121	6.3	5.33	0.070	1.53
11	PAE, 1.0; CMPS, 1.0	61.5	0.429	7.34	0.279	11.3	0.75	367	17.2	3.91	0.117	15.9	4.17	0.118	7.85	0.401	125	6.6	5.26	0.144	1.66
12	PEI, 1.0; PAA, 0.2	61.6	0.421	6.08	0.276	8.46	0.505	352	18.6	3.43	0.141	14.9	3.28	0.106	5.86	0.478	153	11.3	4.52	0.193	1.31
	Pulp slushed, then beaten 25 min																				
13	Blank Control	63.0	0.448	6.06	0.271	7.55	0.683	400	12.8	2.93	0.090	15.1	3.30	0.106	5.53	0.399	183	5.4	3.84	0.167	1.00
14	PAE, 1.5	63.3	0.477	8.28	0.465	12.1	0.92	442	19.8	3.61	0.163	16.7	5.15	0.268	9.32	0.703	142	9.6	5.03	0.130	1.56
15	PAE, 1.0; CMC, 0.4	60.7	0.478	8.14	0.352	11.3	0.83	421	21.5	3.56	0.173	15.1	5.98	0.293	10.7	0.36	182	10.7	5.10	0.080	1.81
16	PAE, 1.0; PAA, 0.2	62.0	0.469	7.80	0.385	11.0	0.92	425	11.3	3.57	0.223	16.7	4.89	0.185	9.02	0.512	146	5.6	4.94	0.151	1.48
17	PAE, 1.0; CMPS, 1.0	63.1	0.479	8.78	0.555	12.9	1.23	451	19.3	3.68	0.116	15.9	5.33	0.119	9.94	0.611	159	10.9	5.20	0.212	1.62
18	PEI, 1.0; PAA, 0.2	61.2	0.467	7.00	0.226	9.76	0.493	402	14.6	3.45	0.154	15.2	4.08	0.218	6.88	0.612	178	11.9	4.44	0.187	1.24
	Pulp slushed, then beaten 50 min																				
19	Blank Control	63.6	0.503	6.96	0.325	8.93	0.890	468	22.1	2.97	0.162	15.0	4.30	0.185	7.92	0.766	212	8.5	4.26	0.226	1.00
20	PAE, 1.5	61.0	0.511	8.60	0.289	11.4	0.60	464	9.2	3.34	0.092	16.3	6.42	0.245	11.7	0.28	173	5.8	5.34	0.043	1.49
21	PAE, 1.0; CMC, 0.4	62.4	0.520	9.14	0.542	13.3	1.00	501	30.6	3.62	0.100	15.4	6.12	0.144	11.8	0.780	193	10.0	5.28	0.119	1.42
22	PAE, 1.0; PAA, 0.2	61.0	0.520	8.32	0.192	11.4	0.46	451	17.6	3.40	0.174	16.0	5.81	0.423	10.0	0.758	179	11.6	4.87	0.174	1.35
23	PAE, 1.0; CMPS, 1.0	60.8	0.514	8.39	0.374	10.7	1.27	462	14.2	3.22	0.270	16.3	6.13	0.540	11.1	1.24	169	9.1	5.29	0.234	1.43
24	PEI, 1.0; PAA, 0.2	62.0	0.517	7.88	0.496	11.3	1.40	460	17.3	3.49	0.197	15.2	4.70	0.279	8.12	0.633	204	10.6	4.51	0.145	1.09

Table 1 continued. The effect of refining on polymer effectiveness - polymers added to pulp before refining, softwood unbleached kraft - whole pulp.

Set No.	Additives, % Based on Fiber	Freeness ml,CSF	Fines Content, % through 200 mesh	Wet Breaking Length, km Av.	Wet Breaking Length, km SD	Wet Tensile Factor	Dry STFI Compressive Strength lbf/in. Av.	Dry STFI Compressive Strength lbf/in. SD	Moist STFI Compressive Strength lbf/in. Av.	Moist STFI Compressive Strength lbf/in. SD	Moist Compressive Strength Factor
	Pulp slushed 5 min, no beating										
1	Blank Control	725	5.05	0.061	0.011	1.00	5.74	0.608	2.98	0.205	1.00
2	PAE, 1.5	730		1.24	0.052	20.33	8.21	0.606	3.77	0.405	1.27
3	PAE, 1.0; CMC, 0.4	740		1.45	0.030	23.77	8.07	0.605	3.89	0.290	1.31
4	PAE, 1.0; PAA, 0.2	740		1.13	0.074	18.52	7.75	0.589	3.80	0.337	1.28
5	PAE, 1.0; CMPS, 1.0	750		1.23	0.075	20.16	8.17	0.847	3.82	0.411	1.28
6	PEI, 1.0; PAA, 0.2	755		0.601	0.056	9.85	7.80	0.709	3.62	0.259	1.21
	Pulp slushed then beaten 10 min										
7	Blank Control	675	6.24	0.127	0.013	1.00	7.51	0.689	3.85	0.376	1.00
8	PAE, 1.5	695		2.04	0.140	16.06	9.00	0.644	4.51	0.391	1.17
9	PAE, 1.0; CMC, 0.4	690		1.94	0.154	15.28	8.88	0.447	4.19	0.362	1.09
10	PAE, 1.0; PAA, 0.2	695		1.51	0.078	11.89	8.19	0.689	4.12	0.376	1.07
11	PAE, 1.0; CMPS, 1.0	710		1.77	0.076	13.94	8.87	0.832	4.12	0.357	1.07
12	PEI, 1.0; PAA, 0.2	710		0.820	0.0601	6.46	8.79	0.646	3.83	0.416	0.99
	Pulp slushed then beaten 25 min										
13	Blank Control	610	6.85	0.189	0.014	1.00	8.31	0.600	4.26	0.313	1.00
14	PAE, 1.5	650		2.63	0.109	13.92	10.4	0.74	4.91	0.444	1.15
15	PAE, 1.0; CMC, 0.4	625		2.11	0.098	11.16	9.18	0.695	4.64	0.364	1.09
16	PAE, 1.0; PAA, 0.2	620		1.78	0.079	9.42	9.12	0.824	4.59	0.431	1.08
17	PAE, 1.0; CMPS, 1.0	640		2.28	0.139	12.06	10.3	0.70	4.55	0.404	1.07
18	PEI, 1.0; PAA, 0.2	660		0.864	0.012	4.57	9.32	0.563	4.38	0.341	1.03
	Pulp slushed then beaten 50 min										
19	Blank Control	470	8.46	0.206	0.029	1.00	9.59	0.562	4.76	0.316	1.00
20	PAE, 1.5	525	13.52	2.76	0.161	13.40	9.89	0.685	5.07	0.385	1.07
21	PAE, 1.0; CMC, 0.4	430	10.62	2.35	0.087	11.40	10.4	0.86	5.02	0.307	1.05
22	PAE, 1.0; PAA, 0.2	420	2.99	1.91	0.037	9.27	9.91	0.637	4.94	0.296	1.04
23	PAE, 1.0; CMPS, 1.0	480	4.29	2.37	0.091	11.50	10.4	0.84	4.94	0.294	1.04
24	PEI, 1.0; PAA, 0.2	510	0.20	0.828	0.018	4.02	10.0	0.54	4.61	0.457	0.97

Table 2. The effect of refining on polymer effectiveness - polymers added to pulp after refining, softwood unbleached kraft - whole pulp.

Set No.	Additives % Based on Fiber	Fines content % through 200 mesh	Basis Weight, g/m²	Apparent Density, g/cc	Dry Strength Properties: Breaking Length, km Av.	SD	TEA, kgm/m² Av.	SD	Et, kg/cm Av.	SD	Stretch, % Av.	SD	Moisture Content % at 91-93% RH	Moist Strength Properties: Breaking Length, km Av.	SD	TEA, kgm/m² Av.	SD	Et, kg/cm Av.	SD	Stretch, % Av.	SD	Moist Tensile Factor
	Pulp slushed 5 min, no beating; 725 mL CSF																					
25	Blank Control	5.05	63.9	0.349	2.79	0.133	3.11	0.421	229	10.7	2.49	0.215	15.4	1.29	0.092	1.87	0.193	103	9.5	3.15	0.158	1.00
26	PAE, 1.5	—	67.3	0.370	4.77	0.263	7.73	0.745	302	12.8	3.57	0.181	15.1	3.01	0.109	6.50	0.464	123	6.4	5.21	0.230	2.33
27	PAE, 1.0; CMC, 0.4	—	64.5	0.381	5.30	0.207	8.61	0.629	303	8.3	3.85	0.290	15.2	3.57	0.208	7.86	0.910	122	9.5	5.65	0.260	2.77
28	PAE, 1.0; PAA, 0.2	—	64.4	0.387	5.69	0.224	9.63	0.962	331	12.1	3.89	0.289	15.2	3.64	0.142	8.30	0.530	135	5.0	5.66	0.205	2.82
29	PAE, 1.0; CMPS, 1.0	—	64.7	0.367	5.27	0.528	8.54	1.614	305	20.3	3.69	0.360	15.2	3.33	0.230	7.83	0.841	127	14.2	5.69	0.225	2.58
30	PEI, 1.0; PAA, 0.2	—	64.2	0.378	4.92	0.305	7.63	0.928	319	17.5	3.50	0.149	15.2	2.69	0.196	5.67	0.770	131	3.4	4.92	0.293	2.08
	Pulp slushed then beaten 10 min; 675 mL CSF																					
31	Blank Control	6.24	62.6	0.407	4.62	0.241	5.30	0.831	339	26.5	2.73	0.368	15.1	2.51	0.051	3.75	0.240	159	9.3	3.45	0.215	1.00
32	PAE, 1.5	—	63.2	0.423	7.32	0.242	10.9	1.02	391	5.0	3.64	0.211	14.9	5.12	0.279	10.4	1.07	163	7.1	5.39	0.278	2.04
33	PAE, 1.0; CMC, 0.4	—	64.5	0.433	7.80	0.408	11.9	1.03	417	18.3	3.67	0.137	15.3	5.52	0.161	11.9	0.81	180	4.5	5.56	0.194	2.20
34	PAE, 1.0; PAA, 0.2	—	60.4	0.427	7.58	0.347	11.0	1.00	379	12.8	3.70	0.167	15.2	5.29	0.279	10.6	0.88	166	13.5	5.41	0.266	2.11
35	PAE, 1.0; CMPS, 1.0	—	64.2	0.420	7.42	0.298	11.1	0.89	401	20.8	3.63	0.235	15.1	4.92	0.415	10.1	1.29	165	9.2	5.26	0.262	1.96
36	PEI, 1.0; PAA, 0.2	—	61.4	0.415	6.69	0.318	9.49	0.693	382	17.8	3.48	0.142	15.1	3.97	0.268	7.70	1.183	166	8.2	4.78	0.430	1.58
	Pulp slushed then beaten 25 min; 610 mL CSF																					
37	Blank Control	6.85	63.0	0.448	6.06	0.271	7.55	0.683	400	12.8	2.93	0.090	15.1	3.30	0.106	5.53	0.399	183	5.4	3.84	0.167	1.00
38	PAE, 1.5	—	63.0	0.464	8.30	0.368	12.5	1.27	421	10.6	3.77	0.235	14.9	6.08	0.213	12.3	1.13	184	3.7	5.23	0.295	1.84
39	PAE, 1.0; CMC, 0.4	—	62.8	0.466	9.00	0.482	13.8	0.95	449	25.5	3.84	0.139	14.9	6.60	0.451	13.3	0.86	202	12.9	5.34	0.103	2.00
40	PAE, 1.0; PAA, 0.2	—	64.7	0.486	8.84	0.531	13.6	1.74	481	7.4	3.74	0.298	14.9	6.43	0.231	14.0	0.71	217	10.0	5.39	0.178	1.95
41	PAE, 1.0; CMPS, 1.0	—	63.7	0.464	7.67	0.233	10.2	1.21	429	19.0	3.23	0.324	14.8	6.01	0.387	12.9	1.13	191	6.3	5.33	0.194	1.82
42	PEI, 1.0; PAA, 0.2	—	61.7	0.466	7.93	0.309	11.4	0.85	437	17.1	3.53	0.172	14.8	5.10	0.396	10.5	0.92	194	16.0	4.87	0.136	1.55
	Pulp slushed then beaten 50 min; 470 mL CSF																					
43	Blank Control	8.46	63.6	0.503	6.96	0.325	8.93	0.890	468	22.1	2.97	0.162	15.0	4.30	0.185	7.92	0.766	212	8.5	4.26	0.226	1.00
44	PAE, 1.5	—	63.8	0.520	9.33	0.994	14.1	2.65	497	21.7	3.64	0.403	14.6	7.37	0.294	15.1	0.92	224	12.4	5.35	0.116	1.71
45	PAE, 1.0; CMC, 0.4	—	61.6	0.516	9.28	0.911	13.4	2.83	479	26.1	3.63	0.425	14.7	7.11	0.248	12.6	0.77	218	3.1	5.20	0.173	1.65
46	PAE, 1.0; PAA, 0.2	—	61.3	0.520	9.90	0.612	14.8	1.12	481	33.6	3.84	0.189	14.7	7.01	0.351	12.2	1.00	218	4.0	5.06	0.216	1.63
47	PAE, 1.0; CMPS, 1.0	—	62.6	0.512	9.14	0.937	13.7	2.32	460	26.9	3.77	0.273	14.6	7.01	0.317	13.2	1.01	218	4.7	5.39	0.171	1.63
48	PEI, 1.0; PAA, 0.2	—	62.9	0.515	8.58	0.520	12.7	1.06	485	29.9	3.52	0.177	14.6	6.14	0.335	11.6	0.96	228	4.7	5.10	0.104	1.43

Table 2 continued. The effect of refining on polymer effectiveness - polymers added to pulp after refining, softwood unbleached kraft - whole pulp.

Set No.	Additives % Based on Fiber	Wet Breaking Length, km Av.	Wet Breaking Length, km SD	Wet Tensile Factor	Dry STFI Compressive Strength lbf/in. Av.	Dry STFI Compressive Strength lbf/in. SD	Moist STFI Compressive Strength lbf/in. Av.	Moist STFI Compressive Strength lbf/in. SD	Moist Compressive Strength Factor
	Pulp slushed 5 min, no beating; 725 mL CSF								
25	Blank Control	0.061	0.016	1.00	5.74	0.608	2.98	0.205	1.00
26	PAE, 1.5	1.30	0.056	21.3	8.05	0.583	4.10	0.278	1.38
27	PAE, 1.0; CMC, 0.4	1.52	0.072	24.9	8.64	0.756	4.14	0.495	1.39
28	PAE, 1.0; PAA, 0.2	1.33	0.083	21.8	8.33	0.804	4.05	0.327	1.36
29	PAE, 1.0; CMPS, 1.0	1.28	0.089	20.98	7.88	0.726	3.80	0.386	1.28
30	PEI, 1.0; PAA, 0.2	0.667	0.024	10.93	8.30	0.862	4.14	0.353	1.39
	Pulp slushed then beaten 10 min; 675 mL CSF								
31	Blank Control	0.127	0.013	1.00	7.51	0.689	3.85	0.376	1.00
32	PAE, 1.5	2.05	0.097	16.14	9.13	0.939	4.38	0.419	1.14
33	PAE, 1.0; CMC, 0.4	2.25	0.117	17.72	9.41	0.939	4.76	0.351	1.24
34	PAE, 1.0; PAA, 0.2	2.06	0.057	16.22	9.33	0.825	4.66	0.343	1.21
35	PAE, 1.0; CMPS, 1.0	1.79	0.157	14.09	9.16	0.837	4.60	0.351	1.19
36	PEI, 1.0; PAA, 0.2	0.941	0.049	7.41	9.16	0.973	4.27	0.417	1.11
	Pulp slushed then beaten 25 min; 610 mL CSF								
37	Blank Control	0.189	0.014	1.00	8.31	0.600	4.26	0.313	1.00
38	PAE, 1.5	2.58	0.107	13.65	9.61	0.531	4.80	0.294	1.13
39	PAE, 1.0; CMC, 0.4	2.47	0.160	13.07	10.0	0.77	5.07	0.361	1.19
40	PAE, 1.0; PAA, 0.2	2.55	0.099	13.49	10.7	1.13	4.92	0.538	1.15
41	PAE, 1.0; CMPS, 1.0	2.29	0.183	12.12	10.3	0.95	4.62	0.372	1.08
42	PEI, 1.0; PAA, 0.2	1.14	0.070	6.03	10.0	1.14	4.65	0.316	1.09
	Pulp slushed then beaten 50 min; 470 mL CSF								
43	Blank Control	0.206	0.029	1.00	9.59	0.562	4.76	0.316	1.00
44	PAE, 1.5	3.16	0.138	15.33	10.8	1.05	5.22	0.351	1.10
45	PAE, 1.0; CMC, 0.4	2.77	0.12	13.45	10.3	0.98	4.94	0.401	1.04
46	PAE, 1.0; PAA, 0.2	2.75	0.196	13.35	10.5	0.77	4.97	0.287	1.04
47	PAE, 1.0; CMPS, 1.0	2.59	0.149	12.57	10.5	0.89	4.99	0.336	1.05
48	PEI, 1.0; PAA, 0.2	1.30	0.062	6.31	10.8	0.70	5.12	0.310	1.08

beating time the treated pulps all have higher freenesses than the blank control does. At 50 minutes beating, however, PAE and PEI/PAA produce higher freenesses than the blank control while the treatment combinations PAE/CMC and PAE/PAA yield lower freenesses. These freeness results at 50 minutes beating do not appear to correlate with either the amount of fines (through 200 mesh) in the pulps nor with the various strength properties. The latter finding means that the increases in bond strength produced by the polymers have a much greater effect on the strength properties than does the freeness level.

In general, better strength was obtained by adding the bonding agent to the pulp after refining. For addition either before or after refining the relative improvement in strength over that of the untreated pulps decreased with increased refining. This supports our earlier findings that the strength additives produce larger relative effects with classified pulps than with beaten whole pulps. As expected, the absolute values of the strength increased with beating (Table 1 and 2).

It is not clear why addition of the bonding agents prior to refining did not produce the desired improvements in the strength properties. Two possibilities can be suggested. First, more than anticipated of the outer surface of the fibers (containing the adsorbed polymers) may be removed during refining. The end result would then be equivalent to addition of the strength aids to the fines fraction, which we have shown to be less effective[1]. Alternatively, the bonding agents adsorbed before refining may be partially overlaid with hemicelluloses or other material released during the refining process. The adsorption of this latter material onto the preadsorbed strength aids would largely nullify the expected improvement. Which, if either, of these explanations is the major contributor to the reduced strength improvement cannot be determined from the evidence in hand. The salient point, however, is that the bonding agents should be added after refining.

Another potential method to improve performance with whole pulps would be to minimize the adsorption of the strength aids onto the fines. It is well-known that fines, because of their large specific surface area, may adsorb a disproportionate share of chemical additives[2-4]. Additionally, because of their small size compared with the long fiber fraction, the fines have a much greater probability of collision (leading to adsorption) with the bonding agents. One method to reduce both the high collision probability and the large specific surface area of the fines is to attach them to the long fibers. If this can be done prior to the addition of the strength aids, their efficiency should be improved.

To achieve this attachment, we first added a polymeric retention aid of the type usually found effective in pulp fines retention. We used a cationic, high molecular weight, low charge density polyelectrolyte. Following a short period of moderate agitation to effect the fines retention, the strength additives were introduced and sheet making proceeded as usual. The results are presented in Table 3. At its low addition level the retention aid used alone had negligible effects on the dry strength properties and may have had a small deleterious effect on the moist properties. In combination with the bonding agents the presence of the retention aid gave reduced strength under both dry and moist conditions when compared with the cases where it was not used. It is not clear why the retention aid reduces rather than enhances the effectiveness of the bonding agents. Further work in progress may help to explain this behavior.

Table 3. The effect of a "fines retention aid" on duopolymer effectiveness; softwood unbleached kraft - whole pulp, 470 mL CSF.

Set No.	Additives, % Based on Fiber	Basis Weight, g/m^2	Apparent Density, g/cc	Breaking Length, km Av.	Breaking Length, km SD	Dry Strength Properties: TEA, kgm/m^2 Av.	TEA SD	Et, kg/cm Av.	Et SD	Stretch, % Av.	Stretch SD	Moisture Content, % at 91-93% RH	Moist Strength Properties: Breaking Length, km Av.	Breaking Length SD	TEA, kgm/m^2 Av.	TEA SD	Et, kg/cm Av.	Et SD	Stretch, % Av.	Stretch SD	Moist Tensile Factor
43	Blank Control	63.6	0.503	6.96	0.325	8.93	0.890	468	22.1	2.97	0.162	15.0	4.30	0.185	7.92	0.766	212	8.5	4.26	0.226	1.00
49	Retention Aid, 0.05	62.9	0.474	6.90	0.413	9.08	0.699	455	20.1	3.07	0.114	15.3	3.94	0.318	6.57	0.622	196	15.5	4.25	0.206	0.92
50	Retention Aid, 0.05; PAE, 1.0; CMC, 0.4	63.4	0.504	9.01	0.627	13.3	1.83	483	18.5	3.56	0.218	14.7	6.42	0.241	12.2	0.53	204	10.5	5.26	0.102	1.49
													6.32	0.523	11.9	1.25	198	10.5	5.37	0.252	1.47
51	Retention Aid, 0.05; PAE, 1.0; CMPS, 1.0	62.7	0.506	8.38	0.421	11.6	0.78	455	25.0	3.41	0.072	15.2	7.11	0.248	12.6	0.77	218	3.1	5.20	0.173	1.65
45	PAE, 1.0; CMC, 0.4	61.6	0.516	9.28	0.911	13.4	2.83	479	26.1	3.63	0.425	14.7	7.01	0.317	13.2	1.01	218	4.7	5.39	0.171	1.63
47	PAE, 1.0; CMPS, 1.0	62.6	0.512	9.14	0.937	13.7	2.32	460	26.9	3.77	0.273	14.6									

Set No.	Additives, % Based on Fiber	Wet Breaking Length, Km Av.	Wet Breaking Length, Km SD	Wet Tensile Factor	Dry/STFI Compressive Strength, lbf/in Av.	Dry/STFI SD	Moist STFI Compressive Strength, lbf/in Av.	Moist STFI SD	Moist Compressive Strength Factor
43	Blank Control	0.206	0.029	1.00	9.59	0.562	4.76	0.316	1.00
49	Retention Aid, 0.05	0.249	0.009	1.21	9.62	0.521	4.54	0.394	0.95
50	Retention Aid, 0.05; PAE, 1.0, CMC, 0.4	2.70	0.069	13.11	10.9	0.83	4.92	6.337	1.03
51	Retention Aid, 0.05; PAE, 1.0; CMPS, 1.0	2.51	0.145	12.18	10.3	0.99	4.86	0.368	1.02
45	PAE, 1.0; CMC, 0.4	2.77	0.102	13.45	10.3	0.98	4.94	0.401	1.04
47	PAE, 1.0; CMPS, 1.0	2.59	0.149	12.57	10.5	0.89	4.99	0.336	1.05

Another explanation for the reduced effectiveness of the strength aids when used with whole pulps concerns the dosages used. These dosages were earlier established[5] as the optimum for classified pulps. It is possible that whole pulps with larger specific surface areas may require higher dosages for maximum effect. Studies to ascertain such optimum dosages are planned for the near future.

Most of the previously reported work on this project was carried out at a pH of about 9. This was owing to the pH of the Appleton city water supply. Because it is thought that at least a part of the interaction of the duopolymer bonding agents with each other and with the fibers is ionic in nature, it was of interest to examine the effect of pH on the systems. A further incentive is that most paper is made under acid conditions.

To isolate the effects of ionic bonding, we chose duopolymer systems that had previously been shown[1] to produce no covalent bonding. These were combinations of the cationic polyethylenimine (PEI) with one of three carboxyl-containing polymers. In order of decreasing carboxyl content they were polyacrylic acid (PAA), carboxymethylcellulose (CMC), and carboxymethylated potato starch (CMPS). As the chosen pH's, PEI[6] has a charge density of 60% (pH 4.5) and 30% (pH 7). The dissociation and anionic charge of the PAA, CMC, and CMPS will increase over this pH range. Thus by varying the pH and the dosage ratio between the cationic and anionic polymers, the relative amounts of positive and negative charge in the system could be controlled. For this purpose the amount of PEI added was maintained constant at 1% (based on pulp), and the amount of the anionic polymer was systematically varied. The results are presented in Tables 4 and 5.

Table 4. The effect of anionic/cationic polymer ratio on strength properties at pH 7 (Softwood unbleached kraft - classified).

Set No.	Additives % Based on Fiber	Anionic/ Cationic Polymer Ratio	Basis Weight, g/m^2	Apparent Density, g/cc	Dry Strength Properties: Breaking Length, km Av.	SD	TEA, kgm/m^2 Av.	SD	Et, kg/cm Av.	SD	Stretch, % Av.	SD	Moisture Content, % at 91-93% RH	Moist Strength Properties: Breaking Length, km Av.	SD	TEA, kgm/m^2 Av.	SD	Et, kg/cm Av.	SD	Stretch, % Av.	SD	Moist Tensile Factor
1	Blank Control	--	59.8	0.427	4.23	0.157	3.7	0.53	336	12.2	2.1	0.21	16.5	2.19	0.073	3.08	0.454	135	6.5	3.3	0.31	1.00
2	PAE, 1.0	--	62.4	0.440	7.05	0.592	9.3	1.28	401	20.3	3.2	0.23	15.5	4.79	0.173	9.18	0.597	143	1.9	5.2	0.09	2.19
3	PAE, 1.5	--	59.2	0.433	7.79	0.524	10.9	1.32	393	15.0	3.6	0.24	15.9	5.07	0.236	9.14	0.433	143	6.7	5.2	0.09	2.31
4	PAE, 1.0; CMC, 0.4	0.4	65.3	0.473	8.57	0.244	13.4	0.57	485	22.9	3.7	0.15	16.1	5.88	0.358	12.3	1.30	172	6.0	5.6	0.18	2.68
5	PAE, 1.0; PAA, 0.2	0.2	64.1	0.466	8.46	0.526	12.9	0.85	472	34.1	3.7	0.12	15.8	5.66	0.308	11.9	1.21	182	4.2	5.4	0.29	2.58
6	PEI, 1.0	--	65.4	0.471	6.06	0.640	8.0	2.25	431	17.8	2.9	0.60	15.0	4.22	0.258	7.51	0.842	193	9.8	4.4	0.39	1.93
7	PEI, 1.0; CMC, 0.2	0.2	61.9	0.463	5.74	0.450	9.27	1.13	418	14.8	3.3	0.22	15.0	4.32	0.180	8.25	0.642	183	8.6	5.0	0.27	1.97
8	PEI, 1.0; CMC, 0.4	0.4	61.8	0.471	7.73	0.698	11.26	1.99	429	26.8	3.6	0.35	15.0	5.24	0.463	10.5	1.74	177	16.0	5.5	0.50	2.39
9	PEI, 1.0; CMC, 0.8	0.8	62.5	0.475	8.43	0.599	12.77	1.91	441	30.3	3.7	0.28	15.0	5.54	0.384	11.1	1.41	194	12.7	5.5	0.28	2.53
10	PEI, 1.0; PAA, 0.2	0.2	60.9	0.476	7.42	0.532	10.86	1.99	432	19.2	3.5	0.42	15.1	4.40	0.305	8.20	0.959	173	5.7	5.1	0.24	2.01
11	PEI, 1.0; PAA, 0.4	0.4	59.2	0.453	7.23	0.739	9.47	1.58	407	43.7	3.3	0.29	15.0	3.96	0.100	6.53	0.295	158	9.9	4.5	0.15	1.81
12	PEI, 1.0; PAA, 0.8	0.8	67.2	0.478	6.14	0.639	7.92	1.67	419	19.0	2.9	0.35	14.9	4.02	0.152	8.04	0.704	193	14.4	4.8	0.22	1.84
13	PEI, 1.0; CMPS, 0.2	0.2	63.2	0.473	6.45	0.352	8.94	0.80	409	14.4	3.2	0.13	15.1	4.21	0.242	7.40	0.947	182	7.4	4.5	0.25	1.92
14	PEI, 1.0; CMPS, 0.4	0.4	64.8	0.483	6.26	0.657	8.76	1.28	414	38.4	3.2	0.15	15.1	4.12	0.258	7.38	0.799	180	6.3	4.4	0.24	1.88
15	PEI, 1.0; CMPS, 0.8	0.8	65.8	0.478	6.91	0.299	10.53	1.38	416	3.0	3.5	0.31	14.9	4.34	0.253	8.07	0.709	189	11.3	4.6	0.17	1.98
16	PEI, 1.0; CMPS, 1.2	1.2	62.3	0.466	6.69	0.443	9.36	0.877	401	27.1	3.4	0.09	14.9	4.01	0.212	6.50	0.562	178	12.8	4.3	0.12	1.83

Table 4 continued. The effect of anionic/cationic polymer ratio on strength properties at pH 7, (softwood unbleached kraft - classified)

Set No.	Additives, % Based on Fiber	Wet Breaking Length, km Av.	Wet Breaking Length, km SD	Wet Tensile Factor	Dry STFI Compressive Strength lbf/in. Av.	Dry STFI Compressive Strength lbf/in. SD	Moist STFI Compressive Strength lbf/in. Av.	Moist STFI Compressive Strength lbf/in. SD	Moist Compressive Strength Factor
1	Blank Control	0.117	0.008	1.00	6.88	0.737	3.19	0.241	1.00
2	PAE, 1.0	1.97	0.070	16.84	8.71	0.625	4.15	0.377	1.30
3	PAE, 1.5	2.07	0.078	17.69	8.50	0.874	3.48	0.489	1.09
4	PAE, 1.0; CMC, 0.4	2.63	0.177	22.48	11.04	1.07	4.18	0.310	1.31
5	PAE, 1.0; PAA, 0.2	2.35	0.106	20.08	10.51	0.741	4.20	0.422	1.32
6	PEI, 1.0	1.016	0.046	8.68	9.74	0.676	4.45	0.397	1.39
7	PEI, 1.0; CMC, 0.2	1.024	0.030	8.75	9.61	0.787	4.59	0.454	1.44
8	PEI, 1.0; CMC, 0.4	1.233	0.120	10.5	9.88	0.644	4.71	0.489	1.48
9	PEI, 1.0; CMC, 0.8	1.257	0.049	10.7	10.7	0.78	5.02	0.566	1.57
10	PEI, 1.0; PAA, 0.2	1.045	0.061	8.93	9.27	0.904	4.30	0.383	1.35
11	PEI, 1.0; PAA, 0.4	0.817	0.101	6.98	8.88	1.42	4.88	0.495	1.53
12	PEI, 1.0; PAA, 0.8	0.633	0.028	5.41	10.4	1.06	5.09	0.729	1.60
13	PEI, 1.0; CMPS, 0.2	0.962	0.051	8.22	9.47	0.742	4.87	0.238	1.53
14	PEI, 1.0; CMPS, 0.4	0.893	0.088	7.63	9.76	1.05	4.79	0.564	1.50
15	PEI, 1.0; CMPS, 0.8	0.938	0.061	8.01	10.5	1.38	4.87	0.503	1.53
16	PEI, 1.0; CMPS, 1.2	0.835	0.028	7.14	9.84	1.16	4.86	0.556	1.52

Table 5. The effect of anionic/cationic polymer ratio on strength properties at pH 4.5 (softwood unbleached kraft - classified).

Set No.	Additives % Based on Fiber	Anionic/ Cationic Polymer Ratio	Basis Weight, g/m^2	Apparent Density, g/cc	Dry Strength Properties: Breaking Length, km Av.	SD	TEA, kgm/m^2 Av.	SD	Et, kg/cm Av.	SD	Stretch, % Av.	SD	Moisture Content, % at 91-93% RH	Moist Strength Properties: Breaking Length, km Av.	SD	TEA, kgm/m^2 Av.	SD	Et, kg/cm Av.	SD	Stretch, % Av.	SD	Moist Tensile Factor
17	Blank Control	---	63.2	0.426	3.61	0.263	3.21	0.62	312	16.2	2.02	0.240	15.0	1.99	0.094	2.95	0.195	136	8.2	3.28	0.242	1.00
18	PAE, 1.0	---	63.6	0.438	6.03	0.336	8.33	0.347	355	26.4	3.29	0.059	15.0	4.43	0.258	8.75	0.415	161	8.7	5.15	0.180	2.23
19	PAE, 1.5	---	61.1	0.433	5.94	0.554	7.67	0.960	341	28.1	3.20	0.120	14.8	4.42	0.323	8.16	0.838	152	7.7	5.03	0.198	2.22
20	PAE, 1.0; CMC, 0.4	0.4	66.5	0.453	7.64	0.682	11.99	1.81	423	27.7	3.67	0.277	15.4	5.41	0.204	11.8	0.81	167	10.1	5.50	0.373	2.72
21	PAE, 1.0; PAA, 0.2	0.2	65.6	0.445	7.08	0.256	11.33	1.283	396	22.2	3.77	0.391	15.1	4.73	0.309	9.97	0.901	167	9.5	5.13	0.506	2.38
22	PEI, 1.0	---	65.4	0.438	4.93	0.249	6.36	0.549	366	23.5	2.87	0.144	15.0	2.96	0.207	5.11	0.584	155	11.6	4.08	0.212	1.49
23	PEI, 1.0; CMC, 0.2	0.2	66.4	0.437	5.26	0.632	6.98	1.474	374	36.8	2.91	0.306	15.0	3.48	0.399	6.54	1.081	158	14.1	4.60	0.275	1.75
24	PEI, 1.0; CMC, 0.4	0.4	68.5	0.452	6.14	0.410	9.65	1.146	395	9.9	3.43	0.210	14.9	3.90	0.180	7.79	0.607	170	7.9	4.82	0.139	1.96
25	PEI, 1.0; CMC, 0.8	0.8	64.0	0.439	6.76	0.604	9.95	1.659	397	17.6	3.45	0.304	15.1	3.59	0.343	6.71	1.210	143	9.5	4.70	0.427	1.80
26	PEI, 1.0; PAA, 0.2	0.2	67.1	0.438	5.94	0.116	8.64	0.801	403	15.8	3.19	0.273	15.1	3.41	0.219	6.39	0.593	174	11.2	4.22	0.194	1.71
27	PEI, 1.0; PAA, 0.4	0.4	60.9	0.422	6.53	0.733	8.69	0.910	377	32.3	3.36	0.208	15.0	3.38	0.307	5.75	0.954	146	7.5	4.35	0.321	1.70
28	PEI, 1.0; PAA, 0.8	0.8	57.6	0.412	7.14	0.413	9.74	1.574	365	7.9	3.57	0.351	15.0	3.81	0.178	6.78	0.693	137	4.4	4.71	0.253	1.91
29	PAE, 1.0; CMPS, 0.4	0.4	60.7	0.423	6.30	0.091	8.72	0.675	341	12.2	3.45	0.267	14.8	4.19	0.183	7.60	0.864	142	3.8	4.89	0.282	2.10
30	PAE, 1.0; CMPS, 1.2	1.2	64.1	0.443	7.09	0.423	10.81	1.305	387	20.2	3.66	0.268	14.8	4.59	0.177	8.84	0.586	152	6.8	5.12	0.143	2.31

Table 5 continued. The effect of anionic/cationic polymer ratio on strength properties at pH 4.5 (softwood unbleached kraft classified).

Set No.	Additives % Based on Fiber	Wet Breaking Length, km Av.	SD	Wet Tensile Factor	Dry STFI Compressive Strength lbf/in. Av.	SD	Moist STFI Compressive Strength lbf/in. Av.	SD	Moist Compressive Strength Factor
17	Blank Control	0.120	0.009	1.00	6.47	0.634	3.51	0.290	1.00
18	PAE, 1.0	1.54	0.057	12.8	7.95	0.687	4.10	0.515	1.17
19	PAE, 1.5	1.57	0.119	13.1	7.40	0.628	3.91	0.346	1.11
20	PAE, 1.0; CMC, 0.4	2.08	0.207	17.3	9.67	1.221	4.54	0.494	1.29
21	PAE, 1.0; PAA, 0.2	1.71	0.097	14.3	9.01	0.618	4.36	0.299	1.24
22	PEI, 1.0	0.679	0.046	5.7	7.83	0.986	4.08	0.496	1.16
23	PEI, 1.0; CMC, 0.2	0.782	0.086	6.5	9.11	1.330	4.35	0.647	1.24
24	PEI, 1.0; CMC, 0.4	0.874	0.055	7.3	9.16	1.170	4.52	0.368	1.29
25	PEI, 1.0; CMC, 0.8	0.769	0.0459	6.4	8.76	1.090	4.24	0.551	1.21
26	PEI, 1.0; PAA, 0.2	0.799	0.044	6.6	8.98	0.874	4.42	0.458	1.26
27	PEI, 1.0; PAA, 0.4	0.708	0.067	5.9	8.04	0.635	3.93	0.420	1.12
28	PEI, 1.0; PAA, 0.8	0.679	0.027	5.7	7.58	0.735	3.66	0.484	1.04
29	PAE, 1.0; CMPs, 0.4	1.44	0.026	12.0	7.40	0.727	3.66	0.363	1.04
30	PAE, 1.0; CMPS, 1.2	1.54	0.095	12.8	8.32	0.869	4.17	0.403	1.19

For almost all the measurements, sheets prepared at pH 7 gave superior results compared with the corresponding sheets at pH 4.5. As noted in previous work[1], additives which can form ionic bonds only give inferior strength compared with covalent bond formers (PAE, PAE/CMC, PAE/PAA). The notable exception is the moist STFI compression strength data at pH 7. Here the ionic-bonding agents give higher values than the covalent bonding materials. Unfortunately, the moisture content for the latter tests was about 1% higher than normal. Whether this is sufficient to account for the apparent reversal in trend is not known. This reversal does not show up in the moist tensile results. However, it has previously been noted[1] that tensile and STFI compression strength are each apparently governed by different fiber and sheet properties.

No consistent trends with respect to the effect of the ratio of cationic to anionic charges on the mechanical properties are evident. For example, for the system PEI/PAA at pH 4.5, the dry breaking length increases with increasing amounts of PAA, but both dry and moist STFI compression strength go through a maximum and decrease thereafter with PAA dosage. Generally, there appears to be a good correlation between the dry or moist STFI data and the dry and moist values of the stiffness (Et). This might be anticipated since the STFI test should be a function both of fiber/fiber bonding and individual fiber stiffness.

If only the dry and moist tensile strength data are considered, with few exceptions strength increased with increasing anionic polymer dosage. As mentioned above, corresponding trends in stiffness (Et), wet tensile strength, and dry and moist STFI compressive strength were not found. This indicates that the additives are affecting the various mechanical properties differently. Much remains to be learned about how the polymeric additives mediate changes in strength and stiffness.

PART TWO: Fundamentals of Bonding

A. Development of techniques for Model II fiber load/elongation recorder.

We have found that plasticized phenoxy resin seems to be a satisfactory hot melt adhesive for gripping a fiber end, thus permitting successful fiber mounting and tensile testing. In work outside this project, one of our students, Garth Kolterjahn, is beginning work in which he will determine the tensile characteristics of individual, pulped, southern pine latewood fibers at various moisture contents.

B. Single fiber/fiber bonds.

We have now completed measurements on the following fibers: loblolly pine (earlywood and latewood), southern pine (lightly refined 570 mL CSF), southern pine (heavily refined, 370 mL CSF), and a western hemlock TMP. For all except the latewood pine we have also determined bond parameters for fibers treated in slurry form with 1% PAE/0.4% CMC. The results are presented in Table 6.

There has been some debate among papermakers concerning the relative bond strengths of earlywood fibers compared with latewood fibers. Intuition would favor earlywood. Its cell wall is thinner, should collapse more easily, and should be more conformable under pressure. The collapsed fibers will also be wider than a latewood fiber with a corresponding larger surface for potential bonding with another fiber. The present results do not bear out intuition. The bond area, as expected, is lower for the latewood, but both the breaking load and specific bond strength are higher. It is difficult to rationalize these findings.

Table 6. Average fiber/fiber bond parameters.

	Type of Fibers				
	Earlywood	Latewood	Lightly Refined	Heavily Refined	TMP
Untreated Fibers					
Breaking Load, g	0.44	0.87	0.73	0.75	0.40
Bond Area, μm^2	2530	1500	2070	1350	760
Specific Bond Strength, $g/\mu m^2$	220	650	360	600	810
Treated Fibers (1% PAE/0.4% CMC)					
Breaking Load, g	1.14	-	1.44	1.47	1.28
Bond Area, μm^2	2970	-	2130	1600	1620
Specific Bond Strength, $\mu g/\mu m^2$	390	-	760	1030	1040

The comparison of light and heavy refining also provides some surprises. The breaking loads are the same while the bonded area decreases with refining. Their ratio (specific bond strength) increases with refining as does sheet strength properties. The reason for the decrease in bond area is not clear. Although increasing internal fibrillation in the cell wall should provide better conformability (and a larger bond area), the increasing disruption of the surface (external fibrillation) may interrupt bonding. The presence of "fines material" in the bond area (between the fibers) was evident in both optical and SEM micrographs. Whether this "fines material" is redeposited fines or outer wall material that is only torn partly free from the parent fiber cannot be determined at present. It would appear that the effect of refining is to "soften" the fiber wall so that more effective bonding can occur in those areas where intimate contact is possible.

The results for the untreated TMP are also interesting. We found it very difficult to produce fiber/fiber bonds from these stiff fibers. Many failed to bond under our pressing and drying conditions, and many more were so weak that they failed during sample preparation. The breaking load for TMP is correspondingly low. Because of the rather rigid character of these fibers, conformability and hence bond area is low. It is surprising then that the specific bond strength for this material is the highest of any (untreated) fibers that we have measured. Whether flow of the lignin and contributions to the bond strength by it are likely at this temperature (105°C) and time (1 hr) are not known. Further work is indicated to resolve this anomaly.

Comparison of the untreated with the corresponding treated fibers gives similar results to those reported previously[1]. All three bond parameters increase upon treatment with the strength aid. The bond area for the TMP fibers increases by more than a factor of two. There is no explanation for this at present. For the treated fibers the same trend with refining is found; breaking load is unchanged, bond area decreases and specific bond strength increases. For the TMP fibers the percent increase in the specific bond strength upon treatment with the additives is much less than for the other pulps. Nevertheless, the treated TMP bonds are among the strongest we have tested.

The results of these studies confirm those on the handsheets[1]. The additives are able to enhance the strength properties of a variety of pulps. The effect can be seen at both the level of the individual fiber/fiber bond and on a large assembly of such bonds (handsheet).

LITERATURE CITED

1. Progress Report Two, Project 3526, Fundamentals of Internal Strength Enhancement, The Institute of Paper Chemistry, 1986.
2. Marton J., Tappi 63(2): 121(1980).
3. Marton, J., Ind. Eng. Chem. Prod. Res. Dev. 21(2): 146(1982).
4. Marton, J., and Marton, T., Tappi Journal. 65(11): 105(1982).
5. Progress Report One, Project 3526, Fundamentals of Internal Strength Enhancement, The Institute of Paper Chemistry, 1984.
6. Lindquist, G. M., and Stratton R. A., Journal Coll. Interface Sci., 55, 45(1976).

THE INSTITUTE OF PAPER CHEMISTRY

Appleton, Wisconsin

Status Report

to the

PAPER PROPERTIES AND USES

PROJECT ADVISORY COMMITTEE

Project 3571

BOARD PROPERTIES AND PERFORMANCE

February 13, 1987

PROJECT SUMMARY

PROJECT NO. 3571: BOARD PROPERTIES AND PERFORMANCE February 13, 1987

PROJECT STAFF: W. J. Whitsitt, R. A. Halcomb

PROGRAM GOAL:

Develop relationships between critical paper and board property parameters and how they are achieved in terms of raw material selection, principles of sheet design, and processing conditions.

PROJECT OBJECTIVE:

- To develop relationships between container performance, combined board and component properties.

- To improve the performance/cost ratios of combined board (including medium).

- The short term goals are directed to (1) using structural models to assess the impact of papermaking factors on combined board and box performance and (2) improving medium end-use and converting performance properties.

PROJECT RATIONALE, PREVIOUS ACTIVITY AND PLANNED ACTIVITY FOR FISCAL 1987-88 are on the Project Form that follows.

SUMMARY OF RESULTS LAST PERIOD: (April 1986 - September 1986)

Section 1 - ECT/Box Compression

(1) Models are being developed to evaluate the impact of papermaking improvements on ECT strength per unit weight of fiber in the components.

(2) Preliminary results suggest that the following papermaking factors can improve strength-to-weight ratios.
a) Increased fiber-to-fiber bonding of the liners and medium.
b) Decreased MD/CD ratios (directionality).

Section 2 - Medium Improvement

(1) For a given Concora, CD STFI strength can vary over a wide range. Higher CD STFI strengths are favored by increased wet pressing, refining, and less directionality.

(2) For heavy weight mediums at least, it should be possible to reduce flat crush levels but increase ECT strengths.

Section 3 - Runnability Modeling

(1) Our runnability model shows that flute fracture speeds and high-lows depend on four properties of the medium. They are MD tensile, MD stretch, hot coefficient of friction and thickness.

(2) Linear and curvilinear relationships between stress ratios calculated from the model and high-lows have been developed. Both forms show high correlations.

(3) At a constant high-low level, a sensitivity analysis shows that changes in stretch and thickness have the greatest effect on operating speeds. Friction and MD tensile have slightly lower effects than the other two properties.

Section 4 - Periodicites in high-low flute formation.

(1) Activities during this period have concentrated on spectral analysis techniques. A significant periodic component with a period of about 5-6 flutes continues to be observed.

Section 5 - Flat crush modeling.

(1) The use of different medium physical properties (E_{MD}, G_{MD-ZD} and caliper) produced significant changes in the load-deflection curves generated by the finite element analysis. Knowledge of the fluted medium physical properties, both before and during loading, will determine the accuracy of the flat crush finite element analysis.

(2) A finite element program capable of material and geometric nonlinear analysis will be necessary to conduct extensive studies of paper materials.

SUMMARY OF RESULTS THIS PERIOD: (October 1986 - March 1987)

(1) For similar papermaking conditions 40-lb mediums give 15-20% lower ECT strengths per weight of medium fiber than 26-lb mediums because they are damaged more in the fluting operation.

(2) Bulky sheets exhibit quite poor flat crush strengths per weight of medium fiber and this is particularly true at high basis weights. This is also a result of fluting damage.

(3) There should be opportunities to improve medium performance by achieving a better balance of ECT and flat crush strengths.

(4) Sheet porosity appears to be adversely affected by increasing fiber alignment in the machine direction.

Section 2. Runnability modeling.

(1) The wrap angle of the medium over the flute tips in the corrugating nip has been verified to be an important factor in our runnability model.

(2) The wrap angles for A-, B-, and C-flute profiles exhibit a sawtooth pattern depending on the relative position of the flute in the nip. This indicates that the medium is subjected to appreciable tension pulses even though the average brake tension is held constant.

(3) Corrugating trials showed that mediums run on B-flute rolls exhibited higher fracture speeds than when run on C-flute rolls.

(4) B-flute board generally gave fewer high-lows at a given speed than C-flute board.

(5) Good predictions of B-flute runnability were obtained using a wrap angle of 2.3 radians in our model. This compares with a wrap angle of 3.09 radians for C-flute.

Section 3 - ECT/Box Compression

(1) Models are being developed to optimize ECT, combined board flexural stiffness and box compression taking into account various papermaking changes in the manufacture of linerboard and medium.

(2) Improvements in liner compressive strength and elastic moduli improve ECT and flexural stiffness and, hence box compressive strength.

(3) Improvements in medium properties increase ECT and box compression but have small effects on flexural stiffness. However, stronger mediums should resist abuse in the distribution system which is a beneficial factor not taken into account as yet.

Date:	1/21/87
Budget:	$160,000
Period Ends:	6/30/88
Project No:	3571

PROJECT TITLE: Board Properties and Performance

PROJECT STAFF: W. Whitsitt/R. Halcomb/J. Dees

PRIMARY AREA OF INDUSTRY NEED: Properties related to end uses.

PROGRAM AREA: Performance and Properties of Paper and Board

PROGRAM GOAL:

Develop relationships between critical paper and board property parameters and determine how they are achieved in terms of raw materials, sheet design, and processing conditions.

PROJECT OBJECTIVE/GOAL:

- To develop relationships between container performance, combined board properties, and component properties.
- To improve the performance/cost ratios of combined board, linerboard, and medium.
- The short term goals are to (1) use structural models to assess the impact of papermaking factors on combined board and box performance and (2) improve medium end-use and converting performance properties.

PROJECT RATIONALE:

There are many aspects of container and component performance which have not been adequately related to board properties through sound structural models. Such models would identify the critical board properties needed for end use performance. They would be used to select papermaking approaches to maintain or improve box performance at less cost. An important step is to incorporate the elastic stiffnesses of the board into such models, if possible. This will enable us to use our knowledge on how papermaking factors affect the elastic stiffnesses to make board improvements.

RESULTS TO DATE:

Past analyses of container failure under several types of load using Rayleigh-Ritz methods have shown that compressive strength (ECT) is the limiting property. Analysis of present ECT vs. component local buckling models indicates they fail to predict ECT performance when the liner or medium density is changed. Therefore new models have been developed which show that combined board ECT is primarily dependent on the compressive strength and/or elastic stiffnesses of the liners and medium. The bending stiffness of the liners appears to have only a minor effect on ECT. The importance of linerboard bending stiffness has been a point of concern to our industry and these results indicate that it is much less important than compressive strength. These results have been experimentally validated and are being extended to combined board flexural stiffness and box compression. Initial results show that basis weight/performance property ratios can be improved via densification and MD/CD changes.

In the case of medium we have shown that the compressive strength is lowered by high bending and shear stresses imposed during forming. These losses in strength lower flat crush and ECT. The losses are inversely related to the density and Z-direction elastic stiffness of the medium. Densification via wet pressing is one way to improve end-use performance of medium.

Our current forming models indicate that satisfactory high speed runnability on the corrugator is dependent on at least four medium properties as well as nip geometry and medium web tension. Better runnability is obtained as MD tensile strength and stretch are increased and the coefficient of friction of the medium and medium thickness are decreased.

PLANNED ACTIVITY FOR FY 1987-88:

As noted above, our short term objectives are directed to (1) using structural models to assess the impact of papermaking factors on combined board and box performance and (2) improving medium end-use and converting performance properties. The structural models we are developing show how the elastic stiffnesses and compressive strengths of the components will affect combined board compressive strength (ECT) and box compressive strength.

During 1987 we will expand these analyses to optimize strength-to-weight ratios. This will include consideration of the impact of papermaking changes on ECT, combined board flexural stiffness and box compression in relation to combined board basis weight. Both commercial and experimental boards will be used to validate the work. Another part of our structural research is directed to identifying the main medium properties affecting the flat crush load-deflection properties of combined board. For this purpose finite element techniques are being used to determine the stresses involved in forming the flute arch and their subsequent effects on converting and end-use performance.

In the converting area we have developed a model which reveals that critical speeds for flute fracture and high-lows depend on four properties of the medium, the nip geometry of the fluting rolls, and the medium web tension. During FY 1987-88 we plan to expand our model to consider other flute geometries and to study the potential effects of papermaking changes on both runnability and compressive strength. Currently data is being collected to determine how strength losses during fluting are related to the model stress predictions.

In another part of our fluting work power spectral techniques are being used to determine why high-lows tend to occur at periodic intervals and to relate the frequencies involved to machine elements. While a part of this work will be shifted over to FKBG, basic research on vibration phenomena as related to high-low generation will continue under this project.

Status Report

BOARD PROPERTIES AND PERFORMANCE

Project 3571

The objectives of this project are to (1) develop relationships between container performance, combined board and component properties, and (2) determine ways to improve the cost/performance ratios of linerboard and medium. Therefore our work is concerned with processing runnability on the corrugator and end-use performance. Our current research is comprised of several parts as follows: (1) medium improvement, (2) runnability modeling, (3) ECT and box compression performance, and (4) flat crush modeling.

We presented two papers at the TAPPI Corrugated Container Conference last fall on compressive strength retention during fluting. Strength losses in fluting were subject of the first paper which has now been published in the February issue of the Tappi Journal. The second article discussed ways to retain more medium strength during fluting and will be published in the Tappi Journal. Copies of the two papers are appended.

Medium Improvement

Medium requirements include both MD and CD strengths for end-use. Good runnability involves MD strength as well as a low friction coefficient and minimum bulk. As papermaking changes are made to increase medium strength it should be possible to square up the sheet to improve CD strength for improved ECT and still maintain adequate flat crush and runnability. As discussed in the last status report we are developing information on papermaking ways to optimize properties considering flat crush, CD compressive strength and runnability. For this purpose experimental 26 and 40-lb mediums were made using combinations of pressing, refining, directionality and basis weight.

Table 1 summarizes selected compression properties of the mediums and the combined board made therefrom. Figure 1 shows that CD short span compression (STFI) strengths can vary widely at a given minimum Concora level. For example, for a minimum Concora level of 1.9 Nm^2/g, CD STFI strengths could vary between about 16 to 30 Nm/g. Combined board flat crush and ECT results show similar trends as discussed in the October status report.

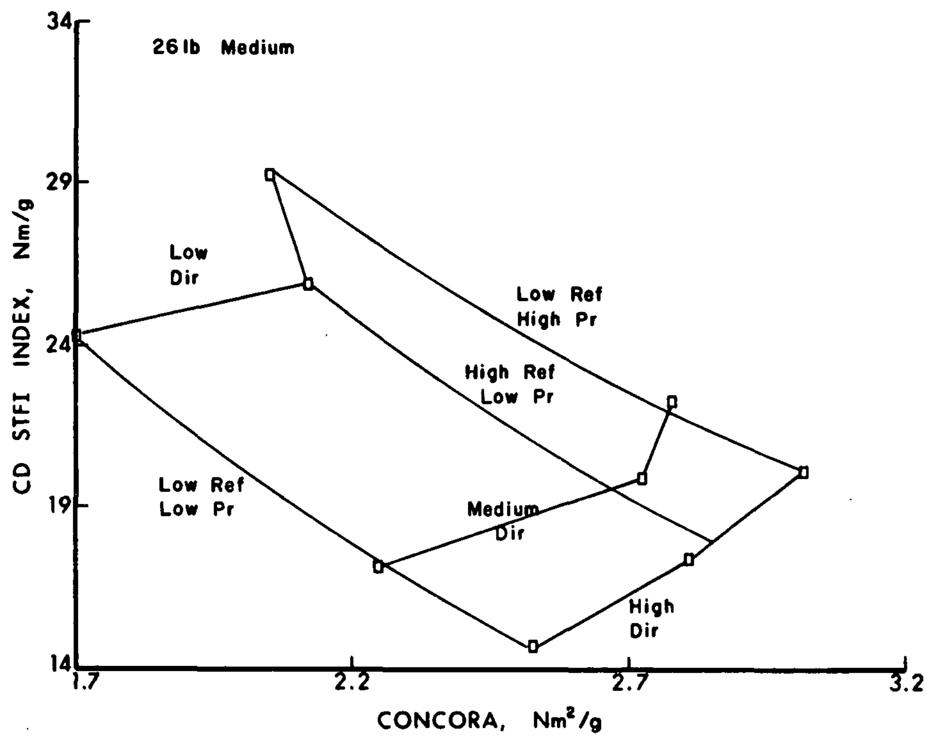

Figure 1. Relationships between CD STFI compressive strength and Concora for 40-lb mediums.

In Table 2 the ECT and flat crush results have been divided by the medium basis weight to compare the effects of the fluting operation on compressive strength. For 26-lb mediums Fig. 2 shows that the ECT strengths per weight of medium fiber ranged from 1.63 to 2.14 lb/in./lb, a difference of about 38%. The sheets with the lower directionality and higher fiber-to-fiber bonding exhibited the higher ECT strength/weight ratios. In this instance the more highly wet pressed mediums gave somewhat higher ratios than the more refined

Table 1. Physical characteristics of experimental mediums.

Lot. No.	Test Factors: Wet Pressing	MD/CD	Refining	Basis Weight, g/m2	Density IPC kg/m3	MD STFI lb/in.	CD STFI lb/in.	MD Tensile lb/in.	CD Tensile lb/in	MD Stretch, %	CD Ring Crush, lb/6 in.	Concora, lb	Flat Crush lb/sq-in.	ECT, lb/in.
3761-43	High	Low	Low	125.80	742	21.8	21.0	42.9	34.0	2.13	51.6	58.0	35.51	55.1
3761-45	High	Medium	Low	130.10	759	29.9	16.6	57.7	22.5	1.83	50.0	81.2	47.88	53.0
3761-46	High	High	Low	131.70	755	32.5	15.1	63.7	19.6	1.74	50.0	89.3	56.04	51.5
3761-34	Low	Low	Low	125.00	524	17.9	17.3	33.8	28.4	1.76	47.6	47.8	27.68	49.1
3761-36	Low	Medium	Low	127.00	540	25.1	12.4	45.4	18.1	1.48	41.2	64.2	37.77	46.5
3761-37	Low	High	Low	133.20	550	29.2	11.2	52.7	16.0	1.44	40.4	75.7	42.97	44.6
3761-24	Low	Low	High	141.00	560	22.1	20.8	41.0	31.7	1.72	62.2	67.2	38.94	53.9
3761-27	Low	Medium	High	133.60	586	29.5	15.2	54.3	22.0	2.05	52.2	81.8	47.94	48.5
3761-28	Low	High	High	128.60	589	29.2	12.8	54.4	17.7	1.51	43.8	81.2	51.16	47.2
3761-48	High	Low	Low	197.40	703	33.9	32.3	62.5	53.4	2.28	109.2	90.8	54.99	68.0
3761-50	High	Medium	Low	201.80	729	46.3	27.5	84.1	38.5	1.96	101.6	107.8	68.35	62.9
3761-51	High	High	Low	204.40	735	50.2	25.1	97.6	33.6	2.02	101.6	136.0	83.34	60.2
3761-39	Low	Low	Low	193.60	526	28.4	26.9	50.9	44.6	1.78	82.2	62.7	31.82	58.5
3761-41	Low	Medium	Low	197.00	553	37.9	21.1	74.2	29.8	1.74	72.8	81.7	35.11	52.7
3761-42	Low	High	Low	205.70	563	45.5	19.5	83.8	28.7	1.61	76.2	97.2	40.41	53.0
3761-29	Low	Low	High	187.90	545	30.0	26.4	53.1	41.8	1.93	89.6	79.8	46.24	59.7
3761-31	Low	Medium	High	191.80	562	38.7	21.7	72.7	32.0	1.92	87.4	105.7	58.93	56.5
3761-33	Low	High	High	197.00	580	44.2	20.7	81.7	29.0	1.62	82.6	125.8	62.49	53.7

Table 2. Summary of combined board test properties.

Lot No.	Test Factors: Wet Pressing	Test Factors: MD/CD	Test Factors: Refining	Medium Basis Wt., g/m2	Medium Density, kg/m3	Basis Weight, lb/M sq ft	Caliper, mil	MD Stiffness, lb-in	CD Stiffness, lb-in	Geom. Mn. Stiff., lb-in	Flat Crush, psi	Flat Crush, psi/lb	ECT, lb/in	ECT, lb/in./lb
3761-43	High	Low	Low	125.8	742	124.2	168.3	140.8	60.7	92.4	35.5	1.38	55.1	2.14
3671-45	High	Medium	Low	130.1	759	125.6	168.7	139.3	57.7	89.7	47.9	1.80	53.0	1.99
3761-46	High	High	Low	131.7	755	127.9	169.4	140.6	56.6	89.2	56.0	2.08	51.5	1.91
3761-34	Low	Low	Low	125.0	524	124.3	167.1	136.0	58.6	89.3	27.7	1.08	49.1	1.92
3761-36	Low	Medium	Low	127.0	540	126.8	168.6	137.3	55.9	87.6	37.8	1.45	46.5	1.79
3761-37	Low	High	Low	133.2	550	126.8	168.3	137.2	54.4	86.4	43.0	1.57	44.6	1.63
3761-24	Low	Low	High	141.0	560	128.7	168.4	141.1	60.4	92.3	38.9	1.35	53.9	1.87
3761-27	Low	Medium	High	133.6	586	127.5	168.7	140.4	55.5	88.3	47.9	1.75	48.5	1.77
3761-28	Low	High	High	128.6	589	125.0	168.2	141.3	55.3	88.4	51.2	1.94	47.2	1.79
3761-48	High	Low	Low	197.4	703	144.8	169.6	140.1	66.4	96.4	55.0	1.36	68.0	1.68
3761-50	High	Medium	Low	201.8	729	144.3	170.0	144.5	61.0	93.9	68.4	1.65	62.9	1.52
3761-51	High	High	Low	204.4	735	146.4	170.4	143.0	58.0	91.1	83.3	1.99	60.2	1.44
3761-39	Low	Low	Low	193.6	526	144.6	169.9	139.1	63.1	93.7	31.8	0.80	58.5	1.48
3761-41	Low	Medium	Low	197.0	553	145.1	169.5	137.1	57.1	88.4	35.1	0.87	52.7	1.31
3761-42	Low	High	Low	205.7	563	148.2	170.1	139.2	56.6	88.7	40.4	0.96	53.0	1.26
3761-29	Low	Low	High	187.9	545	143.1	170.1	143.6	64.4	96.1	46.2	1.20	59.7	1.55
3761-31	Low	Medium	High	191.8	562	144.3	170.0	140.0	60.4	92.0	58.9	1.50	56.5	1.44
3761-33	Low	High	High	197.0	580	144.7	170.6	140.6	57.4	89.8	62.5	1.55	53.7	1.33

sheets but this would be expected to vary depending on the relative amounts of pressing and refining.

The ECT results for the 40-lb mediums in Fig. 3 show similar trends with pressing, refining and directionality. Because of their greater thicknesses they suffer more damage in the fluting operation and, hence exhibit lower ECT strength/weight ratios than the 26-lb mediums. Even so, better wet pressing and lower directionality can significantly improve ECT strengths.

Fig. 4 and 5 compare the combined board flat crush strengths per weight of medium fiber. Flat crush is quite sensitive to fluting damage. For example, for 26-lb mediums the strength/weight ratios ranged from 1.08 to 2.08 psi/lb and from 0.8 to 1.99 psi/lb for 40-lb mediums made under these conditions. Both wet pressing and refining increased the strength/weight ratios as expected however increased wet pressing was particularly effective because of its marked lowering of caliper. The combinations made using low pressing and little refining gave very low flat crush strength/weight ratios at a given directionality

The 26-lb mediums were corrugated at speeds of 600 and 800 fpm; the speeds for the 40-lb mediums were 400 and 600 fpm. None of the mediums fractured at these speeds. Table 3 compares the high-low results in terms of the percent of height differences between adjacent flutes which exceeded 3 and 4 mils. Because of the variability of the process small differences between conditions are not significant. In the case of the 40-lb mediums lower high-lows were generally, but not always, favored by low-to-medium orientation and better fiber bonding. These results will be analyzed in more detail as soon as friction tests are completed.

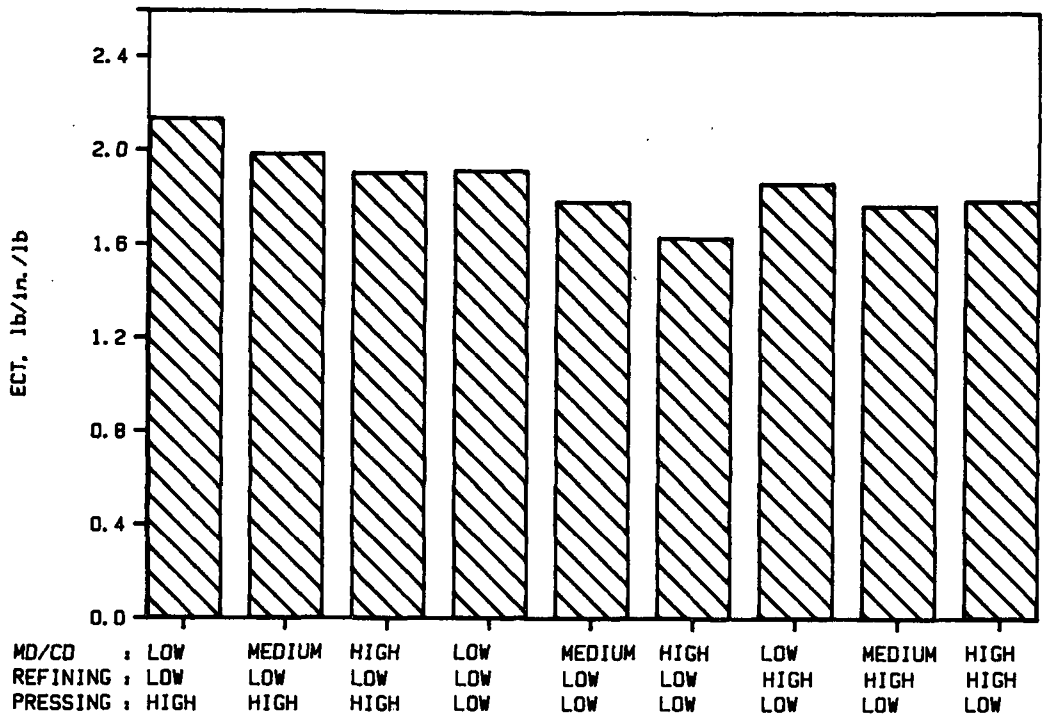

Figure 2. For 26-lb mediums ECT strengths per mass of medium fiber increase with more wet pressing, refining and lower directionality.

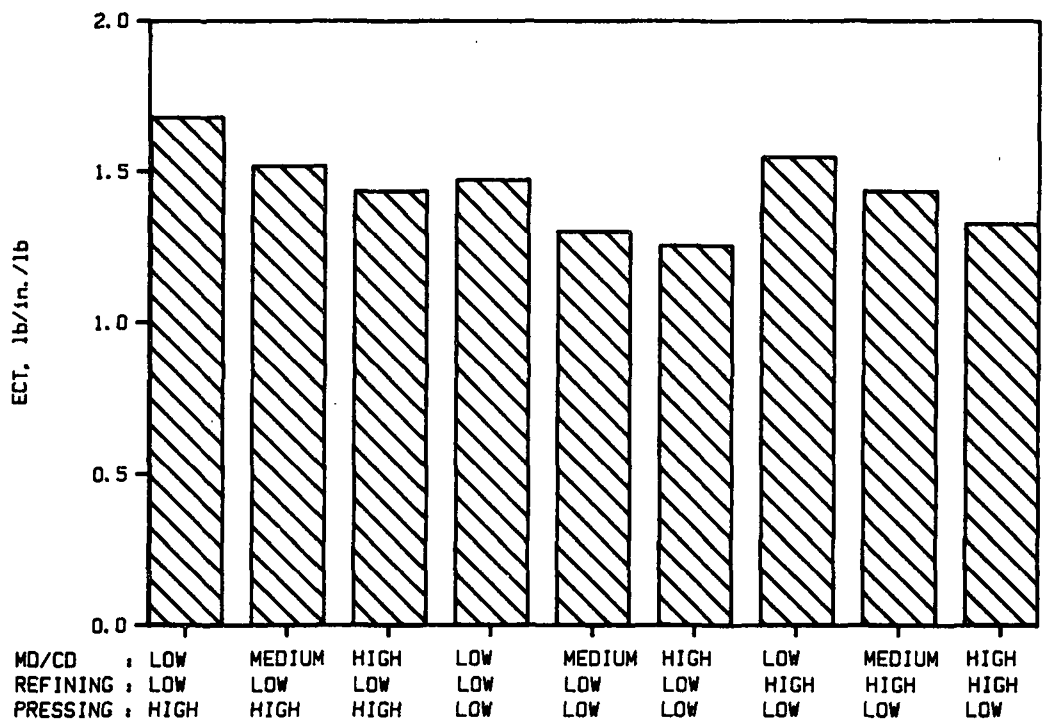

Figure 3. ECT strengths per mass of medium fiber for 40-lb mediums show same trends as 26-lb mediums.

Table 3. Medium density and surface characteristics.

Lot No.	Test Factors: Wet Pressing	Test Factors: MD/CD	Test Factors: Refining	Basis Weight g/m2	Density TAPPI kg/m3	Density IPC kg/m3	Concora, lb	Bendtsen Smooth., ws mL/min	Bendtsen Smooth., fs mL/min	Bendtsen Porosity mL/min	Water Drop, ws sec	Water Drop, fs sec
3761-43	High	Low	Low	125.8	443	742	58.0	2958	2687	329	114	191
3671-45	High	Medium	Low	130.1	465	759	81.2	3135	2911	235	145	219
3761-46	High	High	Low	131.7	449	755	89.3	2904	2857	157	196	194
3761-34	Low	Low	Low	125.0	397	524	47.8	2812	2680	1289	53	73
3761-36	Low	Medium	Low	127.0	407	540	64.2	2812	2562	1164	56	73
3761-37	Low	High	Low	133.2	399	550	75.7	2871	2584	811	106	112
3761-24	Low	Low	High	141.0	417	560	67.2	2728	2625	689	33	35
3761-27	Low	Medium	High	133.6	427	586	81.8	2770	2579	437	115	116
3761-28	Low	High	High	128.6	421	589	81.2	2822	2646	425	191	122
3761-48	High	Low	Low	197.4	498	703	90.8	3194	3032	357	119	99
3761-50	High	Medium	Low	201.8	520	729	107.8	3194	2938	207	94	158
3761-51	High	High	Low	204.4	515	735	136.0	3227	3034	160	97	125
3761-39	Low	Low	Low	193.6	419	526	62.7	3058	2904	1164	51	65
3761-41	Low	Medium	Low	197.0	440	553	81.7	3091	2947	684	91	109
3761-42	Low	High	Low	205.7	457	563	97.2	3114	2752	430	68	88
3761-29	Low	Low	High	187.9	445	545	79.8	2949	2766	747	75	95
3761-31	Low	Medium	High	191.8	461	562	105.7	3034	2746	460	47	51
3761-33	Low	High	High	197.0	580	145	125.8	2931	2902	320	68	92

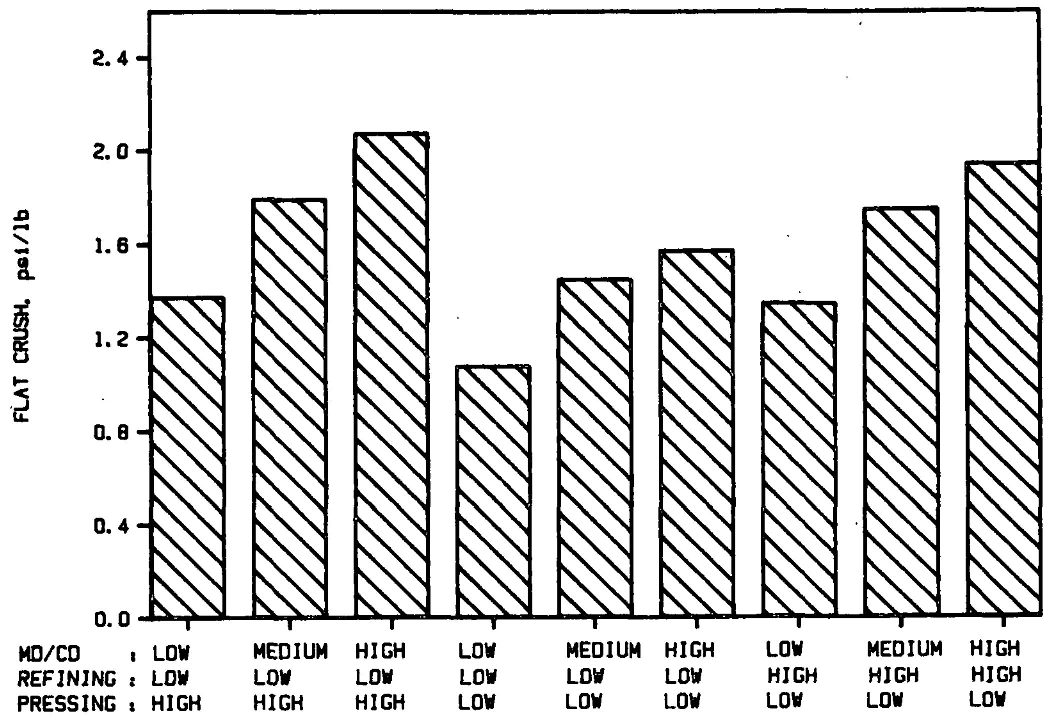

Figure 4. Flat crush strengths per mass of medium fiber increase as directionality and fiber bonding increase (26-lb mediums).

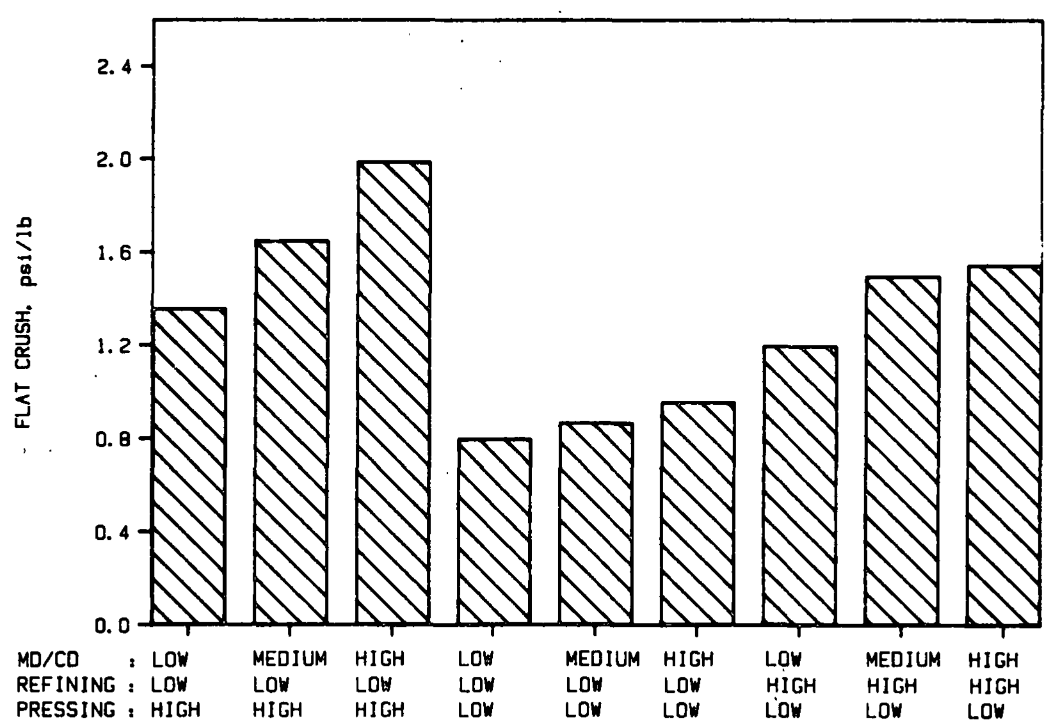

Figure 5. Flat crush strengths per mass of medium fiber of 40-lb mediums show same trends as 26-lb mediums.

All of the mediums corrugated at the selected speeds without any glueing problems. The single-faced boards are now being tested for pin adhesion strength. For comparison with the pin tests the mediums have been tested for smoothness, porosity and water drop (see Table 4). Figure 6 shows that increasing the directionality of the medium makes the sheet less porous. It is speculated that greater fiber alignment results in "nesting" of the fibers and fewer pores for air passage. The effect is consistent for all three 26-lb comparisons in Fig. 6 and can reduce the Bendtsen porosity by as much as a factor of 2. The 40-lb results also show the same pronounced effect of decreased porosity with increased directionality (see Fig. 7).

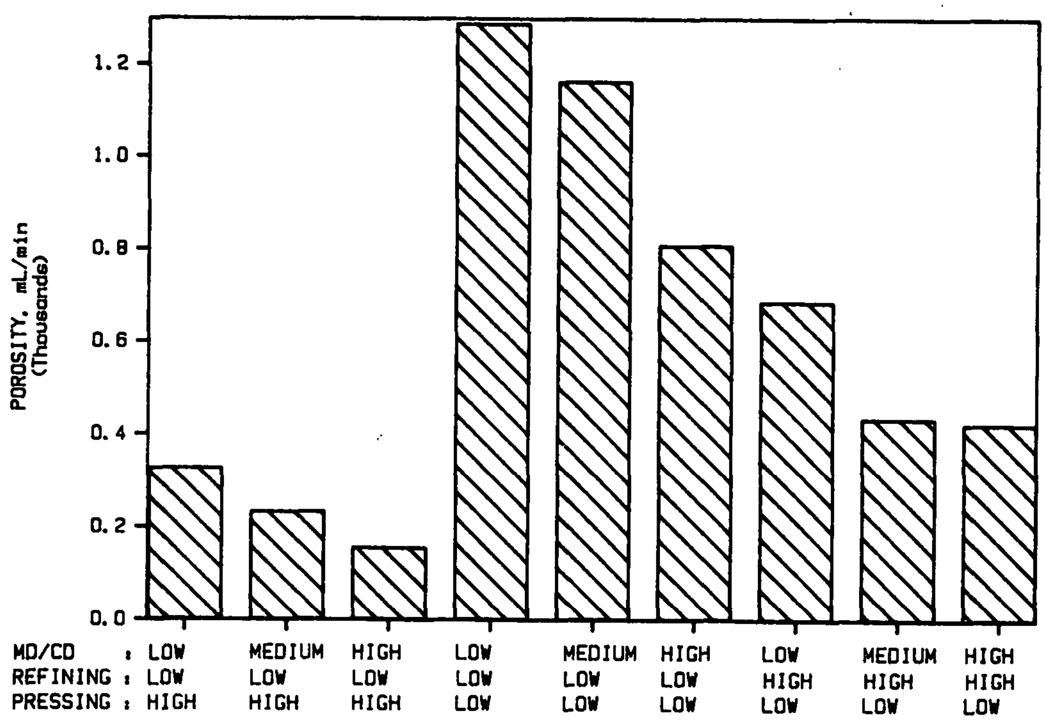

Figure 6. Porosity decreases with increasing directionality and less fiber bonding (26-lb mediums).

Table 4. Comparison of high-low results.

	High-Low Results, %					
	Low Orientation		Medium Orientation		High Orientation	
	High CSF	Low CSF	High CSF	Low CSF	High CSF	Low CSF
26-lb Medium						
Low Wet Pressing						
600 fpm						
% > 3 mils	5.80	5.51	2.20	3.31	3.62	11.40
% > 4 mils	1.82	2.57	0.37	1.10	0.36	1.47
800 fpm						
% > 3 mils	3.73	9.07	8.70	17.74	12.22	18.60
% > 4 mils	1.86	2.24	3.26	8.50	5.18	8.17
High Wet Pressing						
600 fpm						
% > 3 mils	8.82		9.33		4.35	
% > 4 mils	2.94		2.61		2.54	
800 fpm						
% > 3 mils	8.96		14.54		9.83	
% > 4 mils	1.12		3.08		3.28	
40-lb Medium						
Low Wet Pressing						
400 fpm						
% > 3 mils	13.60	5.68	6.34	10.98	11.74	15.15
% > 4 mils	2.57	0.76	0.74	3.79	3.79	4.55
600 fpm						
% > 3 mils	23.19	14.56	12.87	21.78	12.86	20.29
% > 4 mils	8.70	4.01	3.31	8.22	5.00	5.80
High Wet Pressing						
400 fpm						
% > 3 mils	9.47		7.84		19.03	
% > 4 mils	1.90		1.12		5.97	
600 fpm						
% > 3 mils	11.76		12.50		20.22	
% > 4 mils	1.84		3.68		6.98	

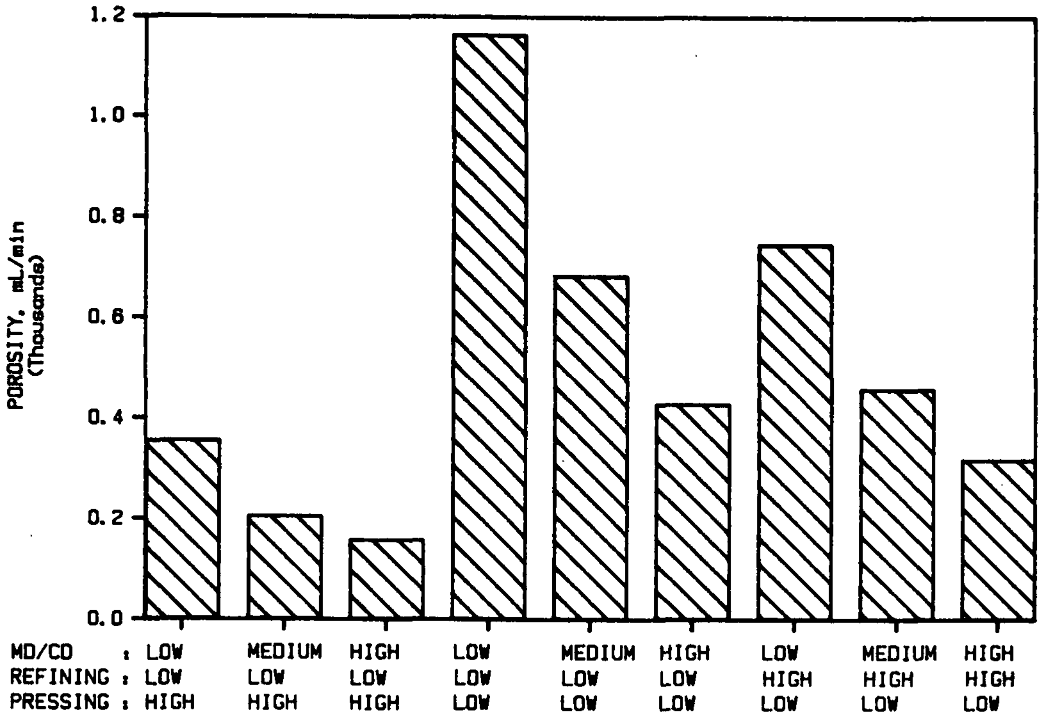

Figure 7. The porosity of the 40-lb medium was significantly lowered by increasing directionality.

Current commercial 26-lb mediums exhibit Bendtsen porosities ranging from about 220 to 1300 mL/min. All but one of the 26-lb mediums fell in this range (see Fig. 6).

Figure 8 and 9 show the water drop results for the 26 and 40-lb mediums respectively. These tests were run using TAPPI T492 so the times are longer than are usually obtained with the TAPPI method for corrugating medium (TAPPI T819). In our current FKBG work water drop values ranging from about 40 to 500+ sec have been obtained on 26-lb mediums so the values shown are within the commercial range. While porosity and water receptivity are usually believed to be important to bonding on the corrugator, we have found it difficult to show that they are well correlated. This will be checked against the pin adhesion strengths obtained on these boards.

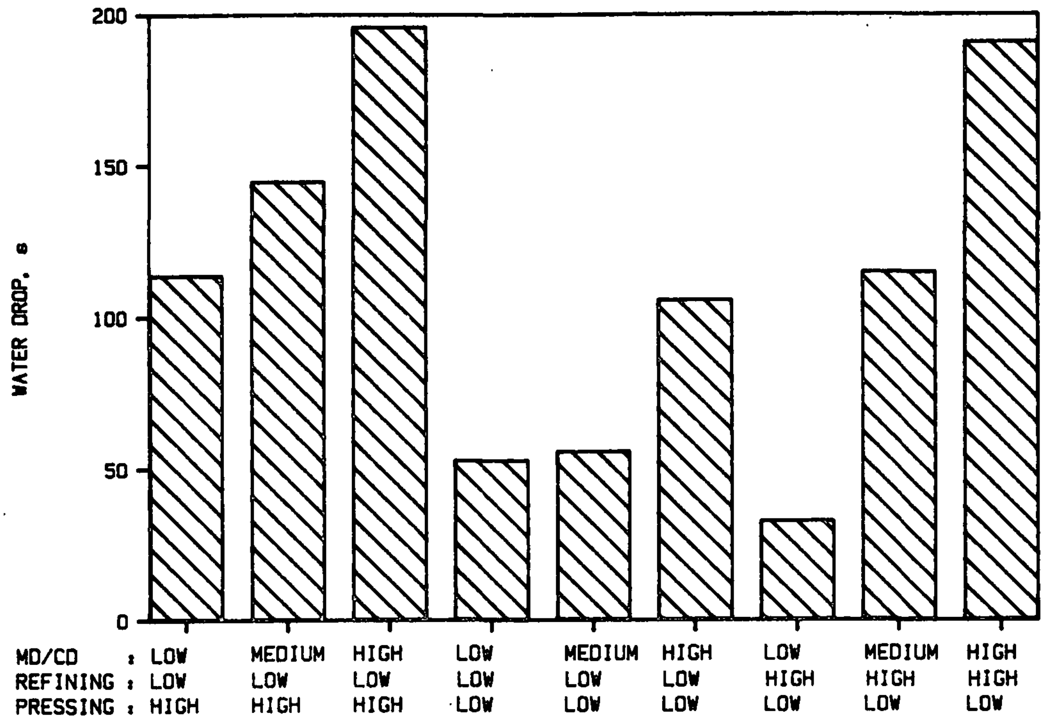

Figure 8. Effect of papermaking factors on the water receptivity of 26-lb mediums.

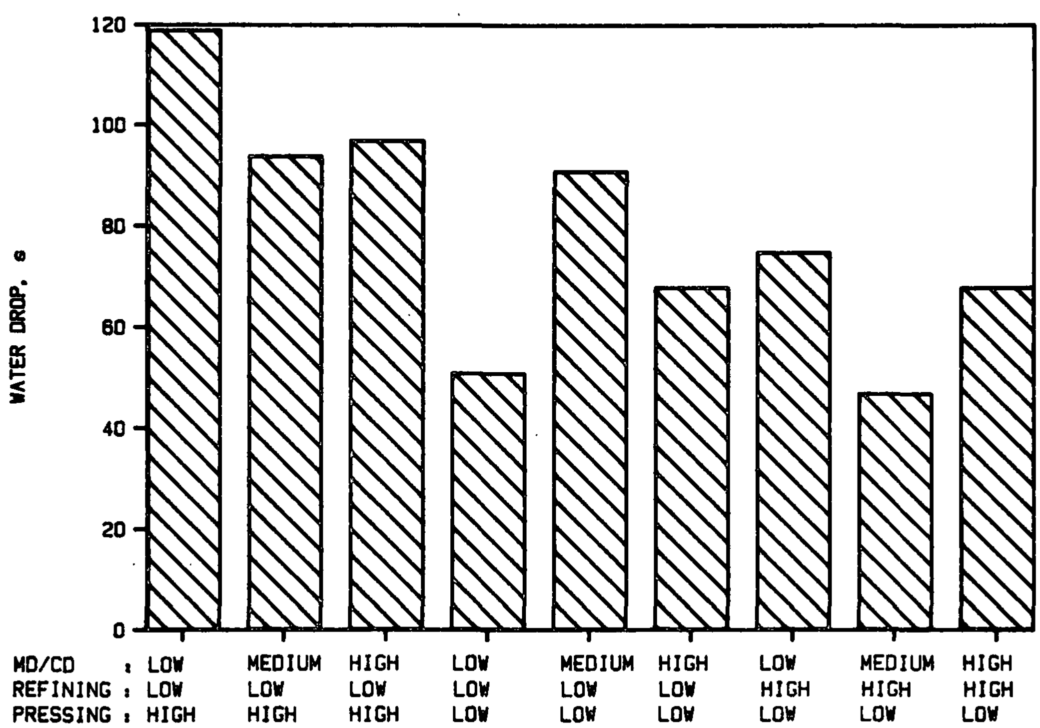

Figure 9. Effect of papermaking factors on the water drop of 40-lb mediums.

Runnability Modeling

Our runnability model shows that flute fracture and high-lows are dependent on medium properties, nip geometry and operational factors. Higher MD tensile strength and stretch and lower medium friction and thickness promote forming board with fewer high-lows and less chance of flute fracture. The nip geometry factors are (1) the total wrap angle in the labyrinth and the radius of the flute tip on the corrugating roll.

To support development of the model we developed a computer program to analyze nip geometry and flute profile effects on wrap angles, draw factor, and flank and tip clearances. From contour measurements taken on C-flute corrugating rolls, our calculations show that the medium draw or slippage is completed before the center of the nip (see Fig. 10). This helps define the total wrap angle in the nip, and hence the tension forces due to friction. Based on Fig. 10 and available data on the fracture speeds of mediums corrugated using our Langston C-flute rolls, a wrap angle of 3.09 radians was used in the runnability model.

The wrap angles which affect the tension in the medium vary cyclically during the formation of each flute (Fig. 11). This gives rise to tension pulses during the formation of each flute. Web tension measurements on the corrugator confirm that cyclical fluctuations in medium tension are usually present. The steep decreases in wrap angle after the peaks do not occur in actual practice; the cushioning effect of the medium and elastic deformations in the machine serve to round off the peaks.

Recently the profiles of our A- and B-flute rolls were obtained. Fig. 12 compares the wrap angles of the B- and C-flute rolls as a function of flute

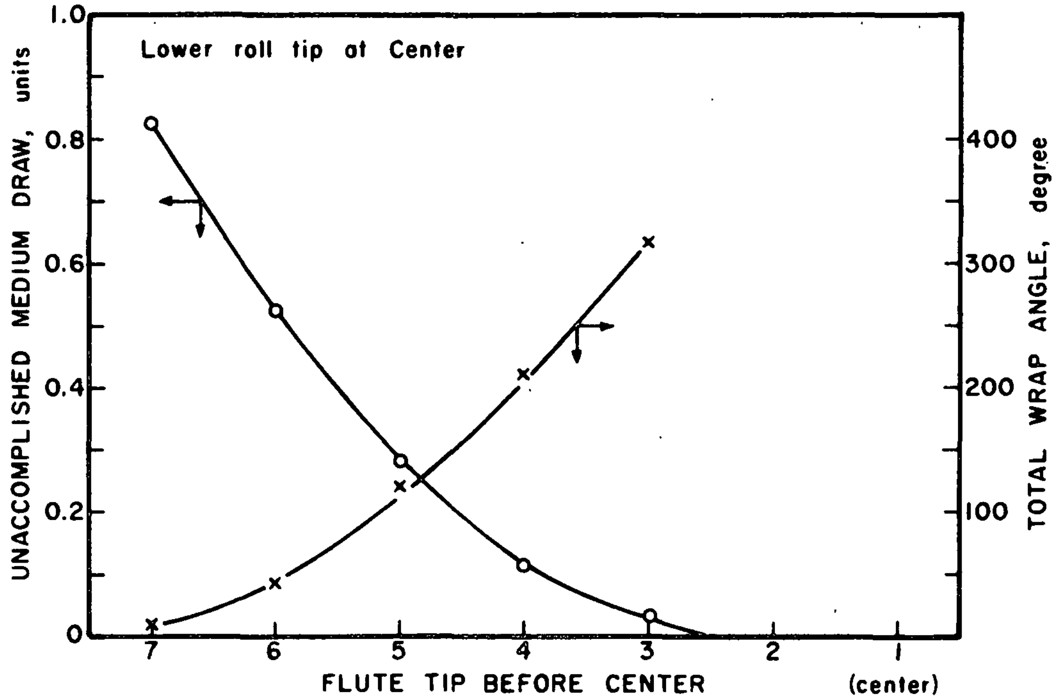

Figure 10. Unaccomplished medium draw and total wrap angle as a function of flute tip position in labyrinth (C-flute).

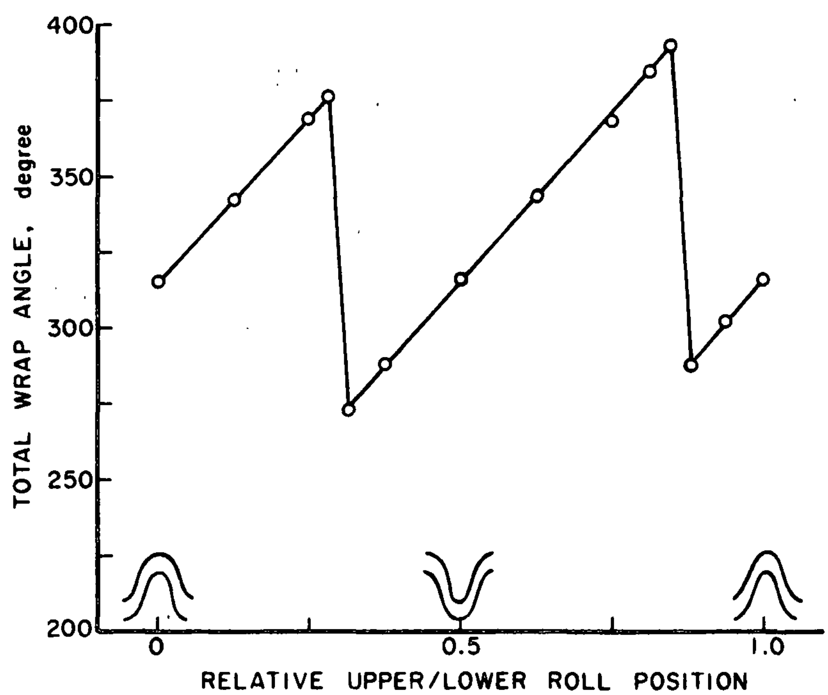

Figure 11. Total wrap angle varies cyclically during formation of one flute, thus tension on medium will also vary (C-flute).

position relative to the roll stack centerline (note: comparison is made at an unnaccomplished draw of 10%). Both the B- and C-flute profiles exhibit similar sawtooth variations in total wrap angle. The A-flute profile (not illustrated) shows a similar pattern.

For our runnability model we arbitrarily chose to average the wrap angles over all flute positions. However it might be equally logical to use the maximum wrap angle in charts such as Fig. 11.

Several criteria for selecting appropriate wrap angles for various flute profiles to use in the runnability model are being considered. They include:

1) using the wrap angle corresponding to 10% unaccomplished draw in the nip,

2) using the wrap angle corresponding to a defined amount of unaccomplished draw in the nip,

3) making the wrap angle proportional to the length of medium included in one flute. The fluted length will depend on the main profile factors, namely, flute height, flute tip radius and the number of flutes per foot.

We have not found an analytical way to determine the criterion which would be expected to provide an appropriate ranking for various profiles. Therefore a limited amount of experimental runnability data was obtained for B-flute rolls to compare with C-flute rolls. Table 5 compares the fracture speeds for 26-lb mediums at 1 and 4 lb/in. medium web tension. The results at 4 lb/in. tension suggest that B-flute fracture speeds are 200 to 400 fpm higher than for C-flute. For this situation using the third criterion results in a wrap angle of 2.30 radians for B-flute and predicted fracture speeds were in reasonable agreement with the observed speeds for the two flutes (see Fig. 13).

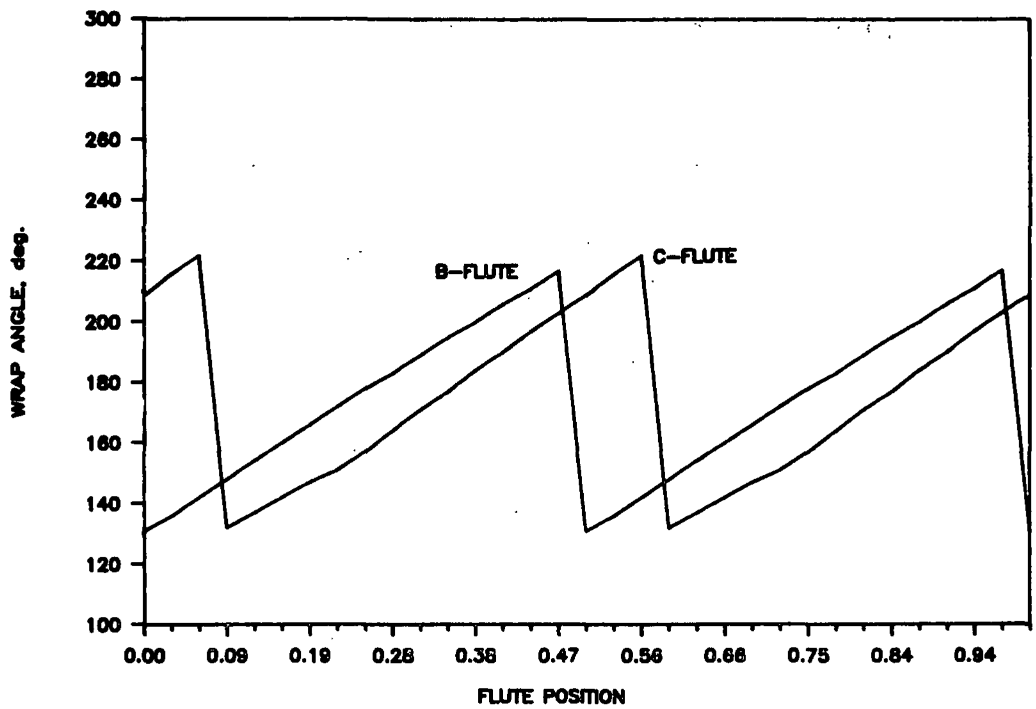

Figure 12. Total wrap angle vs. flute position in the corrugating nip for B and C-flute rolls (10% unaccomplished draw).

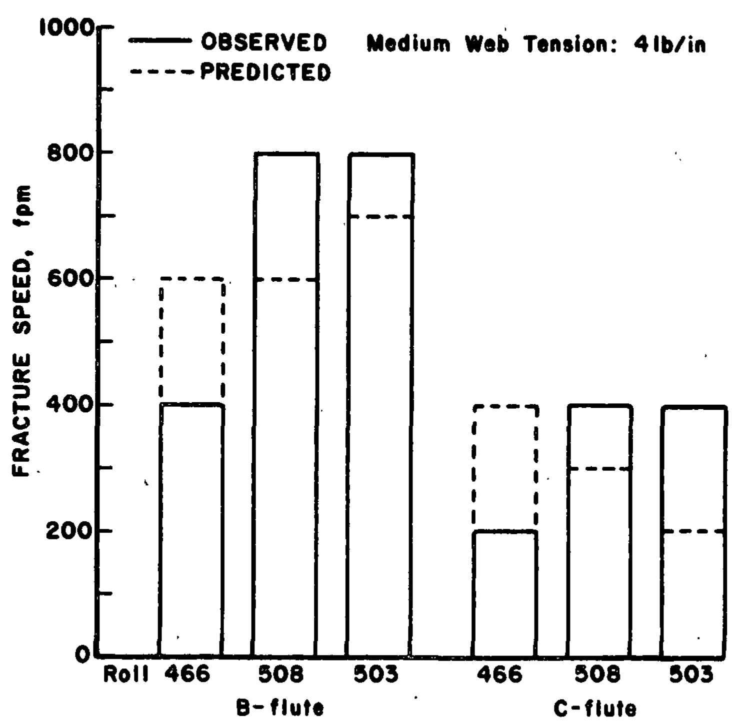

Figure 13. Fracture speeds for mediums corrugated on B- and C-flute rolls.

Table 5. Comparison of fracture speeds using B- and C-flute rolls.

Medium No.	Fracture Speed, fpm[a] B-flute	C-flute	Diff.
	at 1 lb/in. brake tension		
465-6	1000	1000+	--
507-8	1000+	1000+	--
502-3	1000+	1000+	--
	at 4 lb/in. brake tesnion		
465-6	400	200	200
507-8[b]	800+	400[c]	400+
502-3	800	400	400

[a]Evaluated at 200 fpm intervals.
[b]Greater than normal brake tension fluctuations were observed during running due to roll out-of-roundness.
[c]Fractures tended to be cyclical, probably due to out-of-round medium roll.

High-lows for the two flutes were also obtained as shown in Table 6. For two of the three rolls the B-flute single-faced board exhibited much lower high-lows than the C-flute board. Figure 14 compares average high-low predictions for the B- and C-flute boards using 2.30 and 3.09 radians for the two flutes, respectively. Good agreement was achieved for both flutes. The predictions for the individual medium rolls were also in reasonable agreement with the observed results (Fig. 15).

Thus these results indicate that the runnability model can be applied to other flutes if the proper wrap angle is used. Our present results for B- and C-flute suggest that the wrap angles should be 2.30 and 3.09 radians for our

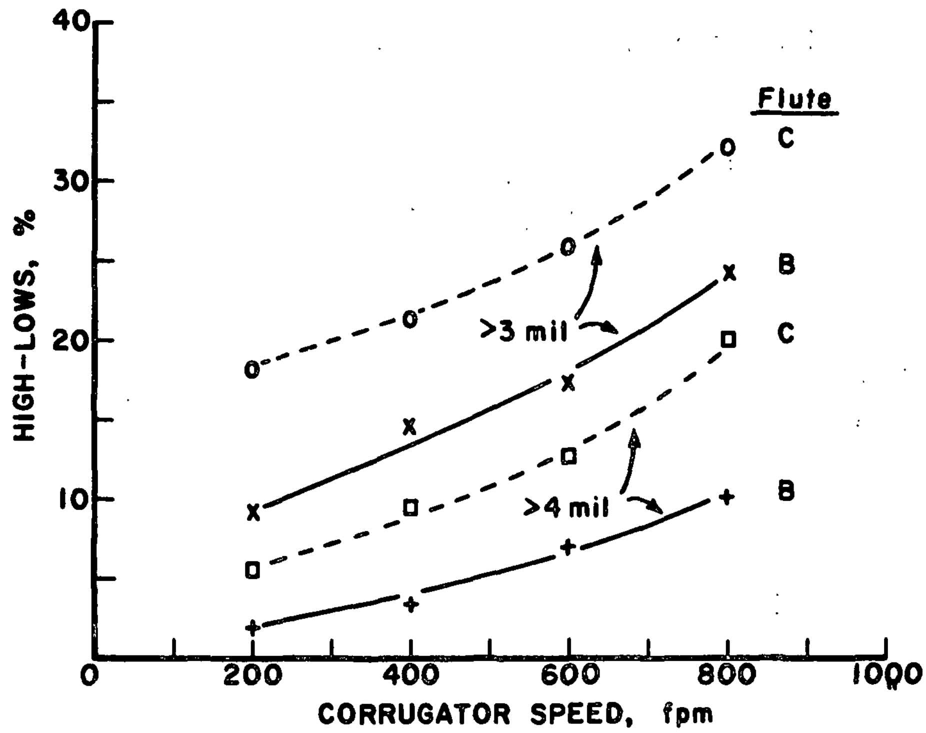

Figure 14. Comparison of average observed (points) and predicted (lines) high-lows for mediums corrugated on B- and C-flute rolls.

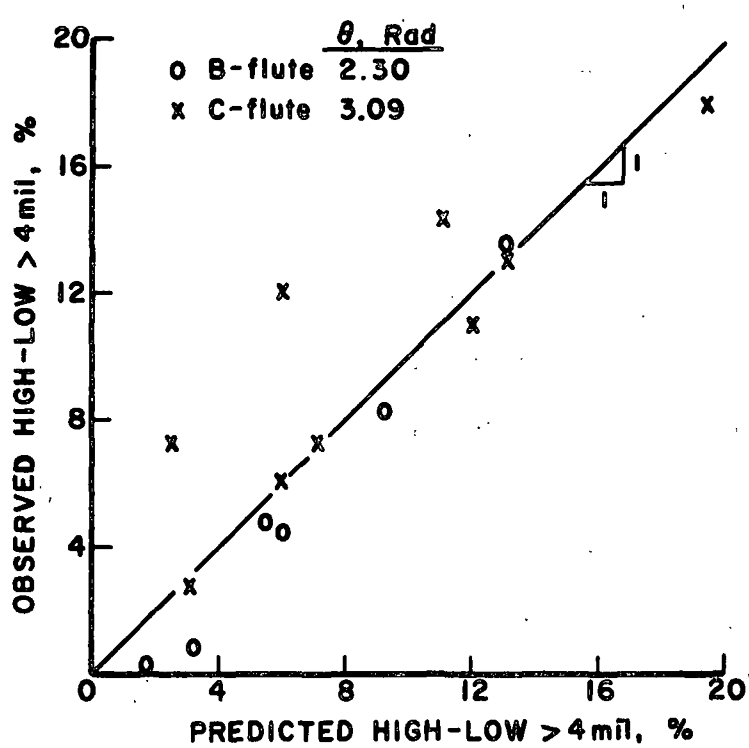

Figure 15. Observed vs. predicted high-lows for mediums flute on B- and C-flute rolls.

Table 6. Comparison of high-lows using B- and C-flute rolls.
(at 1 lb/in. brake tension).

Speed, fpm	Medium 465/6		Medium 507/8[b]		Medium 502/3		Average	
	B-flute	C-flute	B-flute	C-flute	B-flute	C-flute	B-flute	C-flute
				High-low > 4 mil, %				
200	4.9	2.7	0.6	7.2	0.2	7.3	1.9	5.7
400	8.2[a]	6.0	0.8	11.0	0.8	12.0	3.3	9.7
600	13.5[a]	14.2	3.7	10.7	4.5	13.0	7.2	12.6
800	13.9[a]	17.9	6.2	21.5	8.1	20.5	9.9	20.0
				High-low > 3 mil, %				
200	18.4	14.5	3.2	18.2	5.1	21.6	8.9	18.1
400	21.8	17.2	5.4	22.8	6.3	24.0	14.5	21.3
600	29.8	27.8	9.7	25.1	11.9	24.9	17.1	25.9
800	32.5	30.2	17.9	34.1	22.2	31.9	24.2	32.1

[a]Very slight indications of internal fiber wall disruptions.
[b]Greater than normal brake tension fluctuations due to roll out-of-roundness.

Langston profiles. At a convenient time we will install A-flute rolls in our pilot machine to check whether criterion 3 is the best choice. We know it will give a greater wrap angle for A-flute, but somewhat less than would be obtained with the other two criteria.

Periodicities in High-Low Flute Formation

Our goal is to identify periodicities in high-low flute formation using power spectral anaqlysis techniques and to determine what machine elements cause these periodicities. Much of this work is being shifted over to a study for FKBG. The work being carried out on this part of the project has been primarily limited to spectral analysis methodology. We have been analyzing a few IPC and commercial single-face boards in an effort to find the best way to treat the data.

ECT and Box Compression Relationships

An important part of our past work has been directed to developing relationships between combined board ECT and the properties of the linerboard and medium which will be valid under most papermaking conditions. A specific goal is to incorporate the elastic stiffnesses of the components in such relationships. This will allow us to use nondestructive ultrasonic techniques to characterize board and box performance. It also enables us to use our developing knowledge on how papermaking factors affect elastic stiffnesses to assess ways to improve performance.

After study of alternatives we modeled ECT in the same way as the Institute top load box compression formula. This is termed the miniature plate approach. Conceptually ECT is set equal to the sum of the maximum strengths of the individual liner and medium plate elements. Following this approach the contributions of the liners and medium are formulated as the product of two terms:

Liner: $(\text{compressive strength})^{b} \times (\text{mean flexural stiffness of liner})^{1-b}$

Medium: $(\text{compressive strength})^{c} \times (\text{mean flexural stiffness of medium})^{1-c}$

The constants b and c must be experimentally determined and their magnitudes will reflect the relative importance of the two properties. For compressive strength we employ either short span compressive strength values or the in-plane and out-of-plane elastic stiffnesses.

As discussed previously we obtained good predictive accuracies using this approach. The magnitudes of the exponents indicated that ECT is primarily dependent on the compressive strength characteristics of the liners and medium. The flexural stiffness of the medium has a negligible effect; the flexural stiffness of the liners appears to have only a small effect on combined board ECT.

To validate these results experimental linerboards were made wherein we varied the ratio of CD compressive strength to flexural stiffness. This was accomplished by varying the density via wet pressing, directionality and incorporating additives. Good agreement was obtained between observed and predicted ECT values. Thus we are now able to relate ECT to either short span compressive strength or the elastic stiffnesses of the liners and medium. We also modeled the combined board flexural stiffness using an elliptic integral to determine the contribution of the fluted medium. Agreement with experimental results was good.

Currently we are studying ways to optimize box strength-to-weight ratios. As an initial step in developing optimization procedures we considered the effects of selected papermaking changes to improve liner and/or medium properties on ECT strength-to-combined board weight ratios in the last status report.

We used the following equation:

$$ECT = 1.375 \times STFI_L + 1.101 \times STFI_M + 1.212 \quad (1)$$

where ECT is combined board edge crush (lb/in.) and $STFI_L$ and $STFI_M$ are the CD short span compressive strengths (lb/in.) for the liner and the medium respectively. This equation was determined from the experimental data base, reported previously, which included combined boards made with liners and mediums of varying basis weights, densities and MD/CD ratios. This equation may be written in the form:

$$ECT = 1.375 \times BW_L \times SS_L + 1.101 \times BW_M \times SS_M + 1.212 \qquad (2)$$

BW_L = basis weight of liner (lb/1000 sq ft)

BW_M = basis weight of medium (lb/1000 sq ft)

SS_L = CD liner specific compressive strength ((lb/in.)/(lb/1000 sq ft))

SS_M = CD medium specific compressive strength ((lb/in.)/(lb/1000 sq ft)).

In Eq. 2 the STFI strengths in Eq. 1 have been reformulated as the product of basis weight times specific compressive strength, i.e. compressive strength per basis weight.

In this form it is possible to investigate how improved specific compressive strengths will influence the amount of fiber required. It is assumed in Eq. 2 that the basis weights may be changed independently of the specific strength values. For the purpose of the current study the specific strength properties of three liners and two mediums from our past experimental data base were selected. Table 7 below gives the specific compressive strengths for the five components, their codes and an explanation of how the enhanced strengths were experimentally achieved.

Table 7. Component specific compressive strengths.

Component	Specific Compressive Strength (lb/in.)/(lb/10000 sq ft)	Code	Comment
Liner	0.498	RL	Reference liner
Liner	0.565	HL	High density liner achieved by wet pressing
Liner	0.656	SL	Low ratio E_X/E_Y liner achieved by controlling fiber alignment
Medium	0.592	RM	Reference medium
Medium	0.657	HM	High density medium

In order to predict box strength using the McKee formula, estimates of combined board flexural stiffness are needed in addition to estimates of ECT. The simplified flexural stiffness model used for this purpose was

$$FS = 0.74 \sqrt{E_x E_y}\, \frac{2}{3} \left[\left(\frac{H}{2}\right)^3 - \left(\frac{H}{2} - t\right)^3\right] \qquad (3)$$

Where FS = geometric mean flexural stiffness of the combined board (lb - in.)

E_x and E_y = measured ultrasonic elastic moduli of the liner (lb/in.^{2})

H = caliper of combined board (in.)

t = caliper of the liner (in.)

0.74 = scale factor to convert ultrasonic to mechanical moduli

The geometric mean elastic moduli and the specific calipers for the three liners described in Table 7 are shown in Table 8.

Table 8. Additional liner specific properties.

Liner Code	$\sqrt{E_x E_y}$, (lb/in.^{2})	Specific Caliper, (in.)/(lb/1000 sq ft)
RL	677200	2.93×10^{-4}
HL	978100	2.32×10^{-4}
SL	673400	3.09×10^{-4}

Three discrete liner basis weights (38, 42 and 47 lb/1000 sq. ft) and three discrete medium basis weights (26, 33 and 40 lb/1000 sq ft) were chosen to illustrate the dependence of ECT, combined board flexural stiffness and box strength on component basis weights for the component specific properties given in Tables 7 and 8. The liner and medium basis weights were combined to give a total of 6 different combined board basis weights as shown in Table 9.

Table 9. Basis weight combinations.

	Basis Weight, (lb/1000 sq ft)					
Liner	38	42	38	47	42	38
Medium	26	26	33	26	33	40
Combined Board	113.4	121.4	123.5	131.4	131.5	133.6

In Fig. 16 we have plotted predicted ECT (using Equation 2) versus combined board basis weight for constructions made from liners and mediums densified to varying degrees as follows:

HL - HM	high density liner	- high density medium
HL - RM	high density liner	- reference medium
RL - HM	reference liner	- high density medium
RL - RM	reference liner	- reference medium.

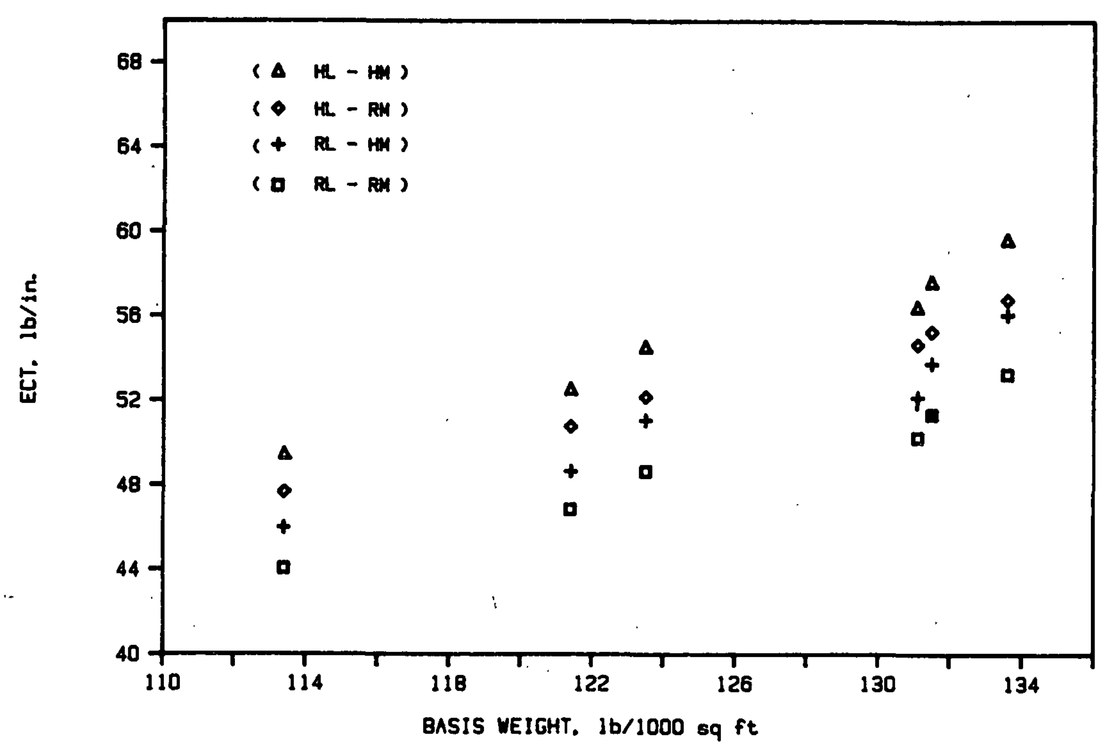

Figure 16. Predicted ECT versus combined board basis weight for liners and mediums made with different densities.

Treating the RL - RM 42-33-42 (131.5 lb/1000 sq ft) combination (indicated in the figures by ■) as the target construction to match or improve upon, we note that comparable ECT's of about 51 lb/in. are predicted for the RL-HM 38-33-38 (123.5 lb/1000 sq ft) and the HL - RM 42-26-42 (121.4 lb/1000 sq ft) combinations with an appreciable savings in fiber.

In Fig. 17 we have plotted similar ECT predictions for the same 6 weight combinations but for the specific property combinations involving liner directionality and medium density:

SL - HM	square liner	- high density medium
SL - RM	square liner	- reference medium
RL - HM	reference liner	- higher density medium
RL - RM	reference liner	- reference medium.

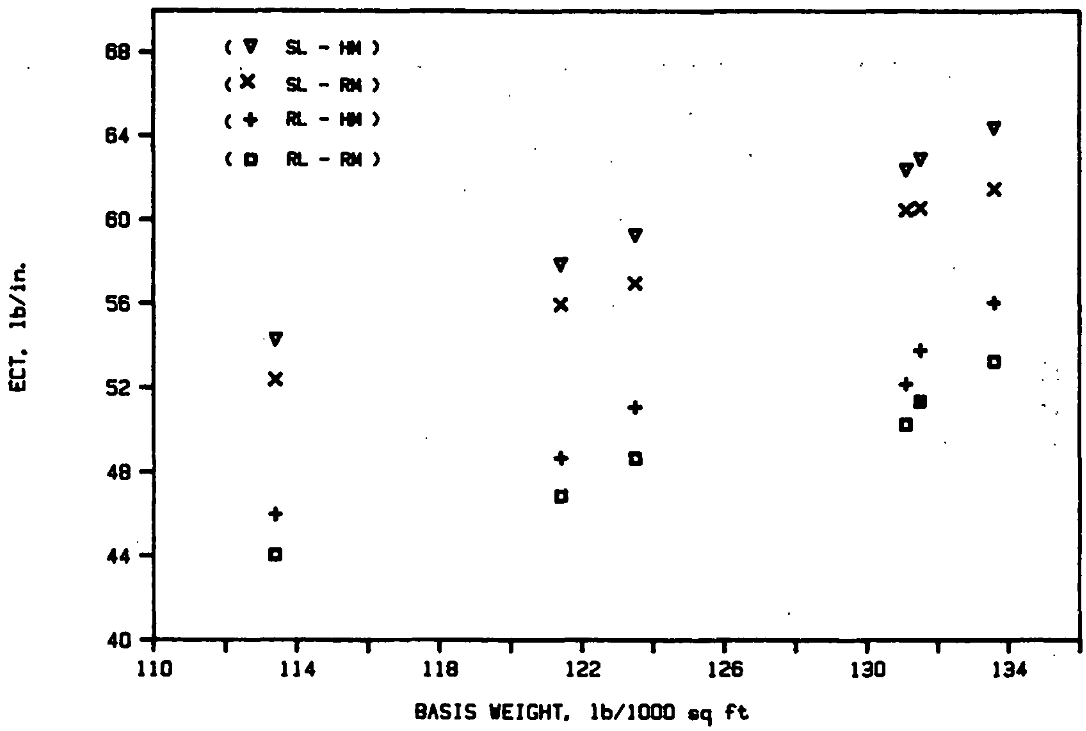

Figure 17. Predicted ECT versus combined board basis weight for liners with varying directionality combined with different density mediums.

These predictions suggest that the SL - HM 38-26-38 (113.4 lb/1000 sq ft) combination would have comparable ECT strength to the RL - RM 42-33-42 target combination.

Figure 18 shows the predicted relative combined board flexural stiffnesses (using Equation 3) for the 6 weight combinations and the 3 specific property combinations, HL - RM, SL - RM and RL - RM. These flexural stiffnesses are plotted relative to the RL - RM 42-33-42 target construction. While the SL - RM combinations give higher predicted ECT's than the HL - RM combinations, the SL - RM combinations are predicted to have lower flexural stiffness than the HL - RM combinations. This trend has been observed experimentally.

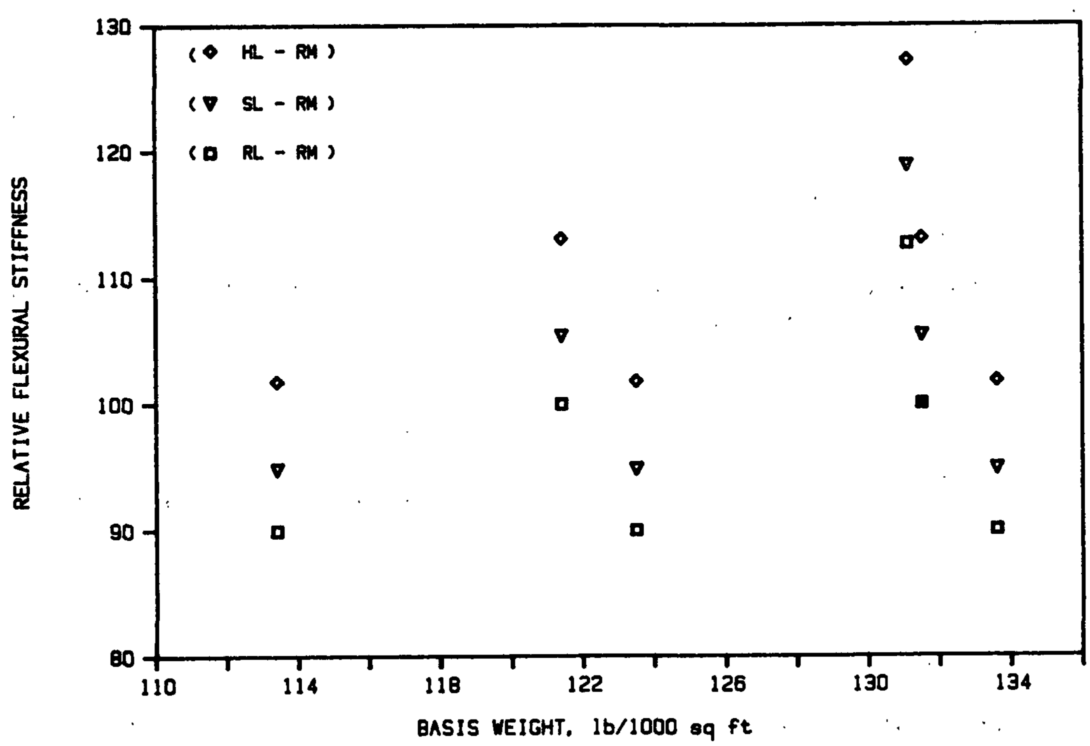

Figure 18. Predicted relative combined board flexural stiffness versus combined board basis weight.

In Fig. 19 the predicted relative box strengths (relative to RL - RM 42-33-42 target construction) for the reference and high density property sets are shown. The figure suggests an appreciable potential savings in fiber may be obtained by using the HL - RM or the HL - HM combinations with the 42-26-42 or 38-33-38 weight combinations.

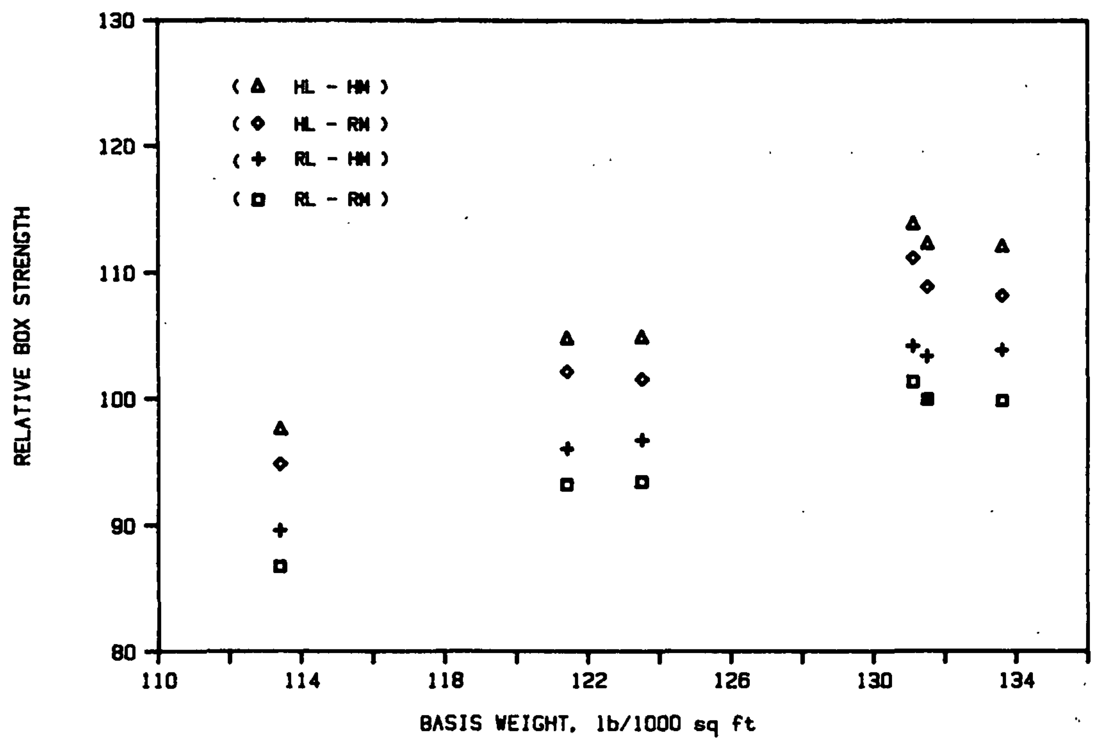

Figure 19. Predicted relative box strength versus combined board basis weight for liners and mediums of varying density.

Figure 20 shows the relative predicted box strengths for combinations where the square liner has been used. The trend is similar to that of Fig. 19 suggesting a sizable weight savings and box strength improvement over the target construction.

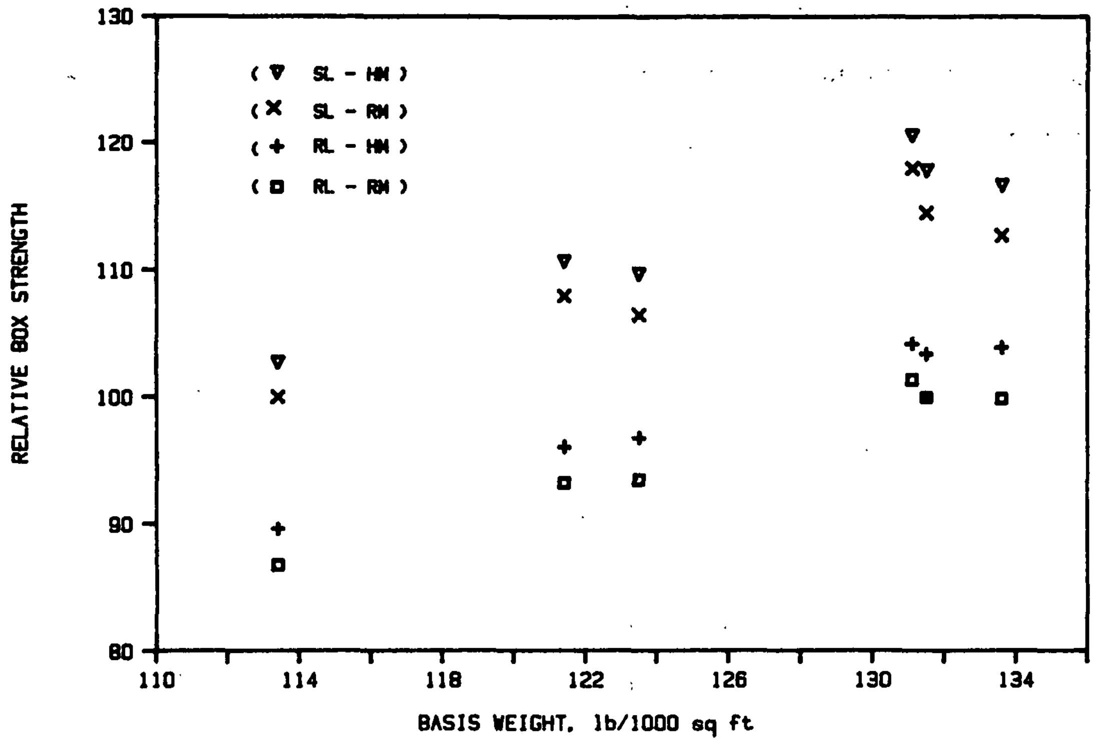

Figure 20. Predicted relative box strength versus combined board basis weight for liners of varying directionality combined with different mediums.

Flat Crush Modeling

The compressive strength and stiffness of corrugated board in its thickness direction (flat crush) depends on the properties of the medium after it is formed into the fluted shape. The properties of the medium which are critical to flat crush performance are its compressive and flexural characteristics. An uncorrugated medium has certain compressive and flexural potentials. The flute formation process results in damage to the medium properties which decrease the potential flat crush performance. Knowledge of the medium properties after corrugating is necessary for an accurate analysis of flat crush. Also, understanding the fluting process is required to provide a basis for improvements in flat crush performance.

A significant amount of research investigating the properties of the medium after corrugating has been conducted in the past. A brief review of the observations from those and other studies pertinent to flat crush performance is as follows:

1) Flexing the medium by bending it around a small radius (radius similar to that at the tip of a corrugated flute) greatly reduced the MD compression strength (Ref. 1). An approximate 50% reduction in the STFI compression strength from the uncorrugated state resulted from flexing of the medium.

2) Test results on the fluted medium indicated much lower compressive strengths than the uncorrugated medium (Ref. 1). The MD STFI compressive strength was measured at various positions around the flute. Overall reductions in the MD compressive strength were about 42%. However, compressive strength reductions were greater at the flute tip and less at the flanks of the flute. Fiber bonding damage was suspected as the cause of the compressive strength reduction.

3) The temperatures in the corrugating rolls had a minor effect on the medium compressive strength after corrugating (Ref. 1). Relatively small differences in the STFI compressive strengths were reported when mediums were formed with hot (350°F) and cold (room temperature) corrugating rolls.

4) Prestressing the medium in tension had little or no effect on compressive strength (Ref. 1). Medium specimens were loaded in tension in the MD direction to failure. The remnants of the speci-

mens were evaluated for their STFI compression strength. While tensile stresses in the medium during corrugating apparently affect its runnability, little change in the medium compressive strength occurs.

5) A study of paperboard beams subjected to bending was conducted and related to the tensile and compressive stress - strain behavior (Ref. 2). Since the compressive strength of paper is lower than its tensile strength, beam failure occurred in compression. Beam failure did not occur when the ultimate strain in compression was reached in the fibers, but rather a plastic yielding of the compressed fibers took place. At failure, an interlaminar crack at the compression side of the board and buckling of the compressed fibers was observed through a significant portion of the thickness. This inelastic bending failure mechanism may also occur in a medium during flute formation and would explain the resulting compressive strength losses after forming. Buckling of the fibers in compression may be prevented due to Z-direction compression of the flute tip by the corrugating roll during flute formation.

The observations from past testing indicate that medium damage primarily results from bending and that flute formation may occur due to inelastic bending. If the properties of the medium remained in the elastic range, the medium would return to its original flat state after passing through the corrugator. The following analysis of bending strains shows that the medium will enter the inelastic range in compression during flute formation.

The analysis of bending is based on the fact that plain cross sections of the bending element remain plain under pure bending. This condition is valid for both linear elastic materials and non-linear inelastic materials (Ref. 3). Therefore, the strains of an elastic or inelastic beam element vary linearly over its height. The ultimate strain in tension of a typical medium is approximately 1.5%. An increase in moisture content and temperature during preconditioning on the corrugator may increase the ultimate strain level in tension. The ultimate strain in compression for a typical medium is not well defined due to difficulties in testing, however, it is probably less than the ultimate strain in tension. Assuming the elastic strain level in compression for a typical medium to be 1.0%, the minimum radius of curvature allowable for elastic bending of a medium can be calculated. For a medium of 0.01 inches in thickness, the minimum radius of curvature in elastic bending is calculated as follows:

$$R = \frac{t}{2\varepsilon} = \frac{0.010 \text{ in.}}{2(0.01 \text{ in./in.})} = 0.5 \text{ in.}$$

where

R = radius of curvature of the deflected shape

t = thickness of the medium

ε = assumed maximum elastic strain in compression.

This radius of curvature (R = 0.5 inches) is much greater than that occurring at the flute tip (R = 0.06). A larger allowable elastic strain due to increased moisture content in the medium would decrease the minimum radius of curvature. Also, shear deformations of the medium would relieve some of the tensile and compressive strain. However, it is unlikely that the moisture content increase and shear deformation would account for the large difference in strain required to form the flute elastically.

The strains in an element experiencing inelastic bending vary linearly over the thickness of the element. For example, the radius of curvature (R) of a typical C-flute tip is approximately 0.069 inches for the inelastic bending case considered here. Under normal conditions the medium does not fail in tension when it is formed. Therefore, the tension strain (ε_t) must be less than 1.5%. The distance from the tension face to the neutral axis of the medium (h_1) would be approximately equal to 0.001 inches as calculated below:

$$h_1 = \varepsilon_t R = (0.015 \text{ in./in.})(0.069 \text{ in.}) = 0.001 \text{ in.}$$

The distance from the neutral axis to the compression face (h_2) would then be equal to 0.009 inches for a 0.010 inch thick medium. The resulting apparent strain in compression (ε_c) would then equal 13.0%.

$$\varepsilon_c = \frac{h_2}{R} = \frac{0.009 \text{ in. } (100)}{0.069 \text{ in.}} = 13.0\%$$

However, the medium may only be effective in compression up to a strain of 1.0% which occurs at a distance of approximately 0.0007 inches below the neutral axis. Therefore, the total effective thickness of the medium at the flute tip area would be approximately equal to 0.0017 inches.

Three sets of finite element analyses of the fluted medium in flat crush loading were conducted. The same modulus of elasticity ($E = 10 \times 10^5$ psi) and shear modulus ($G = 10 \times 10^3$ psi) were used in each case. The following thickness medium values were used:

1) The uncorrugated medium thickness.
2) A reduced effective thickness based on the measured compressive strength at different locations around the flute (based on the results from Ref. 1).
3) A reduced effective thickness in the flute tip area according to inelastic bending analysis.

The results of this analysis are shown in Fig. 21 along with the actual test results from a 26-lb medium. The initial portion of the flat crush load deflection curve is shown up to a vertical deflection of 0.01 inches. Figure 21 indicates the large flat crush potential of the uncorrugated medium. The results also show that the STFI compressive strength losses measured around the flute apparently underestimate the losses when the medium is in the fluted shape. Inelastic bending theory resulted in lower flat crush loads than that of the test medium. The higher flat crush loads for the test medium may be due in part to the reversal in loading on the medium from the flute formation process to the flat crush load. The reversal in loading may allow a partial recovery of the compression fibers in the medium. Further refinement of the finite element model is being conducted.

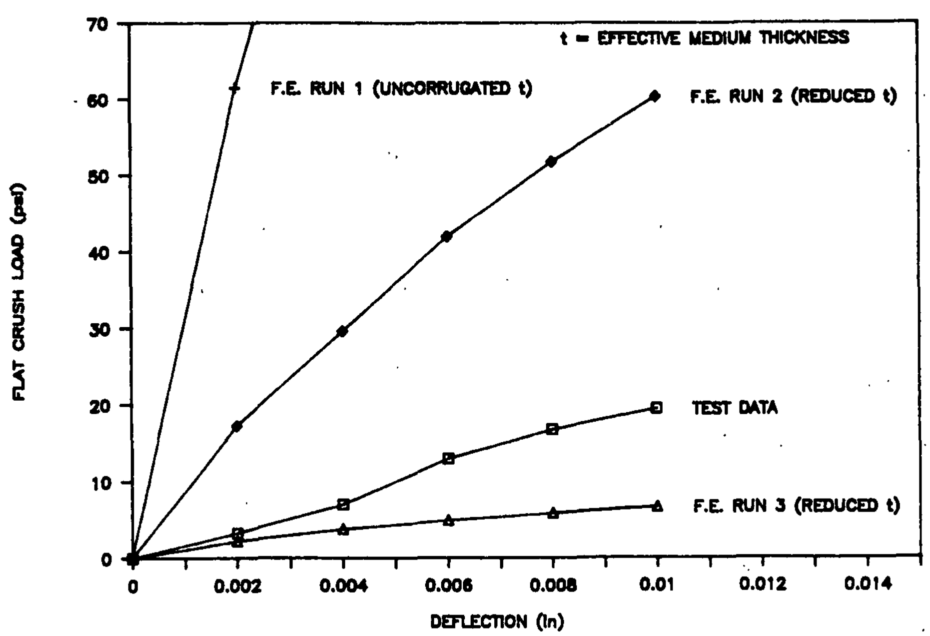

Figure 21. Load-reflection results from finite element analysis.

The compressive strength of the flanks of the flute is reduced according to the results of past testing (Ref. 1). The reduction in compression strength of the flanks may be explained in terms of inelastic bending, if we follow a section of medium as it passes through the corrugator as shown in Fig. 22. At position 1 a medium is in its flat state prior to enter the corrugator. The medium is then pulled into the corrugator and at position #4 the section has probably experienced inelastic bending, with permanent damage to the fibers in compression taking place. This section of the medium continues to be pulled into the labyrinth where it becomes part of the flute flank at position 7. The reduction in compressive strength of the flute flanks will have a great effect on ultimate strength of the corrugated board and flat crush.

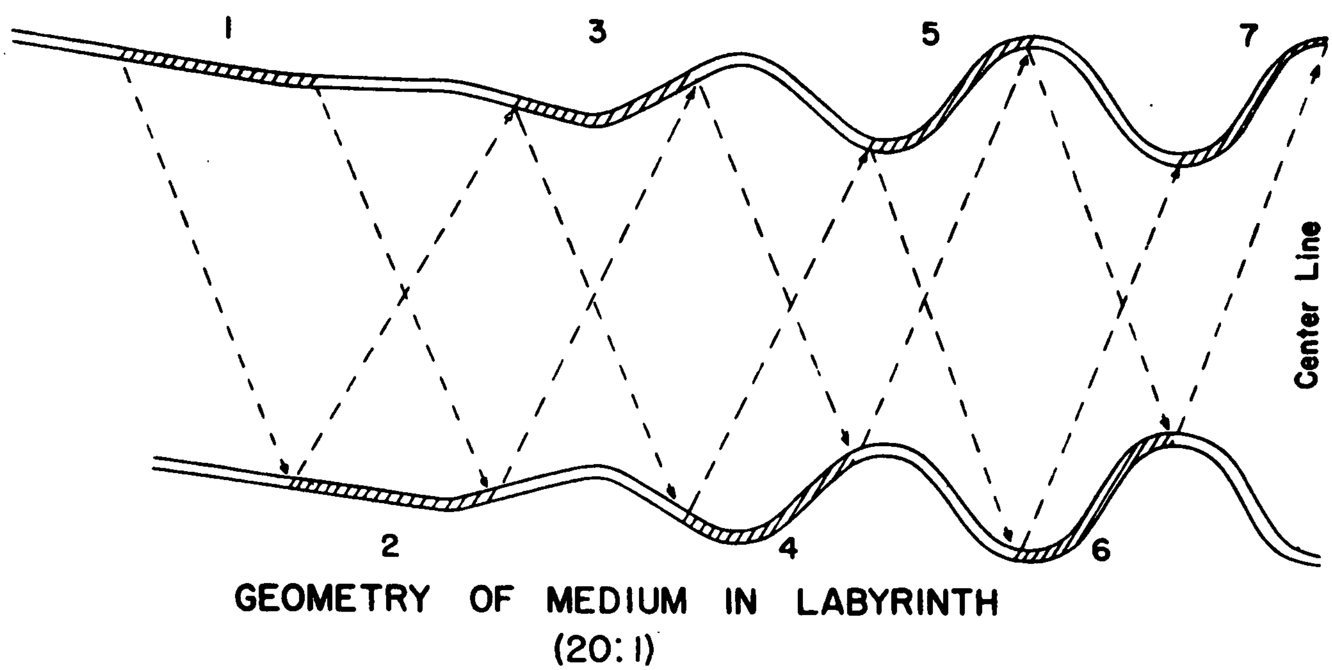

Figure 22. Forming geometry.

Future testing and modeling of the corrugated board in flat crush loading will include the following:

1) Further analysis of inelastic bending of the medium during flute formation. This may include using finite element techniques to model the forming process.

2) Study of the flute formation process using a single flute former.

3) Further establishment of the compression side of the stress-strain curve for the medium.

4) Investigation of the effects of changing the flute shape.

5) Further refinement of the finite element flat crush model.

References

1) Mechanics of Fluting, Project 3396, Report No. 1 to the Members of the Institute of Paper Chemistry, June 15, 1981.

2) Carlsson, L., A study of the Bending Properties of Paper and Their Relation to the Layered Structure, 1980.

3) Gere, J. M. and Timoshenko, S. P., Mechanics of Materials, PWS Publishers, 1984.

APPENDIX A

IPC Technical Paper Series

Number 167

COMPRESSIVE STRENGTH RETENTION DURING FLUTING OF MEDIUM. PART 1. STRENGTH LOSSES IN FLUTING

W. J. Whitsitt and C. H. Sprague

May, 1986

COMPRESSIVE STRENGTH RETENTION DURING FLUTING OF MEDIUM. PART 1: STRENGTH LOSSES IN FLUTING

W. J. Whitsitt
Research Associate
The Institute of
Paper Chemistry
Appleton, WI 54912

C. H. Sprague
Division Director
The Institute of
Paper Chemistry
Appleton, WI 54912

ABSTRACT

This article is the first in a series devoted to factors that affect the compressive strength of medium. In this first article the retention of compressive strength during fluting is discussed. Our results indicate that the flat crush and edgewise compressive strength (ECT) potentials of corrugated board, which are dependent on the medium, are greatly reduced by the fluting process. This occurs because fluting causes large reductions in the edgewise compressive strength of the medium, under both hot and cold forming conditions. The reductions in strength are caused by the high bending and tension stresses induced in the medium during fluting. There are opportunities to improve box performance or save fiber in the manufacture of medium if we can retain more strength during fluting. Developments in this area will be discussed in a subsequent article.

INTRODUCTION

Corrugating performance is limited by a number of factors, several of which directly affect board quality. For example, high-lows, flute fracture, bond quality and board strength all affect corrugator productivity, convertability and end-use performance of corrugated board. Hence, they are of great economic importance to the industry.

Trends to higher corrugating speeds are placing increasing demands on the forming characteristics of medium and our ability to bond the liners and medium. Concurrently our industry is directing attention to improving the end-use performance characteristics of linerboard and medium through changes in papermaking. In these developments it is necessary to make sure that high speed runnability on the corrugator is maintained or improved. To achieve this goal, it is necessary to have a good understanding of the relationships between containerboard properties, forming, and bonding.

During fluting the medium is exposed to high stresses. If these stresses are too high, visible fractures of the medium will occur and the board will be useless. At lower stress levels visible fracturing will cease, but our research shows that there is still heavy damage to the medium, resulting in a serious loss of end-use performance.

This was discovered during our work on the cold corrugating process (1,2). We found that most of the properties of the cold-formed board were comparable to those of hot-formed board, but some mediums exhibited lower ultimate flat crush strengths when formed cold. In seeking the cause of this difference, we found that both hot and cold fluting caused large losses in the edgewise compressive strength of medium. As a consequence, some 30-40% of the flat crush potential of the medium and 15-20% of the ECT potential are lost during fluting. The effects of the fluting stresses on these losses are the subject of this article. Attention will be centered on the hot corrugating process. A second article will identify those medium properties which affect losses during fluting and papermaking changes to improve these properties so that more of the inherent potential of the medium can be retained through the fluting process.

BACKGROUND

In its simplest concept, fluting is a forming operation. The medium is drawn under tension into the nip between the corrugating rolls, termed the labyrinth. In the labyrinth, the medium is shaped to the flute contour under the prevailing stress, temperature, and moisture conditions. At the center of the labyrinth high transverse compressive forces are applied to the medium which serve to help set the fluted shape.

Direct tensile stresses are induced in the medium by the applied brake tension and the frictional drag on the medium as it is drawn over the flute tips. McKee and Gander (3,5) showed that friction causes the web tension near the center of the labyrinth to be much greater than the applied brake tension. This has been confirmed by others (4,6), as well. Some investigators have shown that increasing the brake tension causes fractures to occur at lower speeds and reduces board strengths (2-4,7,8).

Bending the medium around the flute tip contour induces tensile stresses on the convex side of the medium and compressive stresses on the concave side. For pure bending, conformity to the flute tip contour requires bending strains that are greater than the MD stretch of the medium (3,6). These strains would be expected to cause fiber-to-fiber bond damage to the medium with a subsequent reduction in end-use performance of the combined board. This is particularly true because the relatively lower strength of medium in compression (9) was not taken into account in the bending strain estimate above. The pure tensile strains induced by web tension combine with these bending strains to increase total strain on the tensile side and reduce total strain on the compressive side. Acting together, these strains would be sufficient to cause fracture failure in almost every case, but fortunately shear strains are also induced in the medium as it conforms to the flute contour. It is believed these help by reducing the net strain below the stretch limit to permit forming without fracture (5).

At the center of the labyrinth, transverse compressive stresses applied to the medium are sufficient to reduce the tip and root caliper by about 35% (1). This action is similar to dry calendering which reduces sheet strength by disrupting fiber bonds.

McKenzie and Yuritta (10) have shown that the tensile strength of medium is reduced when it is formed in the Concora fluter. Their results indicate that the losses are independent of roll temperature but increase slightly with decreasing medium roll moisture content. Similar losses in tensile strength have been noted in Institute work. However, the effects of forming on the compressive properties of medium have not received attention, despite the importance of compressive strength to end-use performance.

In summary, the medium is exposed to relatively high tensile, bending, shear and transverse compressive stresses during fluting. We believe the stresses are high enough to affect fiber-to-fiber bonding thereby lowering combined board compressive and flat crush strengths.

DISCUSSION OF RESULTS

Strength Comparisons of Formed and Unformed Mediums

To characterize and quantify the strength losses incurred during fluting, considerable experimental work was carried out using four commercial 26-lb mediums: three semichemical and one recycled fiber. To determine the degree of compressive strength loss during forming, short span tests were made on fluted but unbonded sections of cold and hot formed medium. The compressive tests were made on the STFI short span compression tester which employs a test span of 0.7 mm (11). The short test span permits localized strength determinations which are of great value in studying formed flutes.

The machine direction STFI compressive strength results, taken at various positions around both hot and cold formed flutes, are shown in Fig. 1 and 2 for each of the four mediums. In each figure the upper dashed line represents the compressive strength for the unformed medium. The results show that all of the formed mediums exhibit reduced compressive strengths at all positions around the flute, although the losses are most severe at the tips and roots. Both hot and cold formed mediums show similar patterns, although there are some significant differences which are noted below. Overall the reductions in MD compressive strength were about 40%. We believe these reductions in compressive strength reflect fiber bonding damage caused by the high stresses in the forming process.

In Fig. 2 the MD compressive strengths in the flank and tip/flank regions (positions 2-4 and 6-8) tend to be reduced more by cold forming, especially on the trailing flank. These two mediums also exhibited lower flat crush when formed cold. For the mediums in Fig. 1, where the cold and hot flat crush results were comparable, the compressive strengths of the hot and cold formed mediums were also about the same.

Based on past observation and experiment, we believe it is reasonable to expect the flat crush load-deformation characteristics to be related to the MD edgewise compressive properties of the formed medium. Thus the lower ultimate flat crush strength obtained with some mediums under cold forming conditions can be explained in terms of the greater compressive strength degradation in the flank/tip and flank regions of the flute. This is illustrated by Fig. 3, which shows that the STFI compressive strengths of the tip/flank region are related to flat crush for hot or cold formed mediums. In contrast, the STFI compressive strengths of the uncorrugated mediums are not related to flat crush results for either forming method. This supports the hypothesis that degradation of MD edgewise compressive strength during forming is a major factor in reduced flat crush performance.

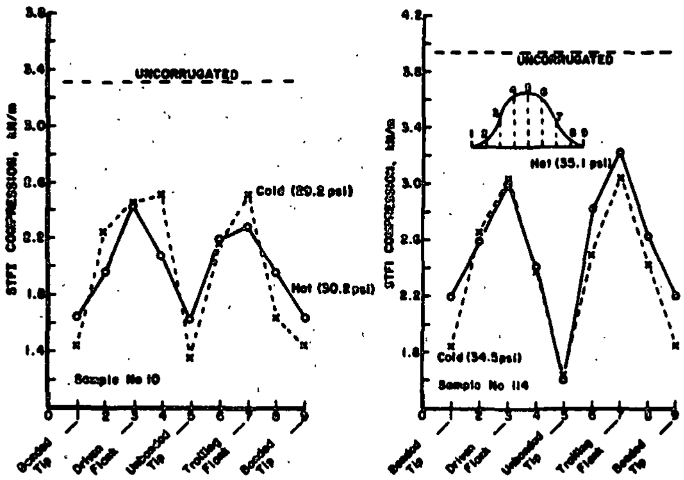

Fig. 1 Machine direction compressive strength after fluting for mediums exhibiting "Equal" cold/hot flat crush ratios (flat crush values in parentheses).

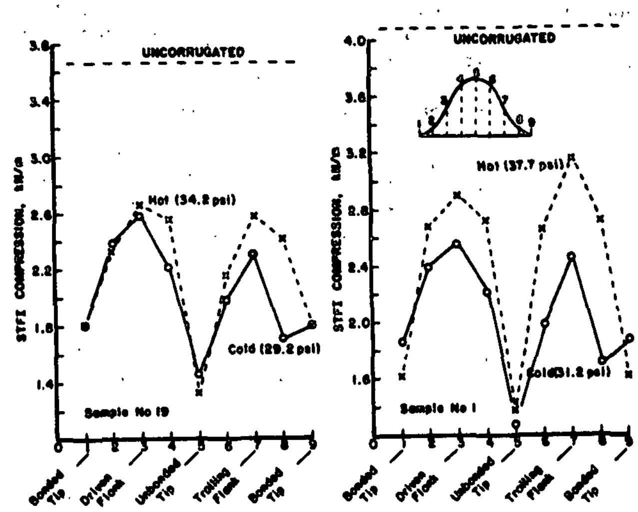

Fig. 2 Machine direction compressive strength after fluting for mediums exhibiting "different" cold/hot flat crush strength (flat crush values in parentheses).

Short span MD tensile tests on the sample 1 hot formed medium also showed reductions in strength, ranging from about 17-44% as compared to the uncorrugated medium (Fig. 4). In all cases studied the percentage reductions in short span tensile strength were less than in edgewise compression. Thus, while forming affects both the short-span tensile and compressive characteristics of the medium, compressive strength is lowered more drastically, at least for speeds before the onset of fracturing. This may occur because compressive strength is sensitive to the shear stresses induced in the forming process.

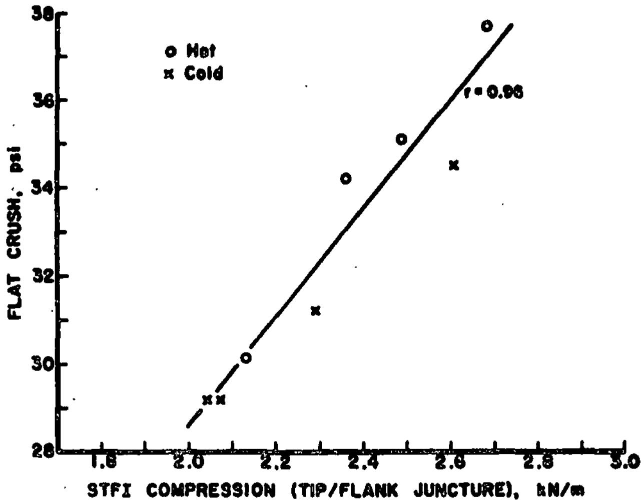

Fig. 3 Relation between compressive strength of the fluted medium and flat crush.

Figure 4 also shows that the cold formed medium exhibits lower tensile strength than the hot formed medium in all flute positions. The tensile strengths, however, vary more erratically with flute position than do compressive strengths. In any case, the reductions in tensile strength do not appear to be directly related to the losses in flat crush potential, although they may affect other board qualities.

STFI edgewise compressive tests were also made in the cross-machine direction on both hot and cold formed mediums. Because the width of the sample clamp is about one flute length, separation by position on the flute was impossible. Figure 5 indicates that forming reduces the average CD compressive strength of the medium about 20%. These reductions are about equal for hot and cold corrugating. Since in many combined board grades, one-third or more of the top-to-bottom box compressive load is carried by the CD strength of the medium, it can be degraded by 7% or more by CD forming losses. These results are significant because they indicate that the corrugating process itself seriously degrades the MD and CD compressive strengths of the medium.

Internal bond strength values, measured by tests of the Viscosity-Velocity Product (VVP) type, were also significantly lowered by forming. It is likely that the reductions in edgewise compressive strength are related to these losses in bonding strength.

Strength Losses from Simulated Forming Stresses

As previously noted, several stress types are induced during forming. To determine the relative significance of each in causing strength losses, a number of special prestressing tests were carried out.

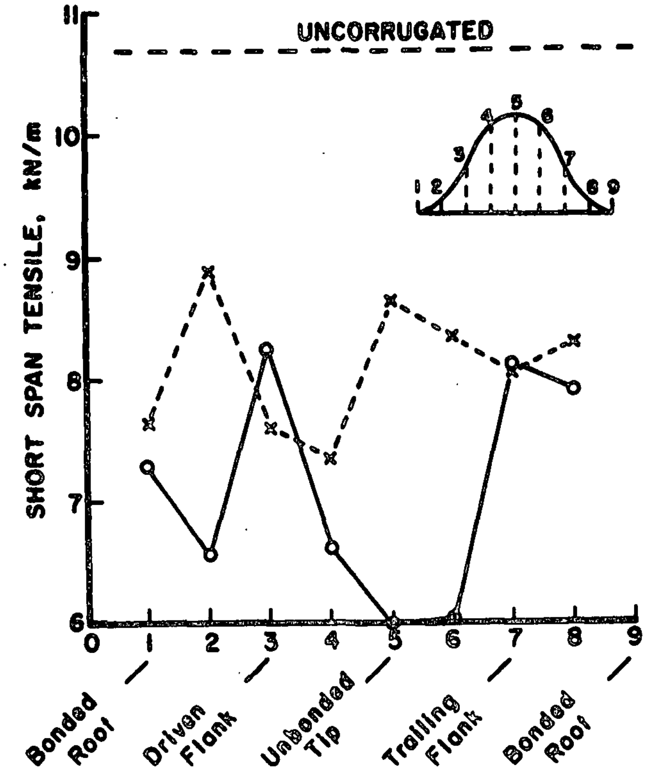

Fig. 4 Effect of forming on short span tensile for sample 1. Compressive strength results for this sample are shown in Fig. 2. (Dashed line = hot formed; solid line = cold formed.)

We first loaded MD specimens of unformed medium in tension to failure. The remnants were then evaluated for compressive strength. Figure 6 shows that prestressing in tension produces no significant degradation in compressive strength, making it an unlikely candidate for causing compressive strength losses.

In corrugating, the onset of visible fracturing occurs gradually over a range of speeds. Fractures also usually occur locally and rarely propagate across the web as in tensile tests. Within the corrugating labyrinth, the medium may be stretched locally far enough to produce bond damage and hence affect compressive strength, but with insufficient stored energy to cause to propagate tensile fractures.

Flexing a medium around a small radius induces bending and shear stresses similar to those incurred in forming. We carried out such experiments. Figure 7 shows that such preflexing greatly reduces the MD compressive strength of the medium. The smaller the radius, the greater the loss in compressive strength. These results suggest bending is a likely contributor to the losses in MD compressive strength. Because the tip and root radii of the corrugating rolls are in the range of about 0.060 inch, both bending and shear stresses would be involved.

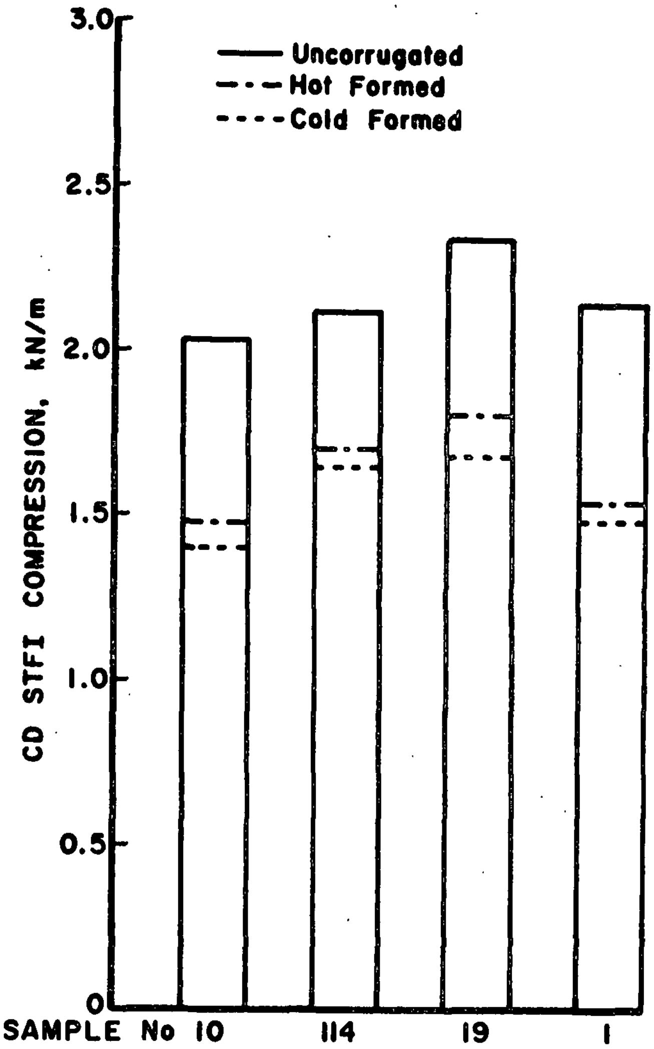

Fig. 5 Effect of forming on cross-direction edge-wise compressive strength.

The combined effects of bending and tension stresses are illustrated in Fig. 8, which shows that the compressive strength decreases rapidly as the wrap angle increases from 0 to 90°. Wrap angles around the flute tip in a corrugator are about 90-120° near the center of the labyrinth (6,7). These angles are large enough to cause a significant loss in strength. The results in Fig. 8 also show that the losses in compressive strength are increased by higher tensions and smaller radii. Past work has shown that high web tensions occur in the corrugating labyrinth as a result of friction between the medium and steel rolls.

The moisture content of the medium at the time of forming will also affect stiffness and moldability. Higher moisture contents should permit the medium to be bent to the flute radius with less damage, assuming that friction is held constant or reduced.

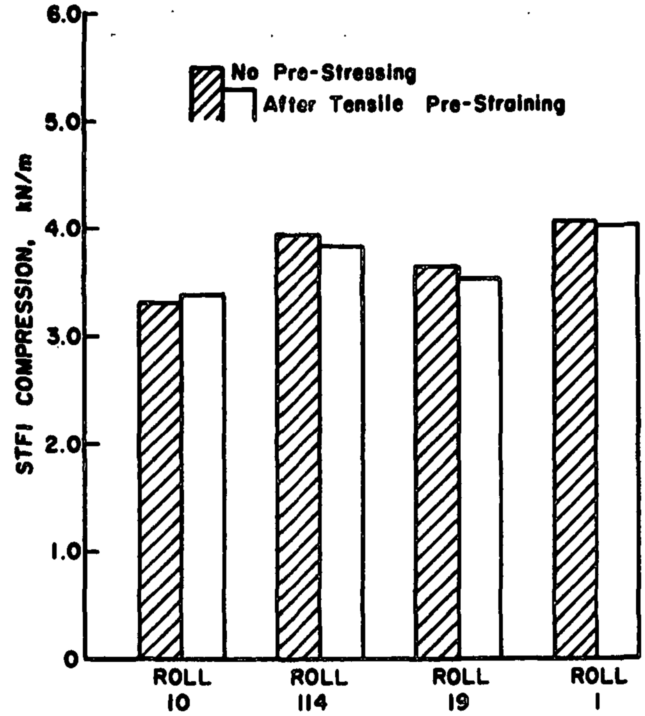

Fig. 6 Effect of tensile prestressing of MD edge-wise compressive strength.

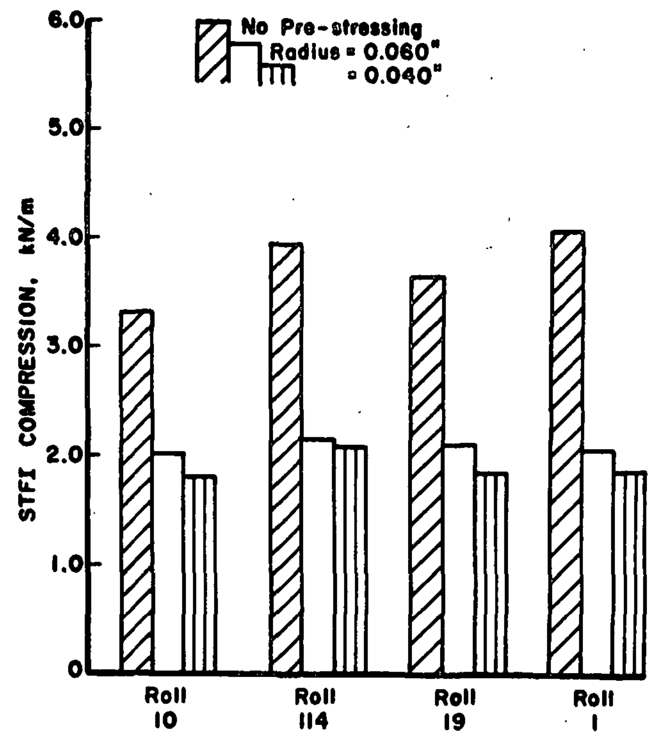

Fig. 7 Effect of bending prestressing on MD compressive strength.

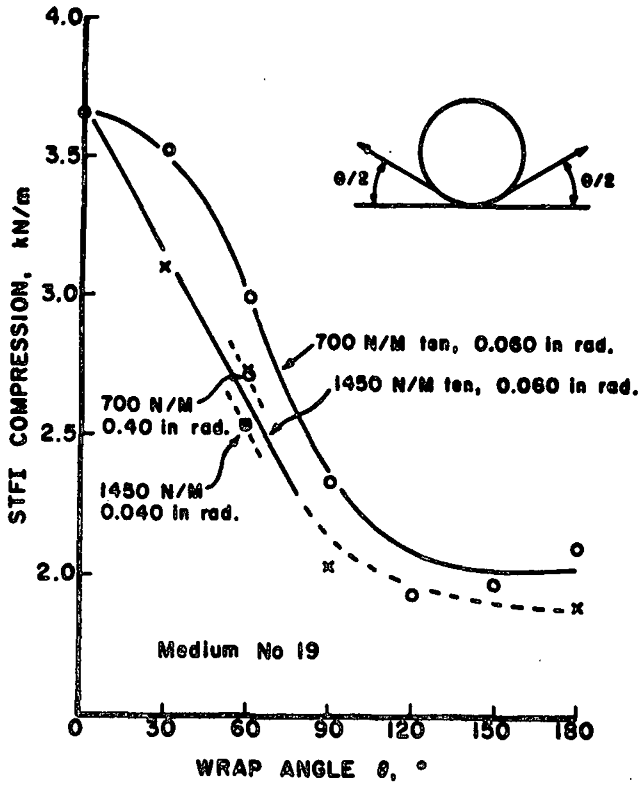

Fig. 8 Effect of tension and flexing conditions on MD compressive strength.

EXPERIMENTAL

Materials

Four commercial 26-lb/1000 ft^2 (ca. 127 g/m^2) mediums were selected for use:

1. Roll No. 1, semichemical
2. Roll No. 10, semichemical
3. Roll No. 19, semichemical
4. Roll No. 114, recycled fiber

Sample rolls 10 and 114 exhibited comparable flat crush levels under both hot and cold corrugating conditions. Sample rolls 19 and 1 exhibited lower flat crush under cold conditions than under hot conditions.

Corrugating

Each roll was corrugated in The Institute of Paper Chemistry's experimental corrugator under both hot and cold conditions. In the "hot" runs the corrugating rolls and preconditioner were maintained at 350°F and the steam showers were used. In the cold runs the preconditioner and corrugating rolls were at room temperature. The mediums were treated on both sides prior to the fluting with a solid "slip" agent comprised of paraffin wax, graphite, stearin, and silicone.

Samples of the formed but unglued medium and single-faced board were obtained at a speed of 200 fpm under both hot and cold conditions.

Test Procedure

The uncorrugated mediums were characterized in terms of a wide array of physical properties as given in Table 1. TAPPI test procedures were employed where available.

Table 1 Properties of the uncorrugated medium

		Roll 10	Roll 114	Roll 19	Roll 1
Basis weight, g/m^2		126.9	137.7	128.4	127.4
Caliper[b], m		259	274	272	234
Density, kg/m^3		486	496	467	538
Concora crush, N		232	297	283	342
Coeff. of friction[a]	73°F	0.58	0.52	0.54	0.54
	310°F	0.44	0.24	0.25	0.28
STFI compressive strength, kN/m	MD	3.31	3.94	3.66	4.08
	CD	2.03	2.11	2.34	2.14
Tensile strength, kN/m	MD	4.52	9.38	6.11	7.56
	CD	2.29	3.06	2.98	2.61
Stretch, %	MD	0.94	1.42	1.22	1.04
	CD	1.30	4.24	1.79	2.57

[a]Kinetic coefficient between medium and a reference steel surface (IPC procedure).
[b]TAPPI T 411.

CONCLUSIONS

(1) The edgewise compressive strength of fluted medium is reduced by the fluting operation in both the machine and cross-machine directions. The reductions range from 35-50% in the MD, while the CD compressive strengths are reduced about 20%. This degradation of compressive strength in both directions decreases box compressive strength, flat crush strength, and other combined board properties.

(2) Simulation experiments reveal that prestressing the medium in bending is probably the greatest factor in reducing edgewise compressive strength. The compressive strength losses are increased further by higher tensions during bending. Greater losses occur as the radius of bend decreases because the strain in the outer fiber layers is inversely related to the radius. These results suggest that the compressive strength losses in the medium - and hence ECT and flat crush losses in the combined board - are due primarily to bending stresses induced during forming.

(3) The transverse bonding strength of the medium

is also reduced by forming. This is consistent with the hypothesis that fiber-fiber bond breakage occurs in the fluting operation.

(4) All mediums tested showed a strong correlation between flat crush strength and the remaining compressive strength in the flank/tip region of the flute after forming. Some mediums showed evidence of greater compressive strength reduction when formed cold. We believe this accounts for the lower flat crush obtained with these mediums under cold forming conditions.

ACKNOWLEDGMENTS

This research was carried out at The Institute of Paper Chemistry (IPC) as part of basic studies on the fluting process and to support development of the cold corrugating process. The latter development was carried out under the sponsorship of the IPC, the Fourdrinier Kraft Board Group, and the Department of Energy, with the active support of the Union Camp Corporation.

LITERATURE CITED

1. Sprague, C. H., and Whitsitt, W. J., Project 3396, Report One to Members of The Institute of Paper Chemistry. June 15, 1981.

2. Whitsitt, W. J., Sprague, C. H., and Kloth, G. R., Tappi 65(10):83-5 (1982).

3. McKee, R. C., and Gander, J. W., Tappi 50(7): 35-40A (July, 1967).

4. Gottsching, L., and Otto, W., Papier 30(10): 417-25 (Oct., 1976); 30(11):457-68 (1976); 31 (2):45-53 (Feb., 1977); 31(3):85-94 (March, 1977); 31(4):12-36 (April, 1977); 31(5):169-79 (May, 1973).

5. McKee, R. C., and Gander, J. W., Project 1108-22, Report One to the FKBG, Feb. 29, 1960.

6. Thomas, C. E., 1979 Corrugated Containers Conference Proceedings. pp. 39-48.

7. McKee, R. C., Tappi 43(3):218-28A (March, 1960).

8. Toroi, M., and Kolhonen, E., Pulp Paper Mag. Can. 77(10):T194-7 (Oct., 1976).

9. Seth, R. S., Soszynski, R. M., and Page, D. H., Tappi 62(12):97-9 (1979).

10. McKenzie, A. W., and Yuritta, J. P., Appita 27(2):106-11 (1973).

11. Cavlin, S., and Fellers, C., Svensk Papperstid., 9:329-32 (1975).

APPENDIX B

IPC Technical Paper Series

Number 168

COMPRESSIVE STRENGTH RETENTION DURING FLUTING

PART 2. IMPROVED MEDIUM STRENGTH.

W. J. Whitsitt and G. A. Baum

May, 1986

COMPRESSIVE STRENGTH RETENTION DURING FLUTING. PART 2: IMPROVED MEDIUM STRENGTH

W. J. Whitsitt
Research Associate
The Institute of
Paper Chemistry
Appleton, WI 54912

G. A. Baum
Division Director
The Institute of
Paper Chemistry
Appleton, WI 54912

ABSTRACT

Previous research has shown that the compressive strength of corrugating medium is degraded in the fluting operation. In this article, attention is focused on papermaking ways to alter the properties of the medium so it can be formed with less damage and thus give more strength to the combined board. At constant basis weight, compressive strength retention is favored by high density (if associated with better fiber bonding) and a high out-of-plane to in-plane stiffness ratio (E_z/E_x). These may be achieved by using higher wet pressing pressures. Higher pressing pressures densify the medium and tend to increase E_z at a faster rate than E_x. The higher out-of-plane stiffness helps the medium resist fiber-to-fiber bond damage during fluting, and hence the medium retains more compressive strength. Densification also reduces caliper, which lowers the bending strains during fluting. As a result of the above, flat crush and ECT increase due to a better retention of strength during fluting and the higher base strength of the medium. Succeeding articles in this series will discuss other aspects of the forming operation and high speed runnability.

INTRODUCTION

In a previous article we discussed the strength losses which occur during fluting (1). Our results indicated that about 40% of the MD and 20% of the CD short span compressive strength (STFI) of the medium is lost in the fluting process. These losses are a result of the high bending strains imposed on the medium as it is fluted and by the high web tensions in the fluting labyrinth. By reducing these losses in strength, it should be possible to improve ECT and flat crush.

There are two approaches to minimizing strength losses during fluting. One approach is to make more effective use of preconditioning heat and steam. From a forming standpoint, the function of preconditioning is to temporarily alter the properties of the medium so it can be formed with less damage. Thus there is potential for improved fluting (minimizing losses) by optimizing the preconditioning heat and steam. Use of this approach will be discussed in a future article.

The second approach is to alter the properties of the base medium during its manufacture so that it can be formed with less damage. This area is the subject of this article.

Other research at The Institute of Paper Chemistry has shown that edgewise compressive strength is highly related to the elastic moduli of the sheet (2). Baum, Habeger and coworkers (3,4) have developed ultrasonic techniques for measuring the in-plane and out-of-plane elastic moduli of paper. High compressive strengths are favored by high moduli in the MD and CD directions (E_x and E_y) and by high thickness direction moduli (E_z, G_{xz}, G_{yz}). Sheet densification to increase fiber bonding is an effective way to increase all of these moduli and hence, compressive strength.

Our past work indicates that the retention of compressive strength during fluting is approximately related to the elastic stiffnesses of the sheet, basis weight and density as follows.

$$RR = 1 - (K/R)(E_x/E_z)^{1/4}\ W/\rho \qquad (1)$$

where RR = retention ratio (ratio of compressive strengths of fluted to uncorrugated medium)
E_x = MD Young's modulus
E_z = out-of-plane Young's modulus
W = basis weight
ρ = density
R = radius of curvature of the fluting rolls
K = constant

Thus in the fluting operation the retention of compressive strength should be favored by high density and a high thickness direction modulus (E_z), and adversely affected by high caliper (W/ρ) and MD modulus (E_x). This is shown in Fig. 1. Our initial research discussed here focused on wet pressing as a means for improving compressive strength retention and improved end-use properties.

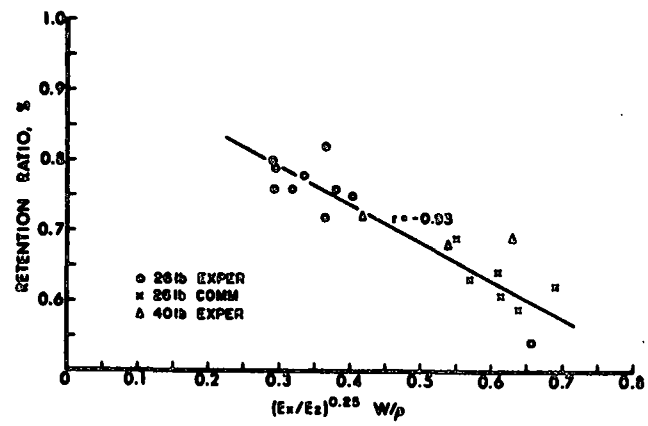

Fig. 1 Retention of compressive strength during fluting depends on elastic stiffnesses, (E_x/E_z), basis weight (W) and density (ρ).

Fluting Performance of Densified Mediums

We made oriented sheets on a Formette Dynamique from a 75% semichemical/25% softwood furnish over a range of densities from about 500 to 1100 kg/m^3, based on IPC soft platen caliper tests (5). To obtain an initial evaluation of corrugating performance, the 26 and 40 lb/1000 ft^2 experimental sheets were spliced into a commercial "carrier" medium, and made into single-faced boards at a speed of about 200 fpm.

All of the experimental and the commercial mediums used as controls corrugated with no difficulties at the low speed used. No bonding problems were encountered; the single face pin adhesion test values were satisfactory for all the mediums.

Figure 2 shows that increasing sheet density increases the retention ratio of compressive strength for both the 26 and 40 lb/1000 ft^2 experimental mediums, as compared to a commercial 26 lb/1000 ft^2 medium. The improvements in retention were less for the 40 lb/1000 ft^2 mediums than for the lighter material because of the greater thicknesses of the 40 lb/1000 ft^2 sheets.

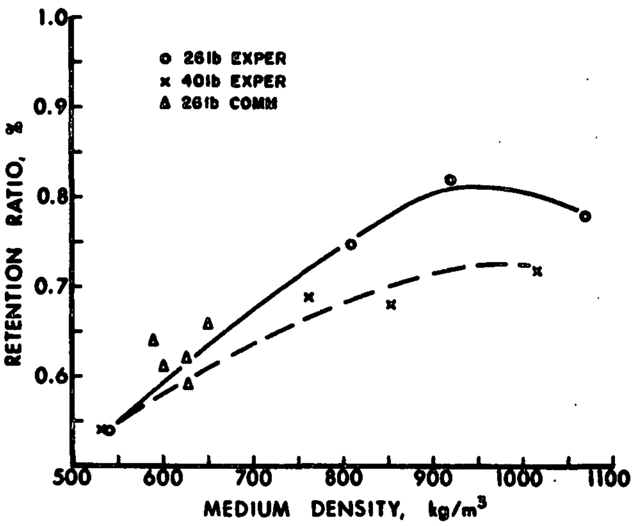

Fig. 2 Effect of density on retention of compressive strength during fluting.

Densification improves most strength properties, thus flat crush strength also increased substantially as density increased, as shown in Fig. 3. At the higher densities the flat crush strengths are greater than those obtained with most commercial mediums. These improvements in flat crush can be attributed to both better retention during fluting as well as the higher MD compressive strengths of the densified sheets.

Compression tests on the combined board show that increasing the medium density markedly increases CD ECT (Fig. 4) as a result of the higher CD compressive strength of the medium.

Increasing medium density monotonically increases CD STFI compressive strength; however, CD ring crush passes through a maximum at a density of 750-800 kg/m^3 (Fig. 5). Thus the shortspan compressive strength results were more indicative of combined board ECT performance. A similar situation prevails when MD STFI and MD ring crush results are compared with the combined board flat crush results (6). Seth (7) also has shown that ring crush passes thru a maximum as wet pressing is increased.

Higher wet pressing pressures also produce substantial increases in the tensile strength of the medium (Fig. 6). The higher tensile strengths should allow higher corrugating speeds before flute fracture occurs because the medium will be better able to tolerate the high tensile stresses imposed during fluting.

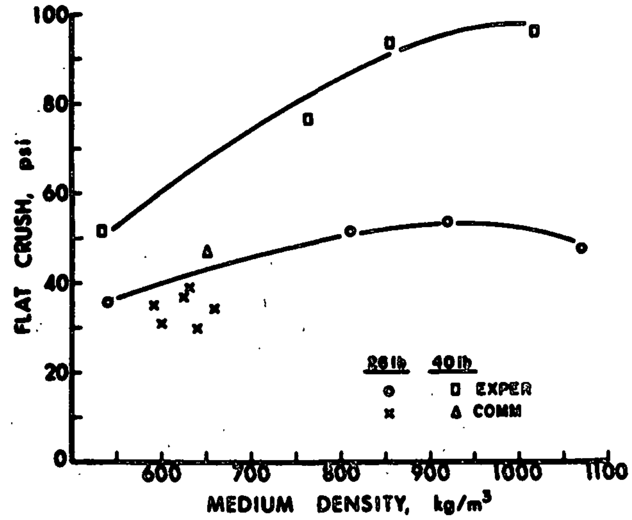

Fig. 3 Increasing medium density improves flat crush.

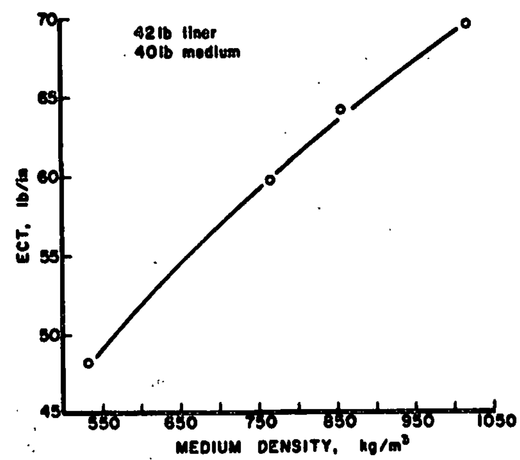

Fig. 4 Increasing medium density improves ECT strength.

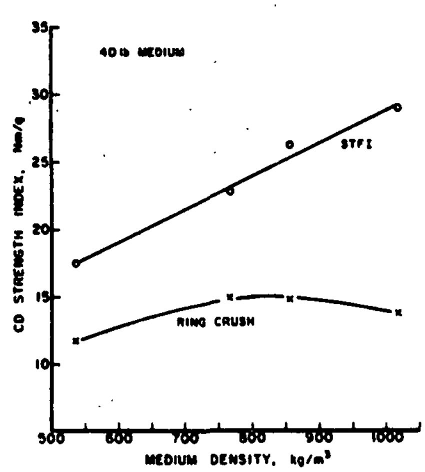

Fig. 5 CD short span compressive strength and ring crush results *vs.* medium density.

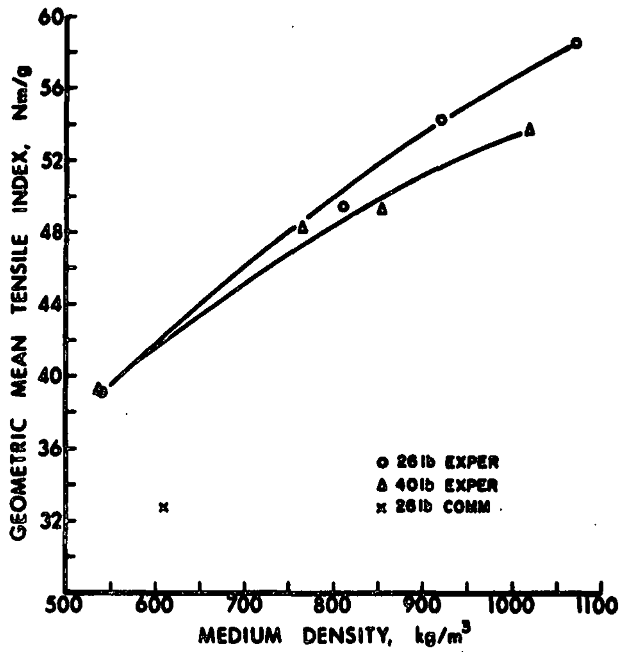

Fig. 6 Increased wet pressing increases tensile strength.

The specific in-plane and out-of-plane elastic stiffnesses also increased with increasing density as shown in Fig. 7. As noted earlier, compressive strength is dependent on the product of $E_x^{3/4}E_z^{1/4}$ or $E_y^{3/4}E_z^{1/4}$ for the MD or CD directions, respectively (2). Because densification increases all three stiffnesses, it would be expected that compressive strength would increase as illustrated in Fig. 5 for the short span STFI compressive strength results.

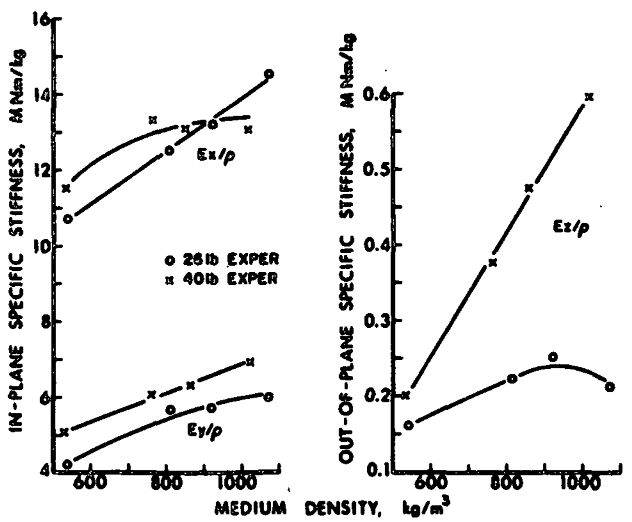

Fig. 7 Effect of density on elastic stiffnesses.

Runnability

Work was carried out to determine whether densification of the medium would adversely affect high speed runnability, including flute fracture, high-lows, and bonding. Because of their greater strength, densified mediums should be better able to resist fracture, but densification could reduce porosity and water receptivity, which would affect high speed bonding.

Oriented medium sheets were made at several densities achieved by wet pressing. The sheets were made with typical MD/CD orientation of about 2/1, using a 75% semichemical plus 25% softwood furnish. Two pressing/drying techniques were employed, namely:

(1) Blotter pressed and dried. One side of sheet was in contact with blotters, while the other side was in contact with a belted rotary press-dryer drum.

(2) Felt pressed and dried. One side of sheet was in contact with a linerboard press felt, with the other side in contact with the belted rotary press-dryer drum.

The blotter and felt-pressed sheets exhibit different compressive strengths at the same density as shown in Fig. 8. The same trend has been observed in other work in progress. This demonstrates that pressing conditions (such as the felt structure) also can affect compressive strength. The elastic stiffnesses of the sheets are affected in a similar way by these drying techniques, as shown in Fig. 9. While the felt-pressed sheets gave lower compressive strengths and stiffnesses, they exhibited higher tensile strengths at the same density, see Fig. 10.

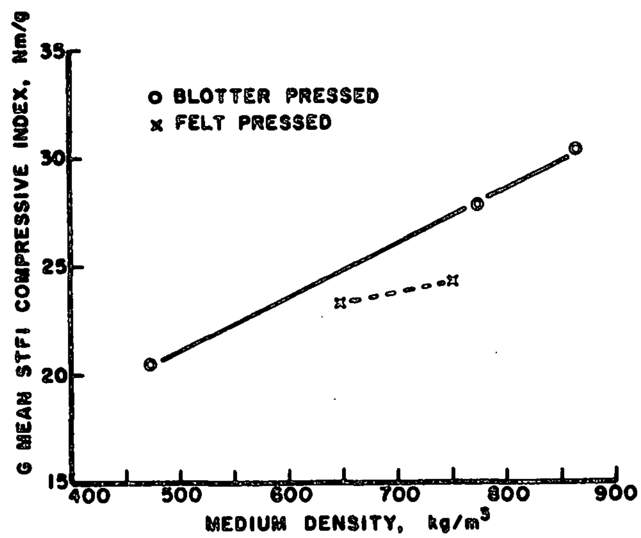

Fig. 8 Effect of densification on geometric mean compressive strength for different pressing/drying conditions.

The air porosity of the sheet decreases, as shown in Fig. 11, as pressing pressures are increased. Commercial mediums, however, exhibit a wide range of porosities. For example, the three commercial mediums used for controls in this study gave Bendtsen porosities ranging from about 350 to 1300 mL/min. Experience indicates that mediums having quite different porosities can be successfully bonded at normal corrugating speeds, although some adjustments in the adhesive or the preheaters and steam showers may be necessary.

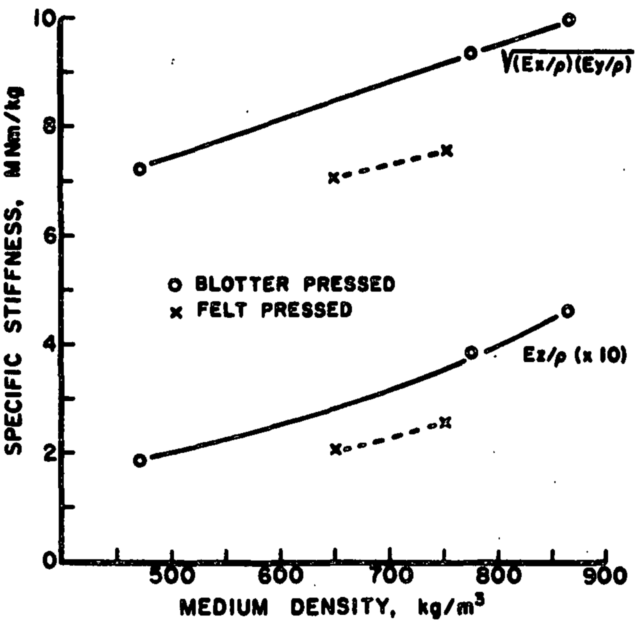

Fig. 9 Effect of densification on specific elastic stiffnesses for different pressing/drying conditions.

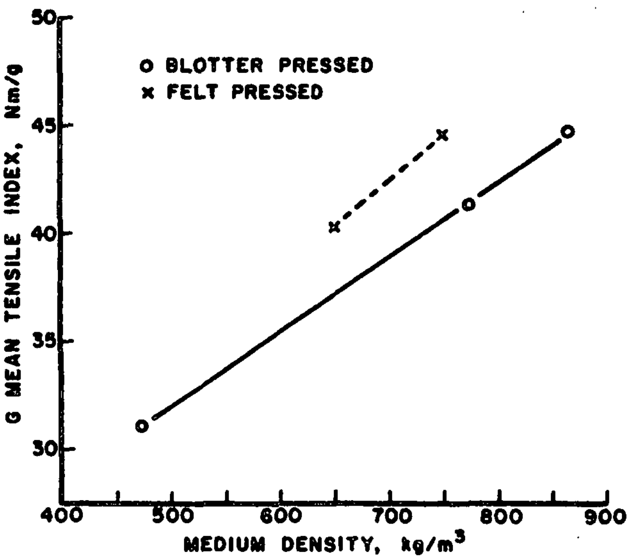

Fig. 10 Effect of densification on tensile strength for different pressing/drying conditions.

The water drop values for the blotter-pressed sheets increased with density, as expected. At the same density, however, the felt-pressed sheets gave lower water drop values, showing that pressing and drying conditions can affect the water receptivity of medium. In general, however, the experimental sheets had water receptivities in the same range as the commercial controls.

All of the mediums corrugated without fracture at speeds up to 650 fpm (Table 1), except that the lowest density sheets exhibited minor fractures in the 400 to 650 fpm range. This was probably due to their lower strength and relatively high caliper, which would increase the bending strain during fluting.

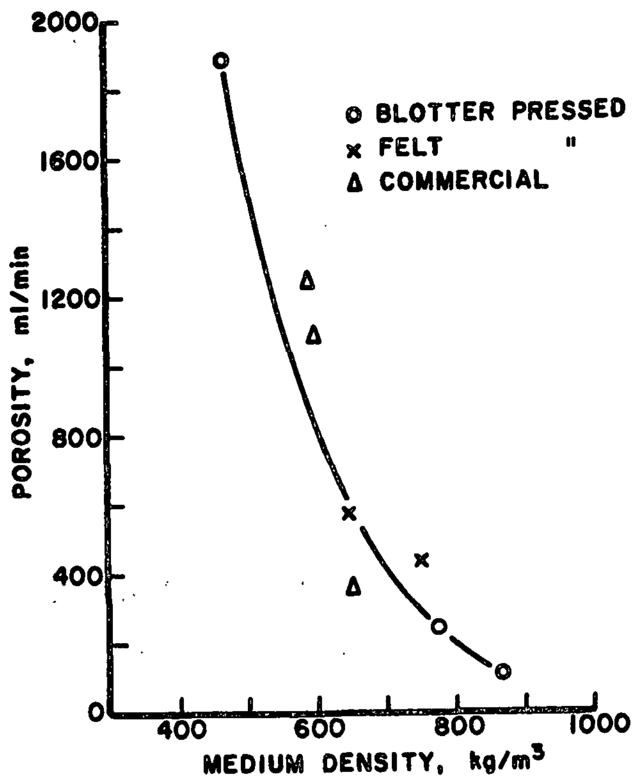

Fig. 11 Effect of densification on porosity.

Table 1. Corrugating results.

	Speed fpm	Low Dens. (185)	Med. Dens. (186)	High Dens. (182)	Felt Pressed[a] Med. Press.[a] (63)	Felt Pressed[a] High Press.[a] (77)	Commercial Controls 6171	Commercial Controls 6208	Commercial Controls 6209
Fracture[b]	400	SlF	No F	No F	No F	No F	No F	No F	No F
	550	SlF	No F	No F	No F	No F	No F	No F	No F
	650	SlF	No F	No F	No F	No F	No F	No F	No F
Pin adhesion lb/ft	400	26.2	37.0	36.5	--	--	38.5	36.0	36.5
	550	28.1	33.1	31.8	--	--	33.0	32.4	31.1
	650	20.1	22.8	--	--	--	18.5	24.8	23.5
High-low,% >4 mil	400	1.0	11.4	6.2	0	4.2	3.6	12.5	15.6
	550	0	7.8	17.2	0	6.2	15.6	--	20.8
	650	1.0	1.0	--	6.2	8.3	11.5	14.6	16.6
% >3 mil	400	6.2	20.8	15.6	2.1	14.6	12.2	27.1	35.4
	550	3.1	15.4	28.9	10.4	22.9	30.2	11.4	27.1
	650	4.2	4.2	--	10.4	27.1	34.0	27.1	35.5
ECT, lb/in.	400	33.1	40.1	41.7	--	--	39.2	36.6	36.2
	550	34.2	40.0	43.0	--	--	36.8	36.6	35.2
	650	33.1	41.6	--	--	--	36.8	34.7	33.5
	Av.	33.5	40.6	42.4	--	--	37.6	36.0	35.3
Flat crush, psi	400	38.1	56.1	59.2	36.5	40.6	34.5	34.8	30.5
	550	39.7	57.1	57.2	35.4	40.1	35.2	36.2	30.8
	650	37.7	57.3	--	38.2	40.2	34.1	35.4	30.9
	Av.	38.5	56.8	58.5	36.7	40.3	34.6	35.5	30.7

[a]Low and high felt pressed sheets, fabricated at a later time with new 42-lb liner roll.
[b]SlF = slight fracture; No F = no fracture.

Figure 12 indicates that the experimental blotter-pressed mediums exhibited high-low levels which were about the same or less than the commercial controls. High-lows were defined as the percentage of flute height differences exceeding 4 mils. They were measured using a SELCOM laser displacement gage. Thus, densification does not appear to increase the proclivity to form high-lows. It is believed this is due to the lower thickness and better fiber-to-fiber bonding achieved by wet pressing.

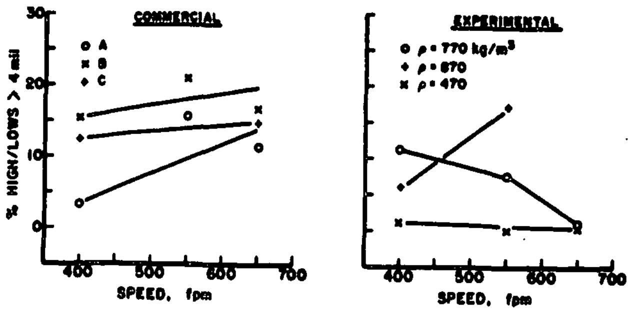

Fig. 12 High/low results on commercial and densified mediums. (A, B, and C are three 26-lb commercial mediums used as controls and corrugated at the same time as the experimental medium).

In Fig. 13 the single-face adhesion results for the densified blotter-pressed mediums are compared to the commercial controls. In general, the densified sheets exhibit about the same pin adhesion strengths as the commercial mediums at the same corrugator speeds. In both cases the adhesion strengths decrease with increasing speed, consistent with other results from our pilot corrugator.

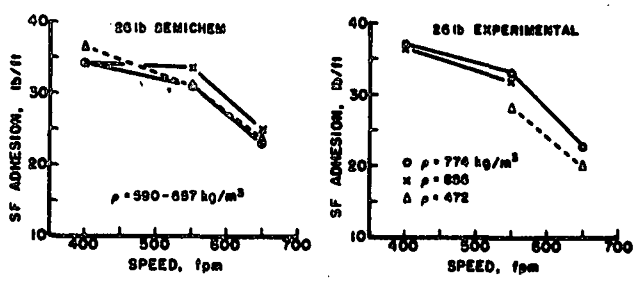

Fig. 13 Comparison of single-face adhesion results on commercial and experimental densified mediums.

Summarizing, these results indicate that densification of medium can be beneficial to high speed runnability. If necessary, adhesive formulations could be changed to optimize adhesion. It would still be possible to adjust the water receptivity of the medium with surfactants as is commonly done today.

CONCLUSIONS

This work explored ways to minimize the strength losses that occur during fluting (1). This would enhance ECT and flat crush strength in combined board. The results show

1. Densification of medium by increasing the wet pressing pressure makes substantial increases in flat crush and the ECT strength of combined board made from the medium. These improvements are due to the retention of compressive strength during fluting and the higher compressive strengths and elastic stiffnesses obtained from densification.

2. The retention of compressive strength during fluting is favored by lower weight to density ratios (caliper) and by a higher out-of-plane stiffness (E_z/ρ) relative to the in-plane stiffness (E_x/ρ).

3. The high density mediums gave single-face bonding levels in the corrugator which were comparable to those obtained with commercial mediums. High-low flute formation levels were also comparable for the experimental and commercial mediums. While these results are not necessarily conclusive because of the small sheet sizes and narrow width of the pilot corrugator, they do indicate that commercial corrugating should be feasible. If necessary, adjustments in surface receptivity or starch formulation could be made.

LITERATURE CITED

1. Whitsitt, W. J., and Sprague, C. H. Compressive Strength Retention During Fluting. Part I, Strength Losses. To be published.

2. Habeger, C. C., and Whitsitt, W. J., Fibre Science and Technol. 19:215-239 (1983).

3. Baum, G. A., Brennan, D. C., and Habeger, C. C., Tappi 64(8):97 (1981).

4. Mann, R. W., Baum, G. A., and Habeger, C. C., Tappi 63(2):163 (1980).

5. Wink, W. A., and Baum, G. A. A rubber platen caliper gage - a new concept in measuring paper thickness. Tappi 66(9):131-133 (1983).

6. Whitsitt, W. J. Compressive Strength Factors and Relationships. Forest Products Laboratory Compression Symposium, Madison, WI, Oct. 1-3, 1985.

7. Seth, R. S., Tappi 67(2):114 (1984).

THE INSTITUTE OF PAPER CHEMISTRY

Appleton, Wisconsin

Status Report

to the

PAPER PROPERTIES AND USES

PROJECT ADVISORY COMMITTEE

Project 3469

STRENGTH IMPROVEMENT AND FAILURE MECHANISMS

February 13, 1987

PROJECT SUMMARY

PROJECT NO. 3469: STRENGTH IMPROVEMENT AND FAILURE MECHANISMS

STAFF: J. Waterhouse, W. Whitsitt February 13, 1987

PROGRAM GOAL:

Identify critical parameters which describe converting and end-use performance and promote improvements in cost/performance ratios.

PROJECT OBJECTIVE:

Establish practical methods for enhancing strength properties (especially compressive strength) during paper manufacture and to evaluate deformation behavior as it relates to sheet composition and structure.

PROJECT RATIONALE, PREVIOUS ACTIVITY and PLANNED ACTIVITY FOR FISCAL 1987-88 are on the attached 1987-88 Project Form.

SUMMARY OF RESULTS LAST PERIOD: (March 1986 - September 1986)

(1) In an attempt to determine the compressive strength potential of pulped unseparated fibers, wood coupons, 16 mm x 16 mm of white spruce have been ultrasonically characterized after 8 hrs and 12 hrs of acid chlorite treatment. Half of the wood coupons were given a mild caustic treatment to facilitate fiber separation and 19 mm diameter handsheets were made. Ultrasonic characterization and compressive strength measurements were also made on these handsheets.

(2) In student related work B. Allender has completed his research project "Morphological Factors in the Refining of Eucalypt and Pinus Radiata Fibers". A paper has been accepted for the PIRA, Paper and Board Division International Conference "Advances in Refining Technologies" Birmingham England, December 1986.

(3) In student related work Tom Bither's doctoral research is entitled, "Strength development through Internal Fibrillation and Wet Pressing" Tom has been evaluating a device for ensuring restrained drying after wet pressing. In addition the response of three different pulps to wet pressing and refining is being determined.

(4) In student related work M. Franke (formerly M. Kemps) master's research is entitled, "Z-direction variation of internal stress and paper properties". Marypat is evaluating the layer removal technique using commercial board and Formette handsheets to determine their Z-direction variation of residual stress and properties.

(5) A progress report is being prepared on our experience with the Formette Dynamique. Results for the effects of furnish, differences in jet-wire speed, consistency, basis weight, refining, wet pressing, drying, synthetic fibers and additives on fiber orientation and sheet anisotropy are included.

SUMMARY OF RESULTS THIS PERIOD: (October 1986 - March 1987)

(1) A paper "Morphological Factors in the Refining of Eucalypt and Pinus Radiata Fiber" was presented at PIRA's Advances in Refining Technologies International Conference, Birmingham, England, December 1986. A copy of this paper is included in Appendix 1.

(2) A number of 16 mm x 16 mm wood coupons (230) of white spruce have been prepared and characterized and will be used primarily to determine the effects of lignin content on compressive strength.

(3) Capital has now been authorized for the purchase of the major components for the API/IPC formation tester which include an x-y table, optical equipment and a beta source.

(4) Commercial samples of newsprint, tissue and fine papers and their furnishes have been obtained for the API/IPC formation study. Noble and Wood's and Formette handsheets have been made for these furnishes. An extensive property evaluation of the commercial and handsheet samples has also been completed.

(5) A series of Formette handsheets have been made and characterized, for the purpose of determining the effects of fiber orientation and furnish composition on the variation of internal stress and properties in the thickness direction of paper.

(6) In student related work Tom Bither's doctoral research is entitled "Strength Development through Internal Fibrillation and Wet Pressing. Tom has established a suitable method for wet pressing and restrained drying of his handsheets, and has measured changes in pore size distribution as a result of refining and wet pressing.

(7) In student related work Maripat Franke master's research is entitled "Z-direction variation of internal stress and paper properties". This project will be completed during this winter quarter.

Date:	1/14/87
Budget:	$90,000
Period Ends:	6/30/88
Project No.:	3469

PROJECT TITLE: Strength Improvement and Failure Mechanisms

PROJECT STAFF: J. Waterhouse/W. Whitsitt

PRIMARY AREA OF INDUSTRY NEED: Properties related to end use

PROGRAM AREA: Improved converting processes and converted products

PROGRAM GOAL:

Identify critical parameters which describe converting and end-use performance and promote improvements in cost/performance ratios.

PROJECT OBJECTIVE/GOAL:

To evaluate deformation behavior and its relationship to sheet composition and structure, and to establish practical methods for enhancing strength properties (especially compressive strength).

PROJECT RATIONALE:

Deformation and strength properties are important in predicting end use performance. An improved understanding of failure mechanisms and ways to improve certain strength properties are important to nearly all grades. The recognized importance of compressive strength in linerboard and corrugating medium to box performance provides impetus for research in this area. The approach is to meet the objectives through new papermaking strategies.

RESULTS TO DATE:

We have shown that compressive strength of paper is highly related to a product of in-plane and out-of-plane elastic stiffnesses. The relationship holds for commercial and experimental sheets made under a variety of conditions. This development suggests it will be possible to monitor compressive strength in the mill using ultrasonic techniques.

Compressive strength is enhanced by high densification, which increases bonding, and high fiber axial compressive stiffness. Thus compressive strength increases with refining and wet pressing. Within a practical range, higher CD compressive strength can be achieved by decreased fiber orientation, loose draws, and/or increased CD restraint during drying. Where limitations to increased refining and wet pressing exist, low levels of polymer addition could be used as a viable means to improve compressive strength. The effect of pulp type and additives on the stiffness-compressive strength correlation has been investigated. A technique involving small wood coupons and mini handsheets has been developed to measure the compressive strength potential of wood fibers.

We have developed a torsion mode technique for measuring the out-of-plane shear stress-strain behavior, and studied ZD shear straining on compressive strength.

Internal stress variations have been determined in the thickness direction together with the variation of in-plane and out-of-plane properties. Measurements of the relative losses in elastic and strength properties due to supercalendering have been made. The layer removal technique has been used to determine the Z direction variation of residual stress.

PLANNED ACTIVITY FOR FY 1987-88.

Non-destructive characterization of wood coupons, pulped wood coupons, and mini-handsheets made from them, will be used to estimate the compressive strength potential of certain softwood and hardwood species as a function of lignin removal.

Work will continue on measuring the deformation behavior of board when subjected to combined stresses, an important aspect of a number of converting processes.

Complete construction of a formation tester capable of the simultaneous measurement of light transmittance, reflectance and beta particle absorption; and provide suitable software for formation analysis.

STUDENT RELATED RESEARCH

T. Bither, Ph.D.-1987.

Status Report

STRENGTH IMPROVEMENT AND FAILURE MECHANISMS

Project 3469

INTRODUCTION

Although this project has well defined goals it nevertheless embraces a number of diverse research areas whose interrelationships are not always obvious. The reason for this, is in part, due to the manner in which the project has evolved. It should be understood that the present project is a combination of two earlier projects namely Project 3469 "Compressive Strength Improvement" and Project 3500 "Shear Deformation and Failure". Currently this project embraces the following areas: Compressive Strength Improvement, Formation Measurements, Combined Stress Measurements and Internal Stresses in Paper and Board as discussed in more detail below.

1. COMPRESSIVE STRENGTH IMPROVEMENT

Work during the previous period demonstrated the possibility of using wood coupons and mini-handsheets to determine the effects of species and yield on compressive strength. Specifically, wood coupons were delignified using an acid chorite procedure. The elastic constants were determined using non-destructive methods on wood coupons before and after delignification. It was relatively easy to separate the fibers after complete delignification and treatment with a mild caustic solution. This was done in a small beaker using glass beads and a magnetic stirrer. Mini-handsheets (19 mm dia.) were made from the separated fibers. Apparent density, elastic constants and compressive strength measurements were then made on these handsheets. This preliminary investigation indicated that the in-plane elastic constants increased significantly with increasing wood density and delignification. However the higher density wood coupons (mainly latewood fibers) resulted in handsheets of lower apparent density and lower elastic constants than fibers from the low density wood coupons. Interestingly the elastic constants of the handsheets were significantly higher than those predicted using the wood coupon measurements and assumming a handsheet having random fiber orientation i.e. $E_s/\rho = 1/3\ E_f$. Where E_s/ρ and E_f/ρ are the sheet and fiber elastic moduli, respectively. The next stage in this investigation is to prepare wood coupons at higher yields and to develop suitable methods for fiber separation wherein damage to the fibers is minimal. Presently wood coupons are being prepared from white spruce.

2. FORMATION MEASUREMENTS

Formation is assumed to be an important factor in many converting operations such as corrugating, calendering, supercalendering and printing. We are specifically concerned with its role in failure properties. The work of P. T. Herdman[1] has demonstrated that small scale basis weight variations (or distribution of mass density) can be effected by papermaking process variables such as forming consistency and drying tension, as shown in Fig. 1. Generally the greater the variation in mass density the lower certain strength properties will be. This is particularly critical in low basis weight papers. The variation of mass density is not the only parameter one can derive from formation measurements, and other representations may be more appropriate to specific situations; e.g., B. Jordan[2] and N. G. Nguyen suggested specific perimeter for print mottle. We would therefore like to determine what formation characteristics might be appropriate for failure properties. Capital has now been authorized for the purchase of the necessary off-the-shelf components for the API/IPC formation tester, including; an x-y table, a beta source, and optical components for light transmission and reflectance measurements. A schematic of the proposed tester is shown in Fig. 2. As part of the API-IPC Evaluation of

Formation Measuring Instruments and IPC Formation Study, furnishes for tissue, newsprint and fine papers have been obtained together with production made samples exhibiting various levels of visual formation. Using these furnishes, handsheets have been made on the Noble and Woods, and Formette Dynamique sheet formers to obtain different levels of formation, color, fiber orientation and basis weight. Wet pressing was held constant. Property measurements have also

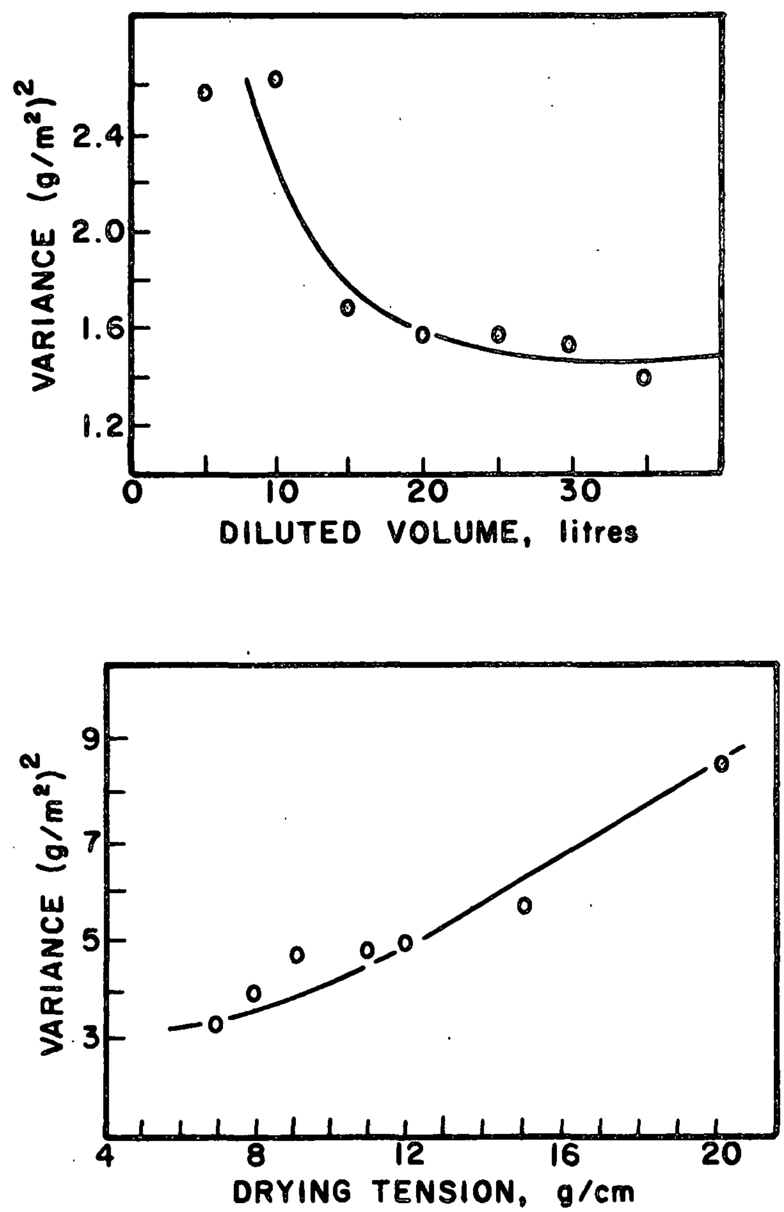

Figure 1. Effect of forming consistency and drying tension on variance of mass density after Herdman[1].

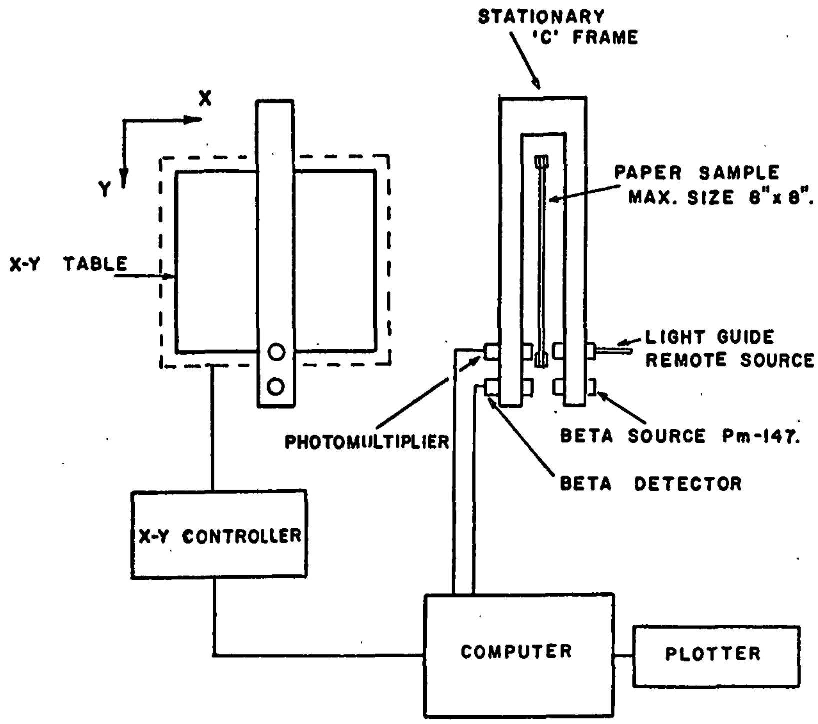

Figure 2. Schematic of API/IPC formation tester.

been made on the commercial and handsheet samples, and include elastic constants, some failure properties, as well as optical and color measurements.

3. COMBINED STRESS MEASUREMENTS

Combined stresses are an important aspect of failure during converting and end use. We are particularly interested in combined out-of-plane stresses as might arise, for example, in corrugating and calendering. It was proposed at our last progress meeting to build an instrument to measure the deformation behavior of paper and board when subjected to combined out-of-plane stresses, i.e., normal and shear stresses. The device conceived by Arcan[3] and suitably modified for our purposes was suggested as the means for inducing this stress situation. A suitable means also has to be found for measuring deformation behavior. This is particularly demanding because of the small deformations involved and possible out-of-plane movement as well.

Different optical techniques for the strain analysis of paper have been reviewed by Rowlands et al.[4]. They concluded and demonstrated that the Moire method offered a lot of advantages; however, it may not have the accuracy required for out-of-plane deformation measurements.

The possibility of using speckle photography and holographic interferometric techniques is also being studied. This approach has been used by Vallat and coworkers[5,6] to study the deformation behavior of adhesive joints. It is possible to measure displacements as small as 1.6 microns and the upper limit is controlled by loss of correlation between the fringe patterns. One disadvantage of the technique is the necessity of producing a speckle photograph for each displacement interval. Advantages of the method are that it is non-contact and displacements at different locations on the sample can be obtained. In the development of a suitable method for measuring combined stress deformation behavior, this could be a useful tool. Image-processing techniques have also been developed by Diez and coworkers[7] to analyze the resulting specklegrams.

4. INTERNAL STRESSES IN PAPER AND BOARD

Research in this area arose out of our work on shear deformation behavior, Project 3500, and the need to explain how properties vary from layer to layer in the thickness direction.

Internal stresses in paper and board are believed to be an important factor in the converting and end use behavior of paper and board. These stresses can be modified during converting and can play an important role in such areas as dimensional stability and elastic and failure properties. In earlier investigations a sectioning technique was employed to measure the variation of residual stress in the thickness direction; and stress relaxation measurement were used to determine the variation of internal stress (drying stress). In student related work referenced below, a layer removal technique is being used to measure the effects of densification by wet pressing and drying on the variation of residual stress and properties in the thickness direction of paper. To further understand the development of internal stresses and their influence on paper properties, a series of Formette handsheets have been made to determine the effects of fiber orientation and furnish composition, some of which have furnish variations in the thickness direction, i.e., triple layered sheets. The composition and properties of these sheets are summarized in Table 1. After sheet characterization, a number of 2 inch X 7 inch MD and CD samples were made and individually characterized, including radius of curvature measurements. To measure the variation of residual stress and properties in the thickness direction each sample will have a certain amount of material removed from its felt side after which radius of curvature and other property measurements will be made.

STUDENT RELATED WORK

1. "Strength Development through Internal Fibrillation and Wet Pressing". This is the title of Tom Bither's doctoral research and it is anticipated that Tom will report on his work to the committee at some future meeting.
2. "Z-Direction Variation of Residual Stress and Paper Properties". This is the title and subject matter of Maripat Franke's masters research project. Some of the main findings of this work will be presented at the forthcoming PAC meeting.

Table 1. Summary of sheet properties.

Sheet Structure & Furnish*	Fiber Orient.	Apparent Density g/cm	In-plane Constant (km/sec)	Out-of-plane Constant (km/sec)	Initial Curvature MD	Initial Curvature CD
100% S.W.	1.13	0.859	9.27	0.266	163	∞
	1.57	0.839	8.80	0.278	47.1	77.9
50% S.W./ 50% unbl. S.W.	1.08	0.814	9.43	0.283	143	86
	1.72	0.801	8.36	0.268	257	22.8
25% S.W. / 50% unbl. S.W. / 25% S.W.	1.15	0.824	9.4	0.287	180	44.2
	1.72	0.830	8.8	0.272	122	64.7
25% unbl. S.W. / 50% S.W. / 25% unbl. S.W.	1.11	0.826	9.6	0.270	124	214
	1.73	0.825	9.42	0.274	62	55

*CSF: S.W. 641 ml., unbl. S.W. 443 ml., 50% S.W./50% unbl. S.W. blend 569 ml.

REFERENCES

1. P. T. Herdman. Measurement of the distribution of mass density in paper, Paper Technology and Industry, September 1978, 246-250.

2. B. Jordan and N. G. Nguyen. Specific perimeter - a graininess parameter for formation and print-mottle textures. Pajeri ja Puu - Papper och Tra 68, 6-7, 1986 (476-482).

3. A. Voloshin and M. Arcan. Pure Shear Moduli of Unidirectional Fiber-Reinforced Materials. Fiber Science and Technology 13, 1980, 125-134.

4. R. E. Rowlands, P. K. Beazley, and D. E. Gunderson. Moire strain analysis of paper. Tappi J. 66 (8) 1983, 81-84.

5. M. F. Vallat, P. Martz, J. Fontaine and J. Schultz. The Application of Coherent Optics to the Study of Adhesive Joints. I. Speckle Photography. Journal of Applied Polymer Science, Vol. 31, 1986 (309-321).

6. M. F. Vallat, P. Smigielski, P. Martz and J. Schultz. The Application of Coherent Optics to the Study of Adhesive Joints. II. Holographic Interferometry, Journal of Applied Science, Vol. 30, 1985 (3953-3959).

7. E. Diez, D. Chambless, W. Simpson and J. Turner. Image Processing Techniques in Laser-Speckle Photography with Application to Hyrid Stress Analysis. Experimental Mechanics 26(3) September 1986 230-237.

MORPHOLOGICAL FACTORS IN THE REFINING OF EUCALYPT AND PINUS RADIATA FIBERS*

B. M. Allender and J. F. Waterhouse

ABSTRACT

Using a solvent exchange, critical-point drying and freeze-fracturing technique, direct evidence of cell wall delamination has been found in *Pinus radiata* and Eucalypt pulps when subjected to refining in a PFI mill. The water retention value (WRV) has been used to measure changes in water uptake in the cell wall with refining. The increases in WRV found for both pulps are mainly affected by fines; however, there is a small but significant change in the WRV for the fines free pulp measured at 3000 g. Furthermore, it appears that apparent density is a sensitive indicator of changes in fiber structure. Limited paper property measurements indicate that the out-of-plane elastic properties of the Eucalypt are superior to those for the *Pinus radiata* and that this measurement is particularly sensitive to fines removal and air drying of the pulp.

*Advances in Refining Technologies, PIRA International Conference, December 9-11, 1986. Birmingham England.

1.0 Introduction

The changes in fiber structure produced by refining and their impact on the papermaking process and paper properties have been reviewed by a number of researchers [1,2,3,4]. The major effects are summarized in the table below:

Major Effects of Refining

- Internal fibrillation
- External fibrillation
- Fiber length reduction
- Fines production
- Curls, kinks, microcompressions, straightening

It can be argued that all of these influence interfiber bonding. There is general agreement that internal fibrillation, external fibrillation and fines make a positive contribution to interfiber bond strength, while curl, kinks, and fiber length reduction can have an adverse effect. Clark[2] has debated the relative merits of internal and external fibrillation and believes that the contribution of external fibrillation has been undervalued. In this paper our interest will be mainly focused on internal fibrillation, since it is probably one of the most important effects occurring in the early stages of refining.

Leading proponents of the importance of internal fibrillation include Campbell[5], and Emmerton[6]. Manifestations of the effect include cell wall delamination and increased water uptake. These changes supposedly produce fibers which are more flexible and conformable to one another, and thus lead to improved interfiber bonding, fiber network densification, and improved paper properties. McIntosh[7] and Page and DeGrace[8] reported direct evidence for cell wall delamination and changes in cell wall dimensions. Increased water uptake has long been recognized as a general effect of refining, but the increase due to internal fibrillation alone has not been precisely measured. Techniques for measuring water uptake and changes in cell wall dimensions with refining include the solute exclusion technique,[9] water retention value (WRV),[10,11] and hydrodynamic specific volume[12].

One of the earliest methods of measuring water uptake is the water retention value developed principally by Jayme[10]. Over the course of time the technique has been modified and used to evaluate bleaching, refining, dewatering, and wet pressing. The method is based on the amount of water remaining in a pulp mat after centrifuging. Ellis[11] et al., investigated the change in WRV over a wide range of centrifugal force, and the effects of hardwood versus softwood, refining level and drying. They show that the variation of WRV with log g where g is the acceleration due to gravity generally has two distinct slopes. It is proposed that in the high slope region, water is present both between the fibers in the mat (interfiber water) and within the fibers (intrafiber water). At the "knee" all of the interfiber water is lost, and beyond this point water is removed from within the cell wall with increasing centrifugal force. Scallan and Carles[13] first suggested that an inflection point or plateau would be expected if the pattern of water removal shifted from interfiber to intrafiber with increasing centrifugal force. This idealized interpretation assumes that each layer of the mat is subjected to the same compaction force, which it is not. The effect of fines removal on WRV has been investigated by Thode[14] and Szwarcsztajn and Przybsz[15]. A fines free pulp gives a lower WRV than whole pulp. When using fines-free pulps it might be assumed that the water uptake as measured by the solute exclusion and WRV techniques is due to internal fibrillation only; however, the possible contribution from external fibrillation cannot be ignored.

The above discussion has focused on briefly reviewing a major effect of refining and its measurement, namely internal fibrillation. The results which follow are concerned with the development and measurement of internal fibrillation in a bleached kraft Eucalypt pulp and an unbleached kraft *Pinus radiata* pulp, which have been refined in a PFI mill. There has been relatively little work reported on the internal fibrillation behavior of hardwoods, and currently Eucalypt is enjoying a lot of attention.

2. Experimental

2.1 Pulp Sources and Treatments

Two commercial never-dried kraft pulps produced at the Australian Paper Manufacturer's Maryvale Mill, Victoria, Australia were used in this study. The bleached Eucalypt was 75% Ash Eucalypt and 25% class D Eucalypt, with a kappa number of 12, and a bleachability of 15. The unbleached *Pinus radiata* had a kappa number of 30.

The Eucalypt and Pinus radiata pulps had consistencies of 28.9% and 25.9%, respectively, on delivery and were beaten with no pretreatment. No preservatives were used. A PFI mill (TAPPI Method T 248 pm-74) was used to beat each pulp. (Eucalypt - 0, 560, 1000, 2000, and 3500 revolutions; Pine - 0, 1000, 3000, 5000, and 7000 revolutions).

After beating, the fines were removed from half of each sample in a Bauer-McNett apparatus using a 200 mesh screen. Small (ca. 50 mL) samples of whole and decrilled pulps were kept in a cold room for later microscopic examination. For all treatment levels two liters of 0.25% consistency pulp was made up and stored in a cold room.

A portion of both the whole and fines free pulps was formed into a mat on coarse filter paper in a Buchner funnel. This was allowed to air dry (ca. 20 g OD).

Pulp Examination and Testing

(a) Canadian Standard Freeness measurements (TAPPI Standard Method T 227m-58) were made on all whole pulp samples.

(b) Water Retention Values (WRV) were measured on whole, decrilled and air dried pulps (dried pulp was soaked for 24 hours before British Standard Disintegrator treatment) after storing 0.25% consistency samples for several days.

The WRV method was modifed from Thode[14] et al. (1960). 19-mm ID Plexiglass tubing was turned to fit a standard 26-mm centrifuge tube. A bronze cap was turned and drilled to fit onto one end of the tube. The cap supported a disk of 100-mesh bronze wire. Grooved plexiglass rings (14 mm high) were inserted into the polypropylene centrifuge tubes to allow room for the accumulation of excess water.

A fiber mat was formed onto the 100-mesh wire in the centrifuge tube from 26 mL of 0.25% consistency pulp. This was accomplished by inserting the centrifuge tube end into a rubber funnel attached to a vacuum flask. The pad was formed under a vacuum of 35 kPa, and a quick acting stopcock was turned off as soon as air could be heard passing through the fiber mat and a drop in vacuum pressure registered on the gage.

The plexiglass tube was immediately stoppered and placed in a centrifuge tube. After centrifuging (25 minutes) the bronze cap was removed and the fiber mat was transferred to a preweighed glass vial using a dissecting needle. The vial was stoppered and weighed on a balance (Mettler AE160). The vial contents were dried unstoppered overnight (100° C), cooled in a desiccator and reweighed. The final OD fiber mat weight was about 0.07 g. Water Retention Values (WRV) were calculated:

$$\mathrm{WRV} = \frac{(\text{wet + vial}) - (\text{dry + vial})}{(\text{dry + vial}) - (\text{vial tare})}$$

For each pulp treatment, four replicates of WRV measurements were made at seven different centrifugation levels. For the low range of centrifugal force (70 - 500 g) an IEC model V Centrifuge was used, and for the high range (600 - 42,000 g) a Sorval RC2-B Centrifuge was used.

(c) Fiber length measurements on whole and fines free pulps were made with a Kajaani FS100 Fibre Length Analyser. The weighted average fiber length, the arithmetic mean of fiber lengths in the lower 10% of the fiber population and the percentage fiber fragments (arithmetic) shorter than 0.4 mm were measured (more than 3000 fiber counts per sample). The last two figures provide an indication of the amount of fines present.

(d) Fiber samples of the unbeaten and highly beaten whole pulps and air dried pulps were examined and measured using a Scanning Electron Microscope (SEM). Fibers were taken through an ethanol/water series (5, 20, 50, 70, 85, 95, 100(x3), % ethanol) with at least one hour in each treatment. The samples were CO_2 critical point dried (Ladd Cat. No. 28000), and the fibers were aligned on the edge of clear adhesive tape under a dissecting microscope using fine forceps. The tape was folded over to hold the fibers in position, and then the fibers on the tape were freeze fractured transversely in liquid nitrogen. The tab of fractured fiber ends was glued upright onto a metal stub and coated with gold-palladium (Technics Hummer V) prior to SEM examination.

Fiber dimensions including width, depth, wall thickness and lumen thickness were measured directly from the SEM video screen at magnifications of x1800, x2400 and x3600. At least 30-50 fibers could be counted for each treatment, depending upon the alignment of the fractured fiber ends. Representative photomicrographs were made.

3. Paper Making

Minihandsheets were made in the WRV centrifuge tubes. The forming wire was now 200 mesh bronze (to match standard handsheet forming wires) and the wet mats were made as described in 2(b) above. The minihandsheets were couched using a fitted plastic plunger with a disc of standard laboratory blotter on the end. The bronze cap was removed from the tube and the minihandsheet and blotter were expressed from the tube. The blotter was removed with a dissecting needle.

The wet minihandsheets were arranged on strips of standard blotter and wet pressed and dried for 30 minutes in a laboratory press and dryer combination to minimize shrinkage. The result was a 19-mm diameter minihandsheet having a nominal basis weight of 250 gsm.

4. Paper Testing.

Basis weight and density (IPC soft platen)[16] were measured on six replicate minihandsheets made from whole pulp and selected fines-free and air-dried pulps.

Out-of-plane elastic constant measurements, $C33/\rho$, were made using a 13-mm diameter transducer connected to the IPC laboratory instrument for making such measurements[17]. The disks were then trimmed to 16-mm wide coupons, and the in-plane elastic constant, C_{11}/ρ, measurements were made using the same instrument by carefully standing the coupons on edge. STFI compression strength measurements were then made on the coupons. A trial with commercial medium showed there was no change in measured compressive strength when the sample size was reduced to 16 mm.

Results and Discussion

3.1 Direct observation of cell wall delamination.

Using the fiber preparation techniques described in the experimental section, typical SEM's of sectioned Pinus radiata and Eucalypt fibers are shown in Figures 1, 2, 3, and 4, at different levels of refining. Figures 2 and 4 show that delamination is a feature of the secondary wall of refined Pinus radiata and Eucalypt fibers, respectively. This appears to be the first time this evidence has been reported for these species. In the case of Pinus radiata, Kibblewhite[18] was unable to show secondary cell wall delamination using a freeze-fracture technique. The present demonstration of delamination is attributed to the improved preparation technique of gradual alcohol infiltration, critical point drying followed by freeze-fracturing. No mention of Eucalypt or other hardwood cell wall delamination has been found in the literature.

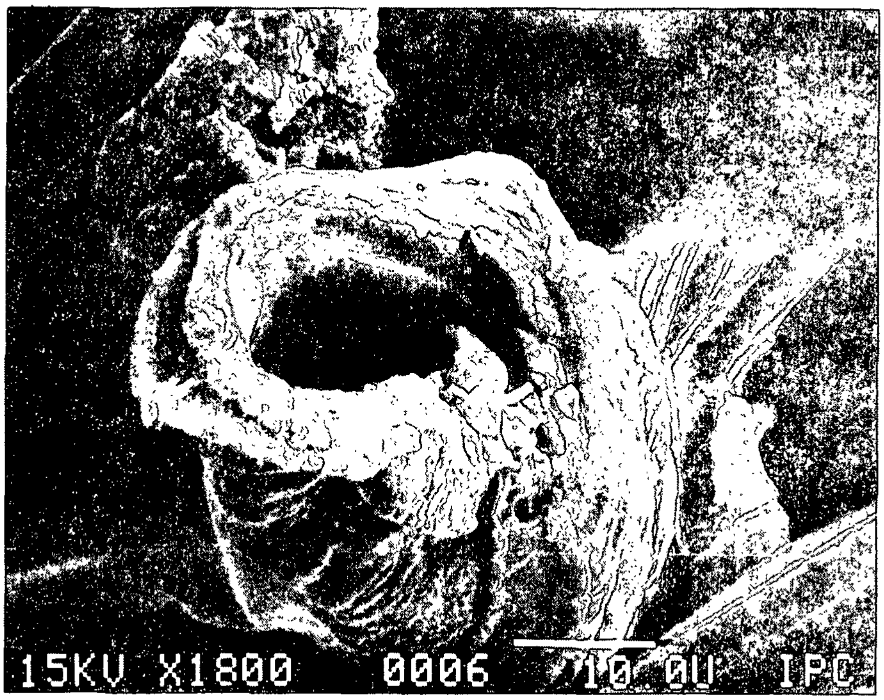

Figure 1. Unrefined latewood fiber Pinus radiata, x 1800.

The number of delaminations was similar in both pulps and varied between two and four major separations and often many other minor layers (Figures 2-4). This agrees with the observations of Page and deGrace[8]. On theoretical grounds, any delamination would greatly improve fiber flexibility (Emerton[6] p. 98).

It was apparent from examining fibers at different refining levels that delamination was a heterogeneous process. In unbeaten Pinus radiata and Eucalypt samples it is estimated that up to about 20% of the fibers examined showed some secondary wall delamination, while at the highest levels of refining about 95% did. The lightly refined Pinus radiata latewood fibers showed more evidence of delamination than the earlywood fibers.

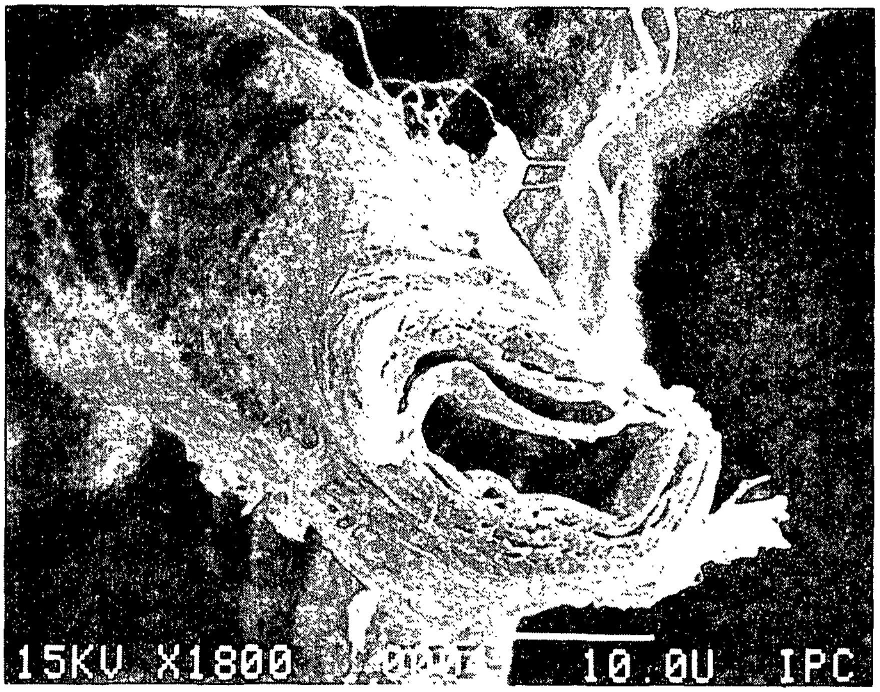

Figure 2. Refined 7000 revolutions PFI latewood Pinus radiata, x 1800.

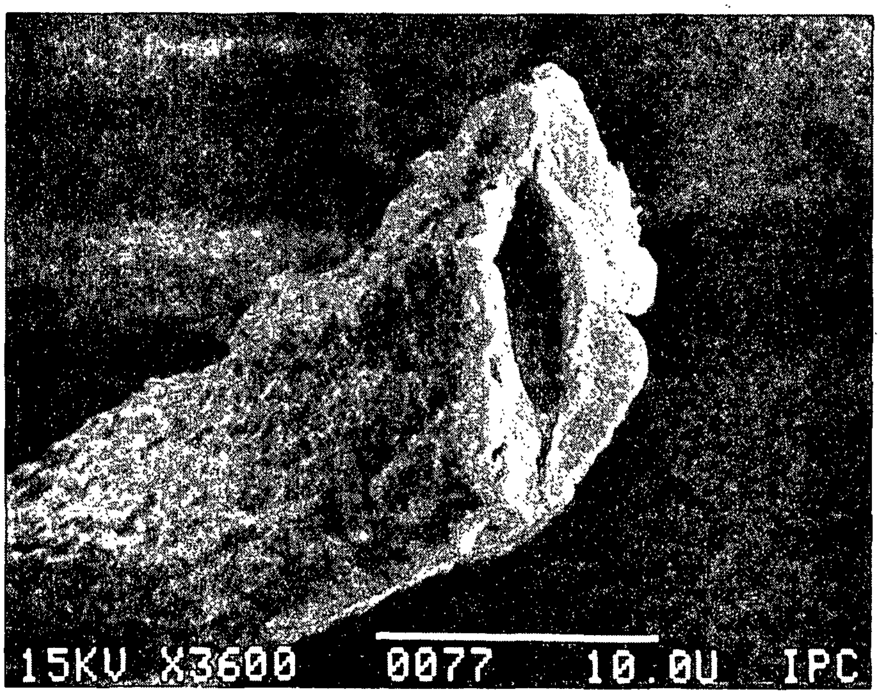

Figure 3. Unrefined fiber Eucalypt, x 3600.

Fiber length and cell wall dimension changes

The weighted average fiber lengths given in Table 1 show effectively no change with refining for the Eucalypt and a slight reduction for the Pinus radiata. Fines production for both pulps was increased with refining but were substantially reduced by the 200 mesh screen (see fines free results Table 1.)

Figure 4. Refined 3500 revolutions PFI Eucalypt, x 3600.

Table 1. Pinus Radiata and Eucalypt Fiber Lengths and Fines

Pulp	PFI Revs	Weighted Fiber Length, mm	Fiber Length Lower 10%, mm	% < 0.4 mm
EUCALYPT (Whole Pulp)	0	0.66	0.13	36.3
	560	0.69	0.11	37.7
	1000	0.69	0.12	36.5
	2000	0.69	0.10	39.7
	3500	0.68	0.09	42.5
EUCALYPT (Fines Free Pulp)	0	0.72	0.32	18.0
	560	0.71	0.26	24.6
	1000	0.71	0.25	24.5
	2000	0.72	0.25	25.0
	3500	0.73	0.27	22.9
PINUS RADIATA (Whole Pulp)	0	1.96	0	46.3
	1000	1.91	0	49.5
	3000	1.90	0	48.7
	5000	1.85	0	50.5
	7000	1.81	0	54.5
PINUS RADIATA (Fines Free Pulp)	0	2.08	0.22	19.8
	1000	2.03	0.29	15.5
	3000	2.07	0.29	15.8
	5000	1.98	0.26	18.5
	7000	1.88	0.23	21.8

Cell wall dimensions are given in Table 2. Unfortunately, the fiber population examined is not large enough to draw statistically significant conclusions. Nevertheless, we shall discuss some of the trends that were observed.

Table 2. Mean fiber dimensions of unbeaten and beaten freeze fractured Pinus radiata and Eucalypt fiber in the swollen state.

PINUS RADIATA	Fiber Width (μm)	Fiber Thickness (μm)	Cell wall Thickness (μm)	Lumen Thickness (μm)
<u>Earlywood</u>				
unbeaten 0 revs.	33.1	16.2	3.5	9.2
unbeaten 600 g	----	----	2.8	7.9
unbeaten 41,000 g	----	----	2.4	5.7
unbeaten air-dried	----	----	2.8	9.3
beaten 7000 revs.	42.3	17.0	6.0	6.1
beaten 600 g	----	----	4.8	6.1
beaten 41,000 g	----	----	3.6	3.2
beaten air-dried	----	----	2.2	2.7
<u>Latewood</u>				
unbeaten 0 revs.	38.0	14.0	3.2	8.3
beaten 7000 revs.	26.5	18.0	5.6	8.9
EUCALYPT				
unbeaten 0 revs.	13.0	6.9	1.7	1.9
unbeaten 600 g	----	----	2.1	3.1
unbeaten 41,000 g	----	----	2.0	3.1
beaten 3,500 revs.	13.9	7.8	2.8	2.1

The <u>Pinus radiata</u> earlywood fibers showed signs of collapse (i.e., their width increased) while the latewood fibers tended to become more circular (i.e., their width decreased while their thicknesses increased) with refining. The changes in the Eucalypt were smaller and showed a slight increase in width and thickness dimensions. Both pulps showed a significant increase in cell wall thickness with refining, i.e, 71% earlywood <u>Pinus radiata</u>, 75% latewood <u>Pinus radiata</u>, and 65% Eucalypt. Centrifuging and air drying reduced the cell wall thickness of the earlywood <u>Pinus radiata</u> fibers, the reduction being greatest for the refined fibers. In contrast centrifuging produced a slight increase in cell wall thickness of the Eucalypt (only unrefined Eucalypt fibers were examined).

The lumen dimensional changes generally follow the cell wall thickness changes. Evidence of fiber collapse (i.e., decrease in lumen thickness) is more prevalent for the earlywood Pinus radiata fibers; refining, centrifuging and air drying all result in a decrease in lumen height. The latewood Pinus radiata and Eucalypt fibers, despite the paucity of data, do not show evidence of collapse, and if anything an increase in lumen height is found.

3.2 Water Retention Values.

The variation of WRV with centrifugal force is shown in Figures 5 and 7 for the whole pulps of Pinus radiata and Eucalypt at three PFI refining levels. The separation of the curves with refining in the low slope region is not as pronounced for the Eucalypt as it is for the Pinus radiata pulp. The effect of fines removal on WRV's is shown in Figures 6 and 8. The curves for each refining level tend to collapse onto a common curve, particularly for the Eucalypt pulp in both the high and the low slope regions. However, as we shall see shortly, there are still significant changes in WRV as a function of refining in the low slope region. In the high slope region, water is centrifuged out from the network, and since the network is not incompressible, its compaction will also aid in further water removal. The rate of water loss in the high slope region is greater for the Eucalypt and is relatively insensitive to refining. The Pinus radiata does show an increase in water removal rate with refining, although it is still less than the Eucalypt at the highest level of refining. Mat compressibility behavior is presumably an important aspect of WRV. In this situation, however, the mat is not uniformly densified. As the mat is densified the free water will be readily removed, and finally a steady state is more or less arrived at where the centrifugal force will no longer remove water from certain sizes of capillary. The model of fiber mat compaction proposed by Osaki[19] et al., suggests that mat compaction in the high slope region could result from an increase in the number of fiber contacts, whereas the low slope region is controlled by fiber cell wall compaction. Fiber compaction will be dependent on fiber structure and composition.

Examining in more detail the effects of refining, fines removal, and drying on changes in the cell wall, the variation of WRV at 3000 g with PFI revolutions is shown in Figures 9 and 10. A small but significant increase in WRV of 9.1% and 5.4% for the Pinus radiata and Eucalypt pulps with fines removed is found over the refining range used for each pulp. Air drying results in a 31% and 33% loss in the unrefined WRV values for the Pinus radiata and Eucalypt pulps, respectively.

Furthermore, since there is no significant change in water retention value with refining when the pulps are air dried, then one effect of internal fibrillation (i.e., increase in WRV) is lost upon drying. This does not necessarily imply that related refining effects are lost upon drying, i.e., fiber flexibility, fiber collapse.

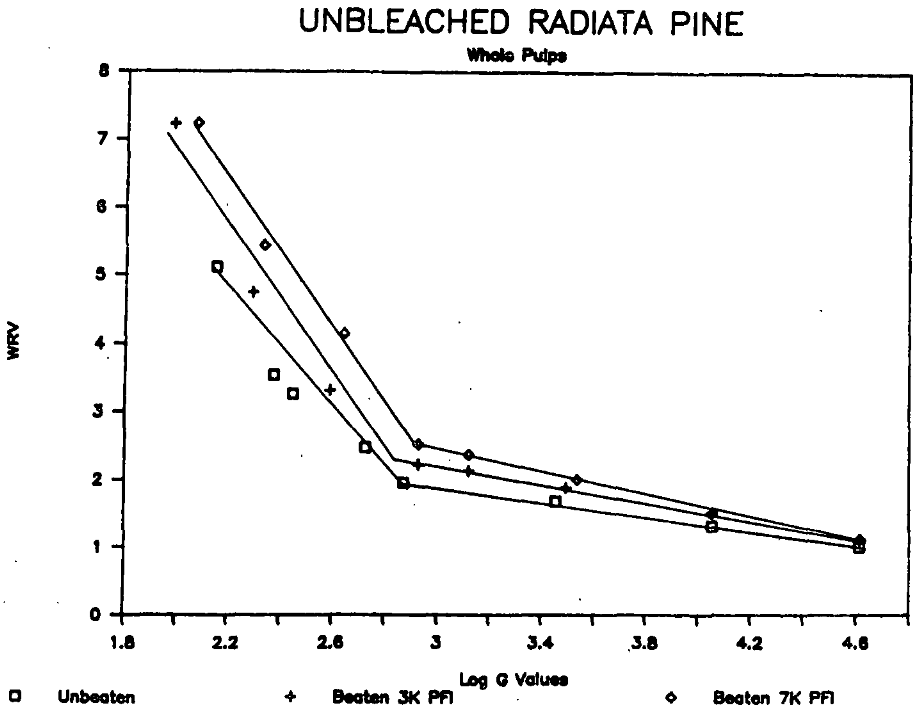

Figure 5. Variation of water retention values with centrifugal force.

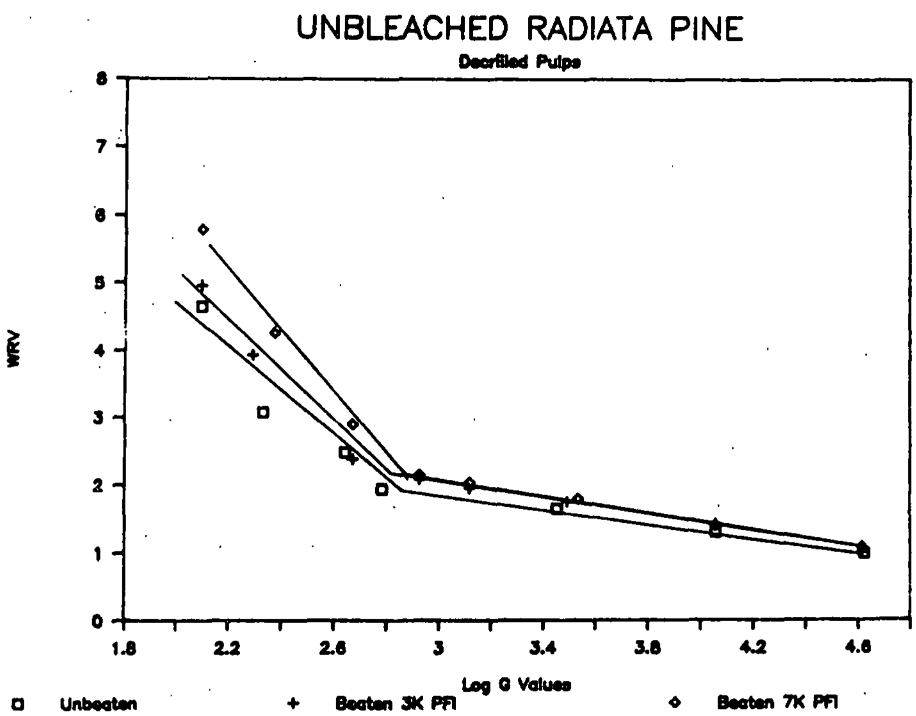

Figure 6. Variation of water retention values with centrifugal force.

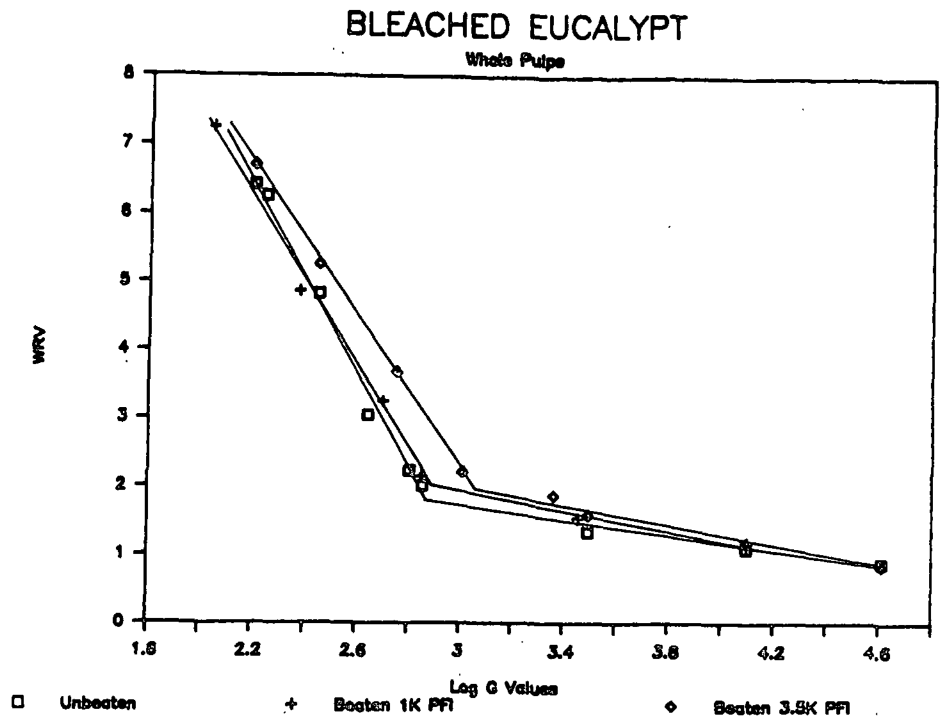

Figure 7. Variation of water retention values with centrifugal force.

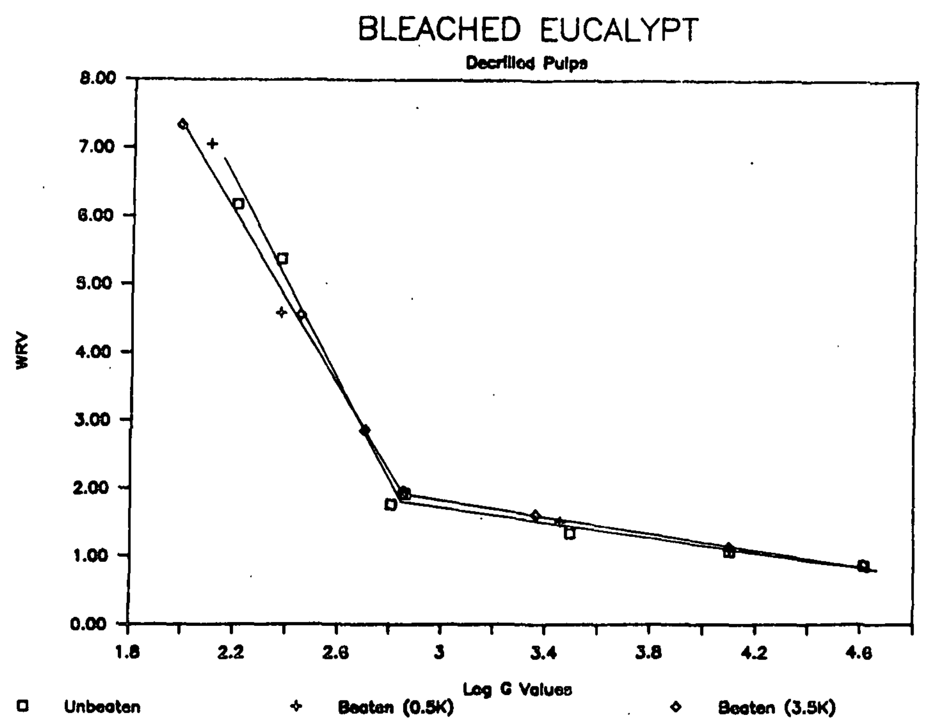

Figure 8. Variation of water retention values with centrifugal force.

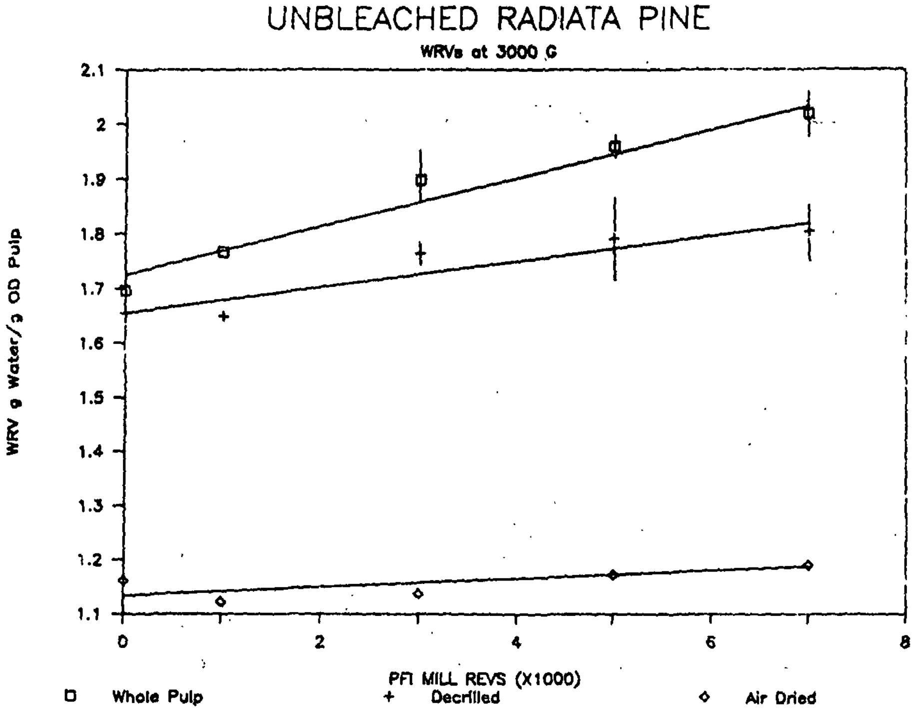

Figure 9. Variation of water retention value with PFI revolutions.

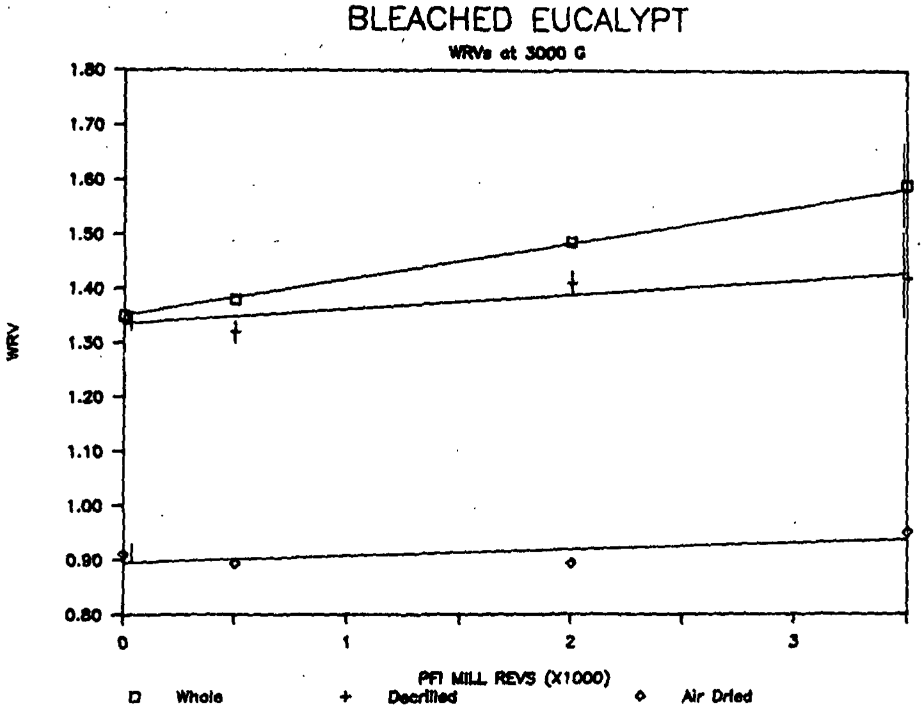

Figure 10. Variation of water retention value with PFI revolutions.

3.3 Paper Properties

Limited paper property measurements were made on minihandsheets (19-mm dia.) having a nominal basis weight of 250 g/m^2. These included basis weight, caliper, ultrasonic elastic constants and compressive strength measurements.

The results are summarized in Table 3 together with WRV's at 3000 g. The variation of apparent density with WRV is shown in Figure 11 for handsheets made from whole pulp, fines-free and air-dried whole pulps. The dominant effect of fines is again seen when we compare the whole and fines free pulp curves. At the highest refining level, removal of fines produces a large reduction in WRV, and only a small drop in apparent density for the Pinus radiata. Essentially the same changes are seen for the Eucalypt except that the change in apparent density is negligible. The overall change in apparent density of the fines-free handsheets is 23.4% and 24.2% for the Pinus radiata and Eucalypt pulps, respectively, which correspond to changes of 9.1% and 5.4% in WRV, as noted above. We might therefore conclude that apparent density is a more sensitive indicator of changes in cell wall structure (internal fibrillation). Air drying, as we have already seen, produces a large overall reduction in WRV. It is believed that drying effectively negates the effect of fines and internal fibrillation, as well as reducing the amount of intrafiber water present, i.e., the changes in WRV with refining are not significant at least for the two pulps examined here. Nevertheless, the effects of refining on sheet densification are still evident, since the change in density from unrefined to the highest level of refining is 17% and 10% for the Pinus radiata and Eucalypt, respectively.

It has been found that many strength related properties correlate with apparent density. Furthermore, a reasonable correlation between relative bonded area and apparent density has been demonstrated by Waterhouse[20], which for a given pulp, is independent of the level of wet pressing and refining. Therefore, to a first approximation, apparent density may be used as a measure of relative bonded area.

The variation of in-plane and out-of-plane specific elastic constants with apparent density (produced by refining) are shown in Figures 12 and 13. At a given density level the Pinus radiata gives a slightly higher in-plane elastic constant; however, the out-of-plane elastic constant of the Eucalypt is significantly higher than the Pinus radiata. A good correlation has also been found by Baum[21] between out-of-plane strength, e.g., ZDT, and out-of-plane specific modulus, Therefore the Eucalypt would be expected to have superior out-of-plane strength when compared with the Pinus radiata at a given apparent density.

The changes in properties with fines removal and air drying are summarized in Table 4 for two levels of refining. The greatest property change experienced by both pulps when fines are removed is a reduction in the out-of-plane elastic constant. The changes in in-plane constants are much smaller by comparison. This result coincides with the expectation that the out-of-plane elastic constant will be more sensitive to interfiber bonding, and thus fines level, than the in-plane elastic constant. As already noted the largest change in WRV is at the highest level of refining for both pulp types.

Table 3. WRV and minihandsheet properties.

PFI Revs.	CSF	WRV 3000 g	Basis Wt. g/m^2	Density g/cc	$\overline{C}/\rho$ $(km/sec)^2$	C_{33}/ρ $(km/sec)^2$	STFI $\sigma c/\rho$ Nm/g
Bleached Kraft Eucalypt							
0	612	1.347	260	0.808	9.14	0.097	24.9
500	555	1.376	258	0.840	10.44	0.193	31.6
1000	520	1.537	253	0.886	11.34	0.231	35.3
2000	460	1.486	248	0.889	11.78	0.280	36.1
3000	345	1.586	271	0.923	12.13	0.349	37.4
Fines Free							
0	---	1.342	207	0.744	8.80	0.0729	23.7
3500	---	1.415	221	0.924	12.78	0.235	36.5
Air Dried							
500	---	0.893	223	0.737	7.65	0.0655	18.4
2000	---	0.894	223	0.773	7.92	0.0751	21.1
Unbleached Kraft *Pinus radiata*							
0	737	1.696	212	0.849	10.63	0.068	31.0
1000	694	1.766	250	0.908	12.43	0.144	35.4
3000	610	1.897	246	0.941	13.78	0.181	42.6
5000	526	1.958	268	0.957	14.17	0.181	42.9
7000	420	2.018	243	0.994	14.38	0.189	43.9
Fines Free							
0	---	1.655	228	0.788	9.57	0.044	28.7
7000	---	1.804	212	0.972	13.21	0.123	43.1
Air Dried							
0	---	1.160	255	0.695	6.99	0.018	17.8
7000	---	1.190	230	0.869	9.43	0.106	29.1

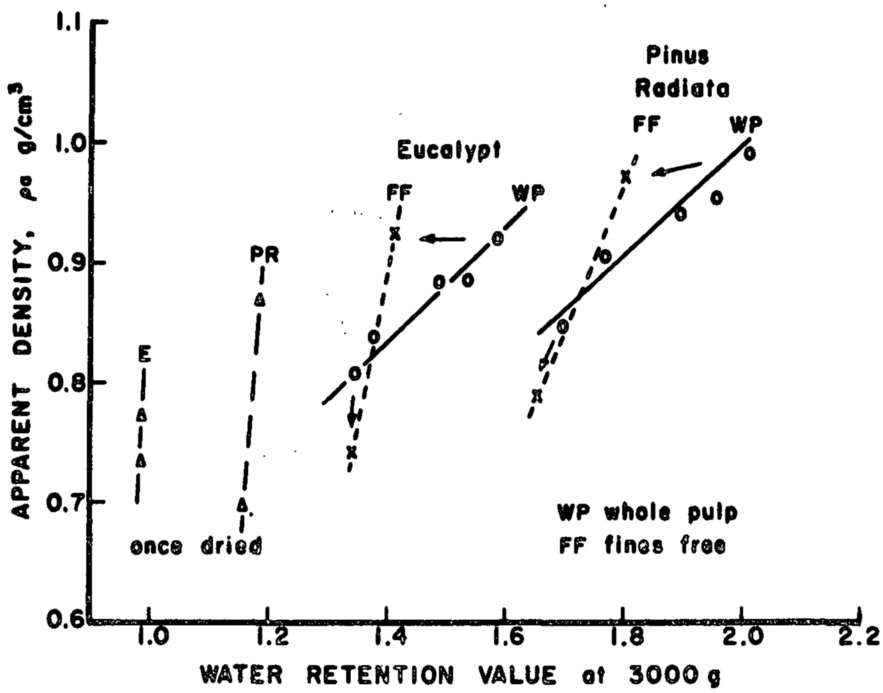

Figure 11. Variation of sheet density with water retention value.

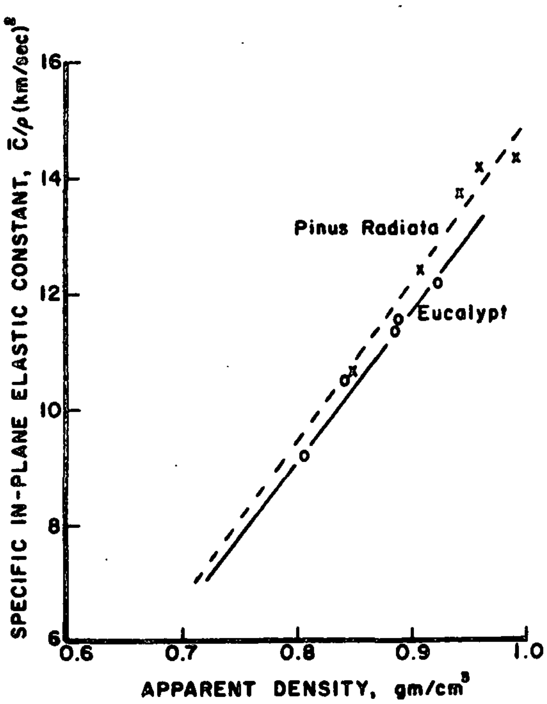

Figure 12. Variation of elastic constants with apparent density.

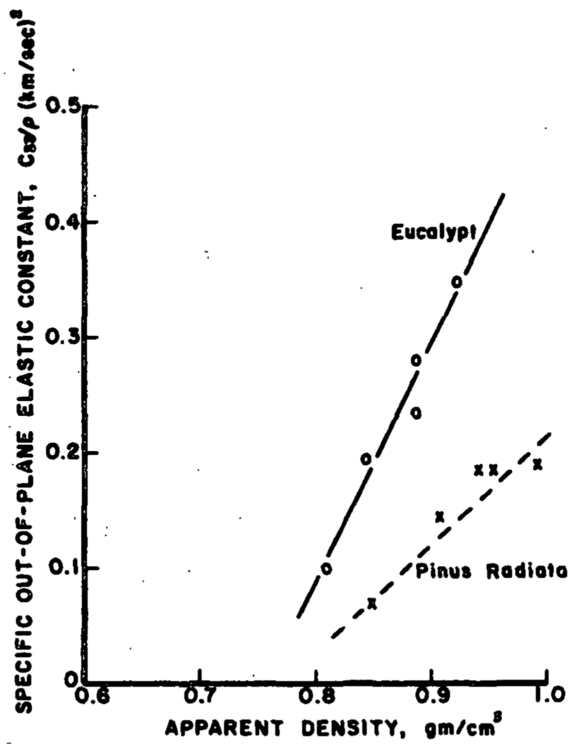

Figure 13. Variation of elastic constants with apparent density.

Table 4. Changes in Properties with fines removal and air drying relative to whole pulps.

EUCALYPT					PINUS RADIATA				
CSF mL	Apparent Density %	WRV %	In-plane Elastic Constant %	Out-of-plane Elastic Constant %	CSF mL	Apparent Density %	WRV %	In-plane Elastic Constant %	Out-of-plane Elastic Constant %
CHANGE IN PROPERTIES WITH FINES REMOVAL									
612	-8	0	-4	-32	737	-7	- 2	-11	-34
345	0	-11	+5	-33	420	-2	-11	- 7	-37
CHANGE IN PROPERTIES WITH AIR DRYING									
EUCALYPT					PINUS RADIATA				
555	-12	-35	-27	-66	737	-24	-32	-34	-74
460	-13	-39	-33	-73	420	-13	-41	-34	-44

Air drying produces large reductions in all of the properties measured, with the largest change again occurring in the out-of-plane elastic constant. The reduction in both in-plane and out-of-plane elastic constants is presumed to be due, in the former case, to a reduction in both interfiber bonding and fiber modulus, and in the latter case, to a reduction in interfiber bonding.

The variation of STFI compressive strength with densification (by refining) for the Pinus radiata and Eucalypt pulps is shown in Figure 14. The performance of the two pulps is almost identical, and it is noted that the fines-free results do not deviate significantly from the whole pulp correlation (based on the data of both pulps).

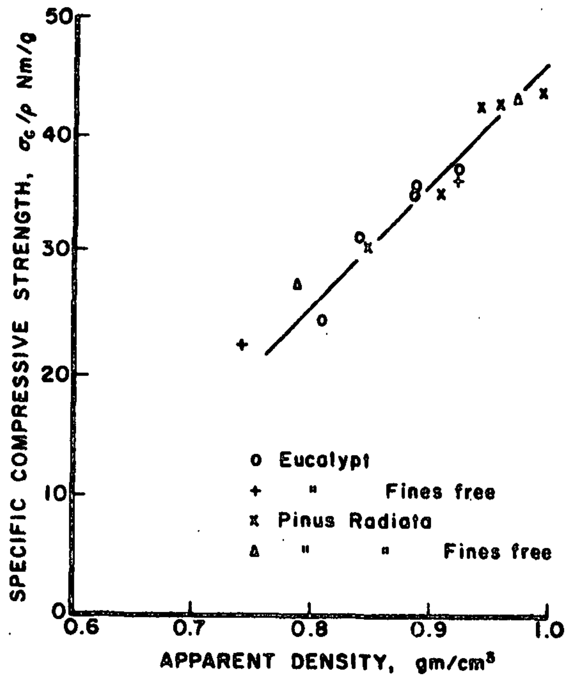

Figure 14. Variation of specific compressive strength with apparent density.

Conclusions

Using a solvent exchange, critical-point drying and freeze-fracturing technique, direct evidence of cell wall delamination has been found in Pinus radiata and Eucalypt pulps when subjected to refining in a PFI mill. The water retention value (WRV) has been used to measure changes in water uptake in the cell wall with refining. The increases in WRV found for both pulps are mainly affected by fines; however, there is a small but significant change in the WRV for the fines free pulp measured at 3000 g. Furthermore, it appears that apparent density is a sensitive indicator of changes in fiber structure. Limited paper property measurements indicate that the out-of-plane elastic properties of the Eucalypt are superior to those for the Pinus radiata and that this measurement is particularly sensitive to fines removal and air drying of the pulp.

Literature Cited

1. Higgins, H. F., and De Yong, J. "The Beating Process Primary Effects and their influence on Pulp and Paper Properties" Formation and Structure of Paper Vol. 2 Trans. Fundamental Research Symposium held at Oxford, September 1961.
2. Clark, J. d'A., Pulp Technology and Treatment for Paper, 2nd Edition, Miller Freeman Publications, Inc. 1985.
3. Ebeling, K., "International Symposium on Fundamental Concepts of Refining" Proceedings. The Institute of Paper Chemistry, Appleton, Wis., Sept. 16-18, 1980.
4. Giertz, H. W., "International Symposium on Fundamental Concepts of Refining" Proceedings. The Institute of Paper Chemistry, Appleton, Wis., Sept. 16-18, 1980.
5. Campbell, W. B., "The cellulose-water relationship in Papermaking" Forest Service Bulletin 84 Dept. of the Interior, Canada 1933.
6. Emerton H. W. "Fundamentals of the Beating Process" The British Paper and Board Industry Research Association 1957.
7. McIntosh, D. C., Tappi 50(10): 483-488, 1967
8. Page, D. H., and DeGrace, J. H., Tappi 50(10): 489-497, 1967
9. Scallan, A. M., "The Accommodation of water within pulp fibers" Fiber-Water Interactions in Paper Making Trans. 6th Fundamental Research Symposium held at Oxford, September 1977. Vol. 1.
10. Jayme, G., and Rothamel, L., Das Papier 2(1/2) 7-18, January 1948.
11. Ellis, E. R., Jewett, K. B., Smith, K. A., Ceckler, W. H., and Thomson, E. V., Journal of Pulp and Paper Science: 1983 TR-12 to TR-15.
12. Ingmanson, W. L., and Andrews, B. D., Tappi 42(1): 29-35, January 1959.
13. Scallan, A. M., and Carles, J. E., Svensk Papperstidning 75(17): 699-703, 1972.
14. Thode, E. F., Bergomi, J. G., Jr. and Unson, R. E., Tappi 43(5): 505, 1960. 505-512.
15. Szwarcsztajn, E., and Przybysz, K. Cellulose Chemical Technology 9: 597-607 (1975).
16. Wink, W. A., and Baum, G. A., Tappi 66(9): 131(1983)
17. Habeger, C. C., and Wink, W. A., Journal Applied Polymer Science, 32: 4503-4540 (1986).
18. Kibblewhite, R. P., Paper Och Tra 11:709-714, 1972
19. Osaki, S., Fujii, Y., and Kiichi, T. "Z-Direction Compressive Properties of Paper" 1981 Papermaking Conference Preprints. Japanese Tappi, Tech. Sect. CPPA Joint Conference, October 20-22, 1981 Tokyo, Japan
20. Waterhouse, J. F., "The ultimate strength of Paper" International Paper Physics Seminar Stockholm. Sweden, June 1984.
21. Baum, G. A., "Elastic Properties, Paper Quality and Process Control" Tappi Proceedings 1986 International Process and Materials Quality Evaluation Conference. Atlanta, GA September 21-24.

Acknowledgments

The authors wish to acknowledge the valuable discussions and assistance of T. Conners, M. Doshi, faculty members of The Institute of Paper Chemistry, and to thank Laura Schumacher and the Editorial staff of IPC for their contribution in preparing this paper. This paper is based on a research project performed by Bruce Allender while a special student at The Institute of Paper Chemistry.

THE INSTITUTE OF PAPER CHEMISTRY

Appleton, Wisconsin

Status Report

to the

PAPER PROPERTIES AND USES

PROJECT ADVISORY COMMITTEE

Project 3332

ON-LINE MEASUREMENT OF PAPER MECHANICAL PROPERTIES

February 13, 1987

PROJECT SUMMARY

PROJECT NO. 3332: ON-LINE MEASUREMENT OF PAPER MECHANICAL PROPERTIES

PROJECT STAFF: C. C. Habeger, G. A. Baum February 13, 1987

PROGRAM GOAL: Develop ways to measure and control manufacturing processes.

PROJECT OBJECTIVE:

To develop the capability to measure elastic parameters on a moving paper web. Current emphasis is on out-of-plane measurements.

PROJECT RATIONALE, PREVIOUS ACTIVITY, AND PLANNED ACTIVITY FOR FISCAL 1987-88 are on the attached 1987-88 Project Form.

SUMMARY OF RESULTS LAST PERIOD: (April 1986 - September 1986)

(1) Several preliminary PVDF wheel transducers have been built and tested. Development of improved models continues.

(2) A high speed data acquisition system has been developed for ZD operation. This is described in the report for Project 3467 but most of the work is directly applicable to on-line measurements of ZD properties.

(3) A paper "On-line Estimates of Strength" (IPC Technical Paper Series 187) was presented at the 1986 Control Symposium in Stockholm and will be published in the proceedings of that meeting.

(4) The DOE project, concerned with combined in-plane and out-of-plane measurements on the paper machine is expected to be initiated in the near future.

SUMMARY OF RESULTS THIS PERIOD: (October 1986 - March 1987)

(1) Improved wheel transducers have been designed and constructed. These will be mounted in a frame and subsequently tested for application in the laboratory moving web device.

(2) A caliper gage for use on moving webs has been designed and is currently under construction. The approach is similar to the soft rubber platen measurement scheme. This device will be used with the (low speed) laboratory moving web system, but is also expected to be applicable to the on-machine system.

(3) In DOE work, we intend to attempt to incorporate the above advances into the on-machine system. In addition we are simultaneously developing a second type of transducer wheel, employing a disk type piezoelectric device made from PVDF.

(4) Dr. Maclin Hall has been hired to serve as Project Manager of the DOE project.

(5) In student work, Dennis Macdonald is studying the impact of changes in jet-to-wire speed differentials on sheets properties as a prerequisite to machine control of this variable.

Date: 1/14/87	
Budget: $75,000	
Period ends: 6/30/88	
Project No.: 3332	

PROJECT TITLE: On-Line Measurement of Paper Mechanical Properties

PROJECT STAFF: C. Habeger/G. Baum/M. Hall

PRIMARY AREA OF INDUSTRY NEED: Properties related to end uses

PROGRAM AREA: Control of manufacturing processes

PROGRAM GOAL: Develop ways to measure and control manufacturing processes

PROJECT OBJECTIVE/GOAL:

To develop the capability to measure elastic parameters on a moving paper web. Current emphasis is on out-of-plane measurements. This project is concerned with development of a laboratory device. A related DOE sponsored project is concerned with measurements on the paper machine and subsequent control of the paper making process.

PROJECT RATIONALE:

The ability to measure mechanical properties on the paper machine is valuable from several standpoints. It provides a potential means for control of process variables. It also provides a non-destructive way to assess product quality on a continuous basis.

RESULTS TO DATE:

Developed theory of ultrasound propagation in paper, and developed devices for measuring paper and board in-plane elastic parameters on-machine. Successfully tested devices in mill environments. Constructed and tested a version useful for light weight grades which is also self-calibrating. Developed cross correlation technique for use with in-plane velocity measurements, and initiated work relating to on-line measurements of z-direction properties. Developed a high-frequency, low impedance out-of-plane transducer using a plastic film piezoelectric material which is superior to commercial ceramic transducers. Developed equipment for measuring moisture and temperature effects on paper elastic properties. Most recently, the feasibility of ZD signal transfer between rubber faced transducers at high speeds has been demonstrated with ceramic transducers. Suitable plastic piezoelectric wheel transducers have been developed; these broad band transducers are active over the entire circumference. The design of an apparatus for simultaneous measurement of caliper and ZD velocity is nearing completion.

PLANNED ACTIVITY FOR FY 1987-88:

We will develop laboratory equipment to make out-of-plane ultrasonic measurements on a (slow) moving paper web. We will build high frequency, broad banded, and low impedance wheel transducers. We plan to look at both ceramic and plastic piezoelectric transducer constructions. Hardware and software for a high speed data acquisition system will be designed and built. On-line caliper measurements techniques will be investigated to be used with the ZD measurement system. This work is complementary to the DOE sponsored research program.

The first phase of the DOE project is also concerned with development of a ZD sensor capable of measurements at machine speeds. Later, this will be integrated into a system capable of making both in-plane and out-of-plane measurements at machine speeds, for the purpose of controlling the paper machine.

STUDENT RELATED RESEARCH:

Bernie Berger, Ph.D.-1988, Dennis Mcdonald, M.S.-1987.

Status Report

ON-LINE MEASUREMENT OF PAPER MECHANICAL PROPERTIES

Project 3332

INTRODUCTION

This project is an extension of earlier work which dealt with on-line measurements of the in-plane elastic stiffnesses of paper and board. The current effort is concerned with measurements of z-direction elastic stiffnesses. The IPC funded portion of this project deals with such measurements in the laboratory on a moving web of paper, although at relatively slow speeds. Such equipment is needed for rapid measurements on MD and CD strips and also provides a testing ground for ideas and hardware later intended for higher speed on-machine applications during paper manufacture. Section 1 briefly discusses the wheel transducers. Section 2 is our first report to DOE, describing the developments in somewhat more detail.

SECTION 1. - Wheel Transducers

The 1-inch thick Kynar wheel with silicone coupling purposed in the last PAC report has been built and tested. Flattened copper wire provided adequate electrical contact and larger thickness created a more sensitive and board banded transducer. Although the signal is not of the quality of the 1-inch disc transducer, we feel it is acceptable and the second transducer is under construction.

The transducers now must be mounted in a frame which drives them and allows dynamic caliper measurements. This will hopefully provide a practical laboratory instrument for profiling caliper and ZD velocity by feeding a sample through a nip. In addition, it will be used to explore the difficulties in making dynamic caliper and ZD velocity measurements at the higher speeds encountered on-line. The frame will be similar to the present out-of-plane transducer frames but for greater durability vertical displacement will be achieved through a mechanical slides rather than a graphite piston in a glass cylinder. Since there is a small radial dependence in transducer diameter and transit time, a means is provided to align the transducer to a reference orientation. This makes it possible to do caliper and velocity calibration as a function of angle. A stepper motor will be mounted on the frame to rotate the transducers and feed the sample through the nip. The mechanical design of the frame and drive system is complete. Purchased components are ordered and machining will begin as soon as critical parts are received.

This system also requires additional electronics and software development. The sample and hold digital scope used with the present ZD laboratory gage is too slow to accommodate dynamic measurements. Data acquisition will now be done with a high speed Lecroy 8013A transient recorder, already in house. Significant software development (which has only just begun) is required to interface the transient recorder to the IBM AT, drive the stepping motor, handle the dynamic caliper and acoustic signals, interface to the operator, and report results.

SECTION 2. - DOE Work

SUMMARY

This report describes project activity on the project since its inception on October 1, 1986, and includes a summary of some relevant work conducted prior to contract approval. The first milestone, showing the feasibility of on-machine z-direction measurements, has been accomplished.

GENERAL PROJECT OBJECTIVES

The objectives of this new project are to develop sensors capable of measuring in-plane and out-of-plane mechanical properties of paper during the manufacturing process and to use these to evolve techniques and hardware to control the manufacturing process in both the machine direction and cross machine direction of the paper. Non-destructive ultrasonic techniques will be used to characterize the mechanical properties of the paper in three dimensions, allowing continuous monitoring of product quality as well as means for process control. These benefits will lead to more effective utilization of raw materials and energy.

ACTIVITY TO DATE

Earlier work at the Institute of Paper Chemistry, demonstrated that z-direction (ZD) ultrasound velocity measurements are valuable for characterizing the mechanical properties of paper. This motivated us to begin development of an instrument to make such measurements on a moving web. The first step is to devise a method of transmitting a pulse of ultrasonic energy through a sheet and detecting it on the opposite side, while the paper is moving at high web speeds. A practical gage would also need to measure caliper and determine the pulse transit time with no web present. Thus far, only the critical problem of ZD pulse detection at high machine speeds has been addressed. Transducer requirements for on-line ZD measurements differ from those for the in-plane sensors which are described elsewhere[1,2]. For a ZD device, the transmitter and receiver will be separated by only a single sheet thickness. To get decent resolution of the time-of-flight, the phase shift of the signal through the sample should be as large as possible. This is accomplished on thin specimens by operating at high frequency. The frequency used in our laboratory ZD instruments (1 MHz) is much greater than that used with the in-plane on-line gages (~80 kHz). The on-line ZD equipment must therefore be designed to operate at higher frequencies than the in-plane device, meaning that transducer dimensions must be kept as small as practical.

The coupling requirements are also different in the two cases. The aluminum button used for web contact on the in-plane gage is not acceptable here. From our experience with laboratory ZD gages, we know a conformable coupling between the paper and the transducer is necessary for efficient transfer of energy in the z-direction. We also know that this is simpler to achieve with longitudinal waves than with shear waves; therefore, the first on-line ZD attempt was designed to generate longitudinal waves. The transducer-to-web coupling is done with 1/32 inch thick sheet of soft neoprene epoxied to the face of the transducer. This is the same neoprene used in the IPC thickness gage and in our laboratory longitudinal ZD instrument.

Figure 1 is a drawing of the receiver wheel which we built for on-line ZD work. The wheel, which is machined from a solid piece of aluminum, is 5.0 inches in diameter. Its functions are to provide a rolling contact to the web, to house some electronics and acoustic transducers, and to electrically shield the sensor. The active element itself is made from two piezoelectric ceramic disks (1/10 inch thick P.Z.T. 5A). They are oriented with opposite polarity and epoxied together. The outer surfaces are held at ground potential, while the connected surface form the active electrode. One piezoelectric element is epoxied to a thin aluminum button which is machined to the same radius as the wheel. The button also has a threaded flange for mounting the active element. The neoprene sheet is epoxied to the aluminum button, which is clamped to the wheel. The active element is mounted in a threaded, hollow cylinder made of Delrin. The Delrin piece is clamped by two screws to the wheel housing. Two pieces of 1/8" Coroprene (a sheet material made with cork and neoprene particles) are used to acoustically isolate the active element from the wheel.

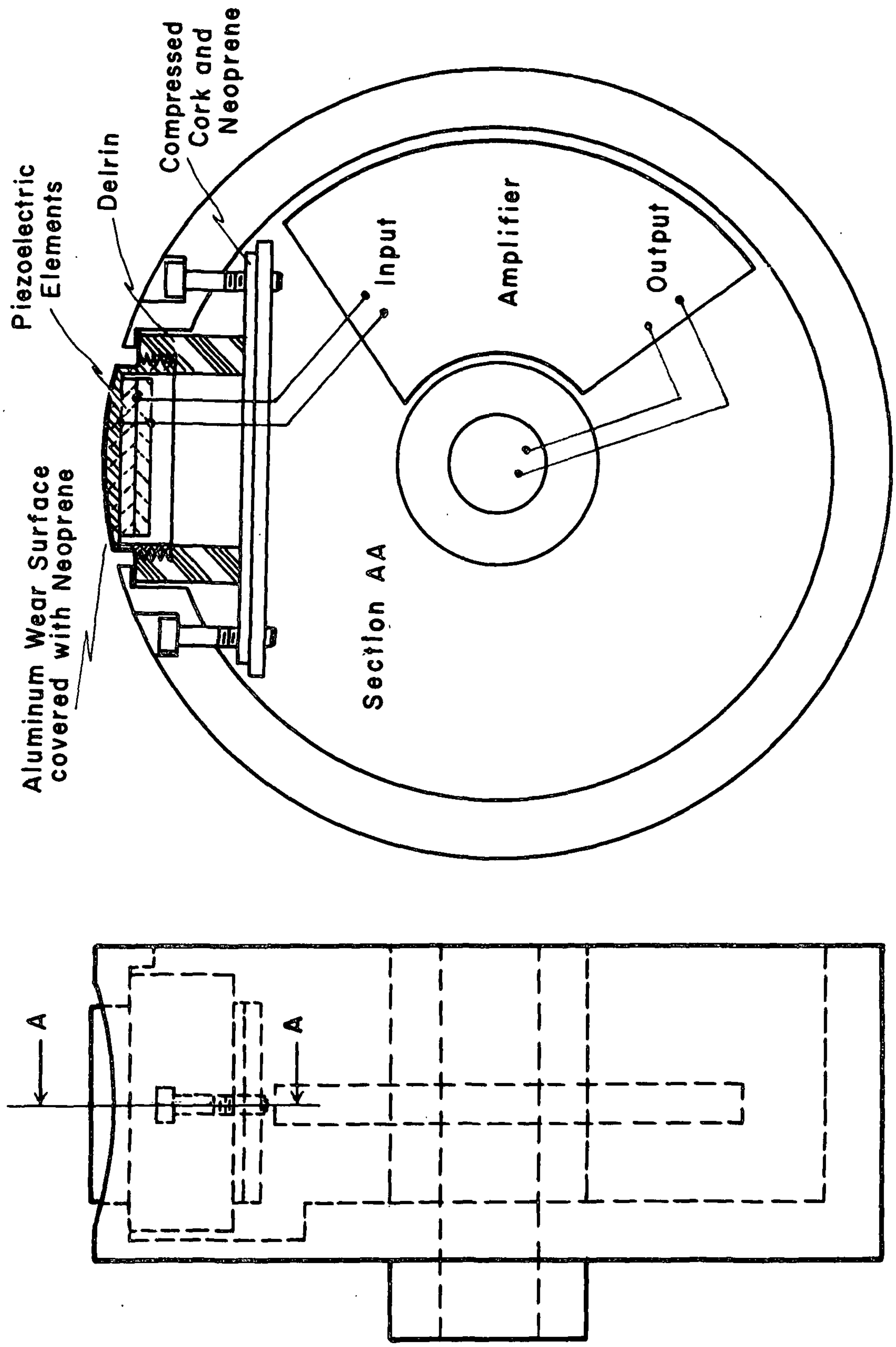

Figure 1. New receiver wheel.

The in-wheel preamplifier is built around a high-speed operational amplifier (Burr Brown 3554 SM). It has a full power band width of 20 MHz and is suitable for the higher frequencies employed in the ZD measurements. To stabilize the high-speed circuitry, the electronic components were mounted and interconnected on a double-sided printed circuit board. This combination of the Burr Brown op. amp. and printed circuit board construction produced a very stable, low noise, high speed preamplifier. A detailed schematic of the preamplifier is given in Fig. 2. The transmitter wheel differs from the receiver only in that no preamplifier is necessary.

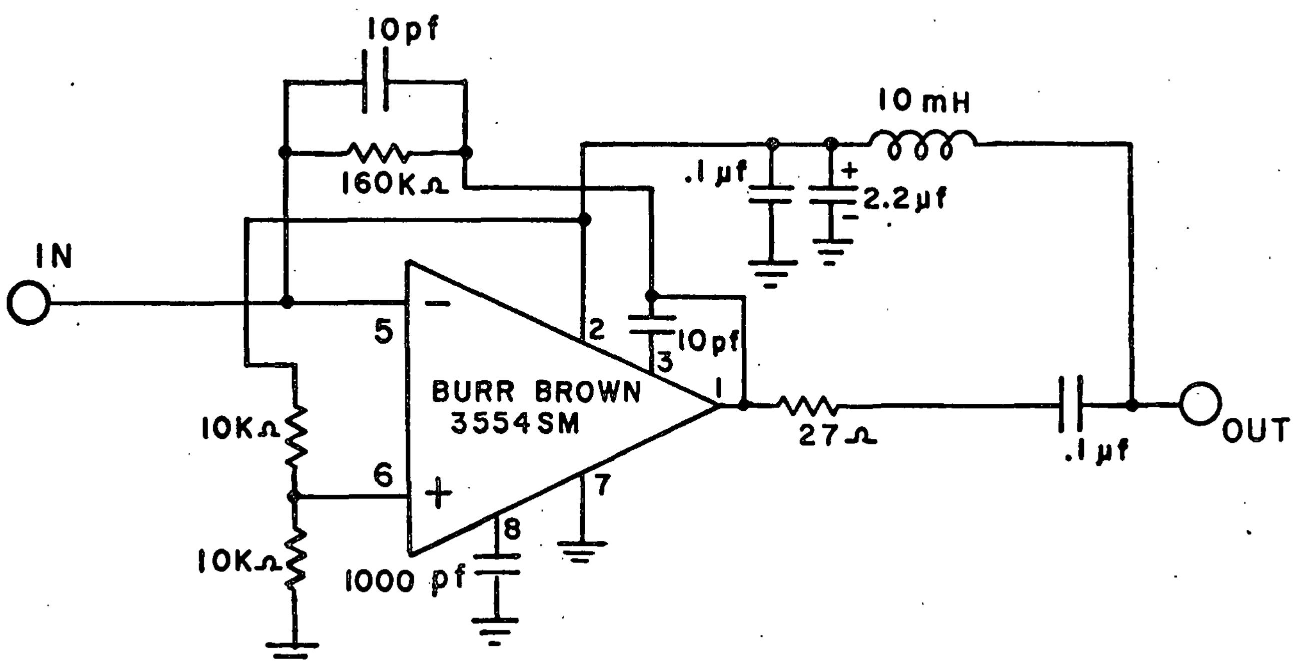

Figure 2. Preamplifier schematic.

The system was mounted on the IPC web strainer and tested at high speed. The transmitter wheel was placed on a shaft and mounted below the paper web which was threaded around the web strainer. The receiver was positioned above the web. The wheels were synchronized by means of gears attached to each shaft off the side of the belt. The time of contact of the transducer to the web was detected with a photoelectric sensor. When transducer contact occurred, an rf pulse was applied to the transmitter and the oscilloscope triggered. The resulting signal at the receiver was viewed on the oscilloscope.

Tests were conducted on 42-lb linerboard and on a low basis weight bond paper. The signal quality was excellent even at the highest speeds available on the web strainer (~2000 ft/min). The signal-to-noise ratio was about 100 to 1. The resonant frequency of the transducers, however, was not as high as desired. They operated well between 100 and 300 kHz, but not at the desired higher frequencies. The frequency response was limited by the transducer, not the preamplifier. The frequency could be raised by eliminating one of the ceramic disks or by decreasing the diameter of the disks. This has not yet been done. However, overall the experiments were judged successful; signals even better than those experienced in-plane were detected at high speed in the ZD. In order to overcome the frequency limitations of the wheel transducers described above, we are now experimenting with a much different design. This is modeled after our low-impedance, broadband, disk transducers which we built for laboratory ZD testing.

Figure 3 is a drawing of one of these off-line transducers. The active piezoelectric elements are polarized polyvinylidene fluoride (PVDF or Kynar) films. Compared to standard ceramic piezoelectrics, the films have a very low mechanical impedance (making them more efficient in coupling energy into paper) and a very low quality factor (making broadband transducer construction practical). A stack of four films, each 110 μm thick, was used. The polarization direction of the two layers on the top is opposite the two on the

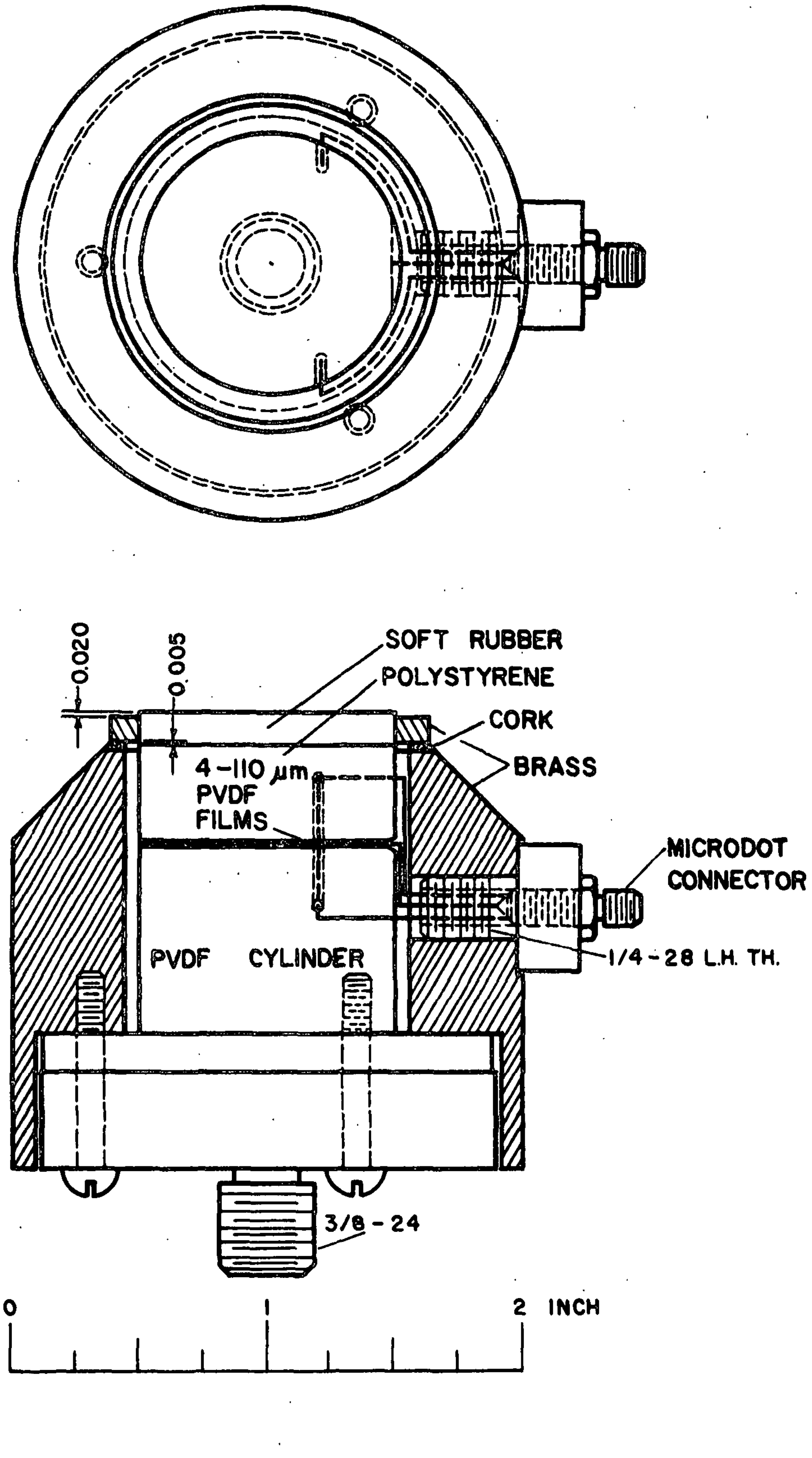

Figure 3. Kynar disk transducer.

bottom of the stack. The active electrode is the stack center and the two outer surfaces are ground. To reduce backside reflections (and increase bandwidth) one end of the stack is epoxied to an unpolarized Kynar disk. The front of the stack is a polystyrene disk. It has low acoustic loss and improves the impedance match to the soft neoprene front face. The soft neoprene conforms to the sample surface giving good acoustic coupling and a reasonable value for caliper. The thickness of the Kynar, polystyrene, and neoprene are all greater than one wavelength of sound at 1.0 MHz, the excitation frequency. This means that a single pulse can be isolated in the received signal and that this pulse has no interference from multiple reflections between transducer interfaces. Cross-correlation techniques can then be used to establish a delay time difference between a sample and a thin aluminum foil.

The aim of the present work is to adapt this design to a wheel transducer. The wheels should be equally active over their circumference. In use they will make rolling contact on opposite sides of the paper and transmit a signal through the paper. Initially we hope to use this in the laboratory. In this case the wheels would be motor driven, and a sample would be fed through the nip. This would give us experience with dynamic caliper and delay time measurements, and perhaps also provide a useful instrument for profiling soft caliper and ZD longitudinal velocity.

Our first attempt was an axially symmetric transducer with the same layering as the disks. A Kynar disk 2 3/8 inch in diameter and ½ inch thick is the base of the transducer. A small v-shaped notch was cut across the disk at one point on the circumference. The films were cut and conductive epoxy was used to secure them to the Kynar disk one at a time. To achieve the intimate contact necessary for acoustic coupling, the films are wrapped around the disk and placed in a circular vise made of teflon. The vise was tightened, extruding epoxy around the periphery. Pressure was maintained until the epoxy cured. A polystyrene ring about 1/4 inch thick was then epoxied to the outer film. To get good contact, the ring, which was undersized a few thousands of an inch, was heated and carefully placed around the core. As the ring contracted a bead of epoxy was extruded at the interface. After the final layer of conductive epoxy had cured, the edges of the layered film ring were machined to remove excess epoxy. Electrical contact to the ground planes at the inner and outer surfaces of the film ring was achieved as in the disk transducers. That is, bare copper wire was inserted in a small hole drilled through the plastic to the surface.

Conductive epoxy was forced into the holes making electrical contact when the curing load was applied. The electrical contact to the film center was made at the notch in the inner Kynar wheel. A hole was drilled through the wheel to the notch. A copper wire was threaded through this hole. During film stack assembly the ends of the two inner films were bent to the sides of the notch while the two outer films were attached to the polystyrene ring. The end of the wire was fixed with conductive epoxy to the stack center in the notch gap. Finally a 1/8 inch thick layer of soft neoprene was glued to the rim of the wheel.

The transducers constructed in this manner were promising, but had some distinct limitations. Compared to the disk transducers, they had only fair sensitivity, and were slightly less broadbanded. We had hoped that the wheels would be of uniform sensitivity over their circumference; however, we encountered a factor of two variability. This was due to inhomogenities in the electrode contact regions, and to nonuniform epoxy thickness at film interfaces. Perhaps the conductive epoxy was too viscous to form a uniform film or uniform pressure was not applied by the ring clamp. Another problem resulted from the physical properties of the polystyrene. It is a brittle plastic with a lower thermal expansivity than the Kynar. This made fitting of the undersized, heated ring to the cool core difficult and stress fractures were often observed in the polystyrene after assembly. Any heating of the completed wheel increased the chance of fracture.

The wheel design was modified (Fig. 4) to eliminate these shortcomings. We decided to sacrifice the better impedance match and transmission coefficient realized from the polystyrene ring and make both plastic pieces from Kynar. Kynar is a very tough material and has a large thermal expansivity. This allowed us to machine a smaller inner diameter to the outer ring and produce a tighter wheel. The tougher Kynar did not fracture and since the design is all Kynar, stresses are not induced by temperature changes. To achieve uniform circumferential sensitivity, we made radical changes in the acoustic coupling of the films and in the method of electrode attachment. Instead of using conductive epoxy, we meter a thin film of silicone grease onto the film surface.

Electrical contact was achieved by inserting copper wire flattened to a thickness of 10 μm in the appropriate interfaces. The ring clamp was unnecessary as coupling at all interfaces was established as the outer ring cooled. The main concern in this design is that the silicone does not interfere with electrical contact between wire and films.

The initial wheels built in this manner were circumferentially uniform in their response. The improved acoustic coupling compensated for the poorer

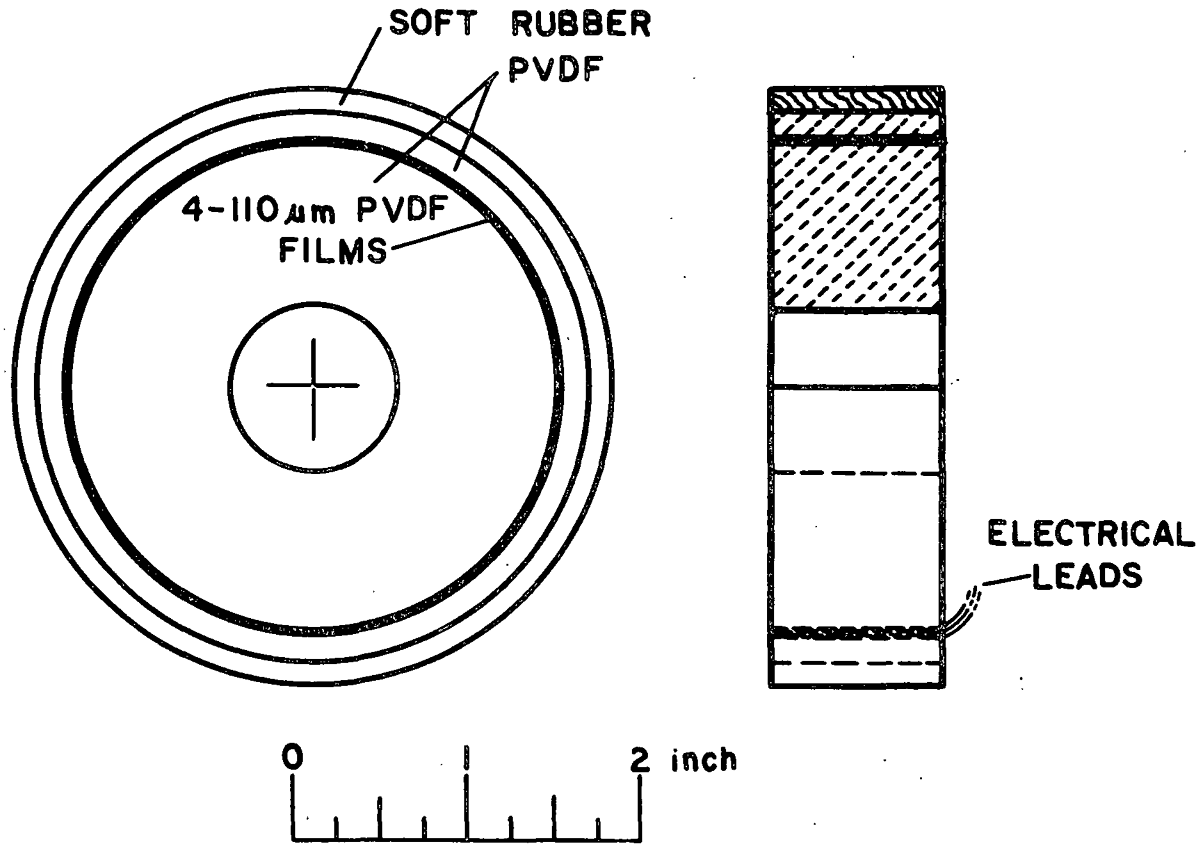

Figure 4. Wheel type ultrasonic transducer.

impedance match, and the sensitivity was approximately equal to that of the sensitive regions of the first wheels. Some contact difficulty was encountered on one of the leads. If necessary, we think we can assure good contact by applying a small amount of silver paint to the flattened electrode. We could also make electrical contact by leaving tabs on the films; however, this would be a less rugged design and increase chances of the films shorting.

From experience building disk transducers of different radii, we think that increasing wheel thickness would lead to a more broadbanded transducer.

This would also increase sensitivity to what we feel is an acceptable level for practical transducers. Our present plan is to build the first serviceable transducers to a one-inch thickness and with silicone grease coupling. We are still experimenting to determine whether film tabs are necessary.

New staff: Dr. Maclin Hall has been hired to serve as Manager of the project. Dr. Hall has many years of experience in industry concerned with sensor development. We expect to fill a second position, for a design engineer, soon.

Future Direction

Plans for the coming month include:

- Continuation of wheel transducer development.
- Make decisions concerning sensor construction.

References

1. Project 2692-4, Report One, A Progress Report to the Fourdrinier Kraft Board Group of the API, May 15, 1985
2. Habeger, C. C. and Baum, G. A. Tappi 69(6): 106(1986).

G L O S S A R Y

GLOSSARY

acid-chlorite delignification	H_2O + glacial acetic acid and sodium chlorite.
breaking load	Force in grams to cause failure of a single fiber/fiber bond in the quasi-shear deformation geometry.
bond area	Optical contact area in the crossed fiber region determined by Page's vertical polarization technique.
bond strength	For single fiber/fiber bonds, the ratio of breaking load to bond area.
classified pulp	Pulp with fines removed.
CMC	Carboxymethyl cellulose.
CMCS	Carboxymethyl cornstarch.
CMPS	Carboxymethyl potato starch.
co-crosslinking	Bonding between fiber and added polymer.
combined out-of-plane stresses	Stresses which act together e.g. normal stress σ_{33}/ρ and shear stresses τ_{12}/ρ or τ_{23}/ρ.
combined board	A completely fabricated sheet assembled from several components such as corrugated fiberboard.
Concora flat crush or CMT:	Refers to flat crush strength of medium fluted in the Concora fluter.
conversions	Pressure: $lbs/in^2 \times 6.895 \times 10^3$ = Pascals Pa. Specific elastic constants: E/ρ or c/ρ $(km/sec)^2 \times 10^3$ = Nm/g. Specific strength: σ/ρ or σ_c/ρ breaking length K.M. x 9.80 = Nm/g
corrugating medium	Paperboard used in forming the fluted portion of corrugated board.
diffuse reflectance	Reflectance in all directions.
distribution of mass density	Small scale basis weight or gramage variation.
draw or take-up factor	Ratio of length of corrugated medium to length of liner for a specified length of corrugated board.
DS	Degree of substitution - in this case, the number of carboxyl groups per monomer unit.

earlywood		Thin walled fibers.
ECT		Edge Crush Test, an edgewise compressive test made on combined board.
effective stiffness		The effective stiffness is the radius of a circle having the same area as that enclosed by a polar diagram.
engineering constants		The set of elastic constants including Young's moduli, shear moduli, and Poisson ratios.
elastic and engineering constants	C_{ij}:	Elastic stiffnesses with units of force/area (GPa). i and j range from 1 to 6. For paper, considered to be an orthotropic material, the only non-zero elastic stiffnesses are C_{11}, C_{22}, C_{33}, C_{44}, C_{55}, C_{66}, C_{12}, C_{13}, and C_{23}.
	E_i:	Young's modulus in the i direction, where i is either 1, 2, or 3 (or x, y, or Z, or MD, CD, or ZD). E_i is considered an "engineering" elastic constant having stress units.
	G_{ij}:	Shear modulus in the ij plane. G is an engineering constant.
	S_{ij}:	Elastic compliances with units of inverse stress (area/force). In general, i and j range from 1 to 6. For paper the only possible values for i and j are those combinations listed under C_{ij}.
	ν_{ij}:	Poisson ratio in the ij plane. ν is an engineering constant. In a uniaxial stress test, it is the ratio of the lateral contraction to the axial extension. It is therefore unitless.
	ε_i:	Strain (dimensionless). i goes from 1 to 6.
	σ_i:	Stress (force/area). σ_i has a range from 1 to 6.
elastic stiffnesses		The C_{ij} defined above. The specific elastic stiffnesses are measured in ultrasonic tests.
extensional stiffness		The product of elastic stiffness and caliper or an engineering stiffness and caliper. In an Instron test, plotting load/width <u>vs</u>. elongation, it is the initial slope of the load-elongation curve.
flat crush:		The force required to crush the corrugations in a specimen of corrugated board.
FLER II		Fiber Load-Elongation Recorder, Model II.
flexural rigidity		A measure of bending stiffness, define as EI, where E is Young's modulus and I is the second moment of the cross-section.

fixed clamp	Specimen-holding clamp of FLER which remains fixed in position during a test.
FTIR analysis	Fourier transform infrared analysis.
geometric mean	The square root of the product of an MD and CD property, e.g. geometric mean stiffness would be $(C_{11}*C_{22})**^{1/2}$.
high-lows	In single faced combined board, a term denoting flutes that are greater than or less than the average. Most often a "high" is followed by a "low".
latewood	Thick walled fibers.
linerboard	Paperboard used for the flat facings of corrugated fiberboard.
medium	See corrugating medium.
MD, CD, ZD	Machine direction, cross machine direction, and thickness direction, respectively, in a commercial paper. Other notations used include x, y, and z or 1, 2, and 3.
MC	Moisture content, %.
mini-handsheets	19 mm diameter made in centrifuge tubes on a 200 mesh screen.
"moist"	Refers to papers conditioned at 91-93% RH usually resulting in a moisture content of 14-16%.
Moist compressive strength factor	The moist breaking length of the treated handsheet divided by that of the untreated control.
moist tensile factor	The moist breaking length of the treated handsheet divided by that of the untreated control.
movable clamp	Specimen-holding clamp of FLER to which a push or pull force is applied and which moves as the specimen deforms.
NSSC	Neutral sulfite semichemical medium.
PAA	Polyacrylic acid.
PAE	Polyamide polyamine epichlorohydrin.
PDDAC	Polydiallyldimethyl ammonium chloride.
PEI	Polyethyleneimine.
polar diagram	A polar graph plotting longitudinal or shear stiffness as a function of angle from the MD.

PVDF	Polyvinylidene fluoride, a plastic material which can be polarized to be made piezoelectric.
ring crush	One of several methods in use for measuring the ultimate compressive strength of paperboard.
soft x-rays	Low energy x-rays.
specific elastic stiffnesses	Elastic stiffnesses divided by sheet density or C_{ij}/density. These are the quantities determined in ultrasonic measurements. They are equal to a square of a sound velocity.
STFI	Swedish Forest Products Laboratory
STFI short span compressive strength test	A test devised by the Swedish Forest Products Laboratory to measure the ultimate compressive strength of paperboard.
wet tensile factor	The wet breaking length of the treated handsheet divided by that of the untreated control.
Whitsitt/Habeger compressive strength correlation	$\sigma_C/\rho \propto E/\rho^{0.75} E_Z/\rho^{0.25}$.
wood coupon	16 mm x 16 mm tangential wood sections.
wrap angle	The sum of the angles of contact between medium and the corrugating roll flute tips from the entrance to the corrugating nip to a defined point in the nip.
WRV	Water retention value, the water remaining in fiber mat after centrifuging (gms of water/gm of fiber).